

## ABSTRACT

Title of Dissertation:

**DATA-DRIVEN ANALYSIS OF INDIVIDUAL  
THERMAL COMFORT WITH PERSONALIZED  
COOLING**

Daniel Alejandro Dalgo Reyes,  
Doctor of Philosophy Mechanical Engineering,  
December 2018

Directed By:

Jelena Srebric, Ph.D.  
Professor of Mechanical Engineering

This dissertation presents numerical and experimental results on the effects of Personal Cooling Devices (PCDs) on the energy consumption of buildings and the thermal comfort of occupants. The objective of this analysis was to quantify the tradeoffs of thermal comfort and energy savings associated with PCD technology. Furthermore, this investigation included an electrical cost analysis associated with PCDs at the building level for different cities across the United States. The results of energy and cost analyses, at the building level, indicated the potential for cooling energy and cost savings associated with shifting the electricity consumption during the peak hours to the off-peak hours of the day. The numerical analysis of human thermal comfort demonstrated the potential for PCDs to regulate human thermal comfort at warm environmental conditions. The thermal comfort level achieved in the numerical simulations were within the limits recommended by ASHRAE Standard 55. In addition, the numerical simulations permitted the evaluation of PCD performance based on thermal comfort, and the amount of sensible heat remove from the human body. The experimental work evaluated the performance of PCDs using both subjective and objective measurements of thermal comfort for 14 human subjects. The results demonstrated the ability of a PCD to change and maintain acceptable thermal comfort micro-environments for

human subjects under warm conditions. Furthermore, the results showed that a PCD had measurable effects on physiological variables that control the thermoregulatory process of the human body. Specifically, variables such as skin temperature and heart rate variability in the time and frequency domain responded to the micro-environment created by the PCD. This research established a relationship between skin temperature, heart rate variability, and thermal comfort. Overall, this investigation performed a comprehensive analysis of the interaction of PCDs with: building energy consumption, human subjects, and human physiological processes; and demonstrated the potential to recognize human subjects' thermal comfort based on physiological signals.

**DATA-DRIVEN ANALYSIS OF INDIVIDUAL THERMAL COMFORT WITH PERSONALIZED  
COOLING**

by

Daniel Alejandro Dalgo Reyes

Dissertation submitted to the Faculty of the Graduate School of the  
University of Maryland, College Park, in partial fulfillment  
of the requirements for the degree of  
Doctor of Philosophy  
2018

Advisory Committee:

Professor Jelena Srebric, Ph.D., Chair  
Professor Bao Yang, Ph.D.  
Professor Liangbing Hu, Ph.D., Dean's Representative  
Professor Jenifer Roberts, DrPh  
Professor Monifa Vaughn-Cooke, Ph.D.

© Copyright by  
Daniel Alejandro Dalgo Reyes  
2018

## Dedication

Mi victoria la llevas marcada en tu nombre y mis fuerzas se alimentan al ver tus ojos. Esta meta cumplida simboliza mi eterno compromiso contigo. Emma Victoria, sueña tan alto como puedas porque la palabra *imposible no tiene significado*, pero sobre todo trabaja fuerte para hacer realidad tus sueños. Te amo

My victory is written in your name and my strength feeds when I see into your eyes. This goal marks my life-long commitment to you. Emma Victoria, dream as high as you can because the word impossible has no meaning, nevertheless work hard to make those dreams come true.

I love you.

## **Acknowledgments**

Dr. Jelena Srebric, it has been a valuable journey that I will treasure in my heart and mind for the rest of my life. I thank you for giving me the opportunity to join your research group, but more importantly for making me feel part of it since day one. Thank you for sharing your analytical, reasoning, and management skills with me. Thank you for the valuable academic and professional lessons that certainly allowed me to grow as an engineer and researcher. More importantly, thank you for the life lessons that have allowed me to grow as a human being with ethics and values to be transparent, strong, and to help people, especially those whom are vulnerable. Thank you for guiding me with your experience, which has been the key for the development of this work. Dr. Jelena Srebric you have certainly marked my life.

I feel grateful to Dr. Jelena Srebric, the “Robotic Personal Conditioning Device”, sponsored by ARPA-E (DEAR0000530), and the University of Maryland College Park for sponsoring my research during the Ph.D. program. Similarly, I thank the GDF-Suez Chuck Edwards Memorial Fellowship for the fellowship received for the academic year 2016-2017.

I extend my gratitude to all the colleagues in the Building Science research group who have helped my research with their experience and expertise, critics, and outstanding work. This has added an enormous value to this research. Thank you all for creating a welcoming and enjoyable working environment. Thank you to Dr. Mohammad Heidarinejad for sharing his enormous knowledge, experience, and talent with me. Thank you to Nicholas Mattise for contributing to my research with his technical expertise, critical questions, and comments that made this work possible. I would also like to thank Dr. Shengwei Zhu for guiding and sharing with me his vast experience in Computational Fluid Dynamics (CFD). Thank you to Mathew, Saber, Seon, Itohan, Harshil, Dr.

Mohammad Nomeli, Sebastian, and Kofi for being part of this journey throughout these years. This work could not have been possible without every member of the research group.

I would like to extend my gratitude to the Center for Environmental Energy Engineering and to all its members for the work in the “Robotic Personal Conditioning Device” and the professional experience of being part of a research collaboration and the lessons learned throughout this work. Similarly, I express my gratitude and admiration to the University of Maryland for embarking in the journey of developing the minds and technology of the present and future. To all the faculty members in the University, specially the faculty in the Department of Mechanical Engineering. Lastly, to the staff of the Department of Mechanical Engineering for their tireless work to help move our research forward.

A mis padres, Marcelo y Raquel, a mis abuelos Teresita y Jorge por todo su apoyo incondicional y sus ánimos para conseguir esta meta. Gracias por siempre creer en mí. Los amo Finalmente y muy importante gracias a mi esposa Estefania por estar a mi lado en cada momento de este largo viaje. Gracias por siempre dar todo de tí para que podamos alcanzar este logro que es tan tuyo como mío. Gracias por tus palabras de aliento en los momentos difíciles y gracias por celebrar cada paso que damos juntos como familia. Sin duda este trabajo no sería posible sin tí y sin tu amor incondicional. Te amo.

## Table of Contents

<i>Chapter 1</i> .....	1
1.1 Statement of the Problem.....	1
1.2 Building Energy Consumption and Personalized Cooling Device .....	2
1.3 Occupants as Energy Consumption Drivers in the Building Environment .....	3
1.4 Building Energy and Indoor Thermal Comfort .....	4
1.5 Structure of This Dissertation Proposal .....	6
<i>Chapter 2</i> .....	8
2.1 Personalized Cooling Devices (PCD).....	8
2.2 Personalized Cooling Devices (PCD) and Energy Savings .....	10
2.3 Personalized Cooling Devices (PCD) and Thermal Comfort .....	12
2.4 Assessment of Thermal Comfort and PCD using Numerical Approaches .....	14
2.5 Assessment of Thermal Comfort and PCD using Experimental Approaches .....	17
2.6 Physiological Responses of the Human Body in Indoor Environments .....	19
2.7 HRV from Electrocardiography (ECG) vs HRV from Photoplethysmography (PPG) .....	25
2.8 Summary .....	27
<i>Chapter 3</i> .....	29
3.1 Research Hypothesis.....	29
3.2 Dissertation Objectives .....	30
3.3 Effect of PCD in the Overall Building Energy Analysis .....	31
3.4 Tasks Overview for each Objective .....	34
3.5 Summary .....	38
<i>Chapter 4</i> .....	40
4.1 Building Energy Simulations and PCD .....	40
4.3 Building Energy Simulations Procedure.....	45
4.4 Building Energy Models and Results .....	48
4.5 Discussion on Manufacturing and Warehouse Buildings.....	57
4.6 Cost Savings Analysis.....	58
4.7 Summary .....	61
<i>Chapter 5</i> .....	62
5.1 Theoretical Analysis of Air-jet Centerline Velocity and Temperature as a Function of Nozzle Diameter .....	62
5.2 Thermal Comfort Numerical Simulations Models .....	68



5.3 Results of Numerical Analysis of Cooling Mode .....	76
5.4 Results of Numerical Analysis of Heating Mode .....	83
5.5 Summary .....	85
<i>Chapter 6</i> .....	<i>87</i>
6.1 Experimental Assessment of Thermal Comfort.....	87
6.2 Information on human subjects.....	88
6.3 Experimental Procedure.....	89
6.4 Physiological Measurements .....	91
6.5 Data Analysis .....	93
6.7 Discussion Section.....	111
6.8 Summary.....	121
<i>Chapter 7</i> .....	<i>122</i>
7.1 Conclusions.....	122
7.2 Recommendation and future work.....	126

## List of Tables

Table 2- 1 Summary of personalized pooling device technology and current products available in the market.....	10
Table 2- 2 Summary of Numerical Studies using PCD and Thermal comfort .....	16
Table 2- 3 Summary of Experimental Studies using PCD and Thermal Comfort.....	18
Table 3- 1 Proposed Research Hypothesis.....	30
Table 3- 2 Proposed Research Objectives .....	31
Table 3- 3 Tasks Associated with Research Objective 1 .....	36
Table 3- 4 Tasks Associated with Research Objective 2 .....	37
Table 3- 5 Tasks Associated with Research Objective 3 .....	38
Table 3- 6 Tasks Associated with Research Objective 4.....	38
Table 4- 1 Outside and Inside Heat Balance Equations.....	41
Table 4- 2 Selected Cities and Climates .....	45
Table 4- 3 Commercial Buildings Electricity Rate in cents/kWh.....	59
Table 4- 4 Time of Use Program for Commercial Buildings .....	59
Table 5- 1 Pressure drops for nozzles of different diameters and flowrates.....	63
Table 5- 2 Discharge Air Velocity and Temperature for each Airflow rate.....	71
Table 5- 3 Convective and Radiative Heat Transfer Coefficient and Thermal Resistances for Seated Model .....	72
Table 5- 4 Convective and Radiative Heat Transfer Coefficient and Thermal Resistances for Standing Model.....	73
Table 5- 5 Airflow Rates and Air Discharge Temperature.....	84
Table 6- 1 Technical Description of Sensors Used in the Experiment.....	93
Table 6- 2 Results of ANOVA test with Skin Temperature Data Between Uncomfortable and Comfortable Conditions.....	98
Table 6- 3 Results of ANOVA test with Heart Rate Data Between Uncomfortable and Comfortable Conditions.....	101
Table 6- 4 Results of ANOVA test with Heart Rate Data Between Uncomfortable and Comfortable Conditions.....	105
Table 6- 5 ANOVA Results Uncomfortable vs Comfortable LF/HF Ratio (p-value < 0.001) ..	108

## List of Figures

Figure 1- 1 End Use Energy Distribution in Commercial Buildings in 2003 and 2012 .....	3
Figure 1- 2 Definition of the thermal comfort boundaries in the psychrometric .....	6
Figure 2- 1 Reported energy savings associated with literature review on extended temperature setpoints while using PCD for thermal comfort.....	12
Figure 2- 2 Predicted mean vote model thermal sensation scale .....	13
Figure 2- 3 PCD and Human Subject Interaction .....	14
Figure 2- 4 Comparison of ECG (RRI) and PPG (PPI) signals from a cardiac test taken simultaneously [114].....	27
Figure 3- 1 Energy Modeling Process .....	33
Figure 3- 2 CFD and PMV Iterative Process .....	34
Figure 3- 3 Objective and Main Task Overview .....	35
Figure 4- 1 External Wall Heat Balance .....	42
Figure 4- 2 Internal Wall Heat Balance .....	43
Figure 4- 3 Building energy models based on building type .....	44
Figure 4- 4 Temperature Schedules for Office Buildings.....	49
Figure 4- 5 Max80 Energy Savings for Office Buildings.....	50
Figure 4- 6 Extended Temp PCD Energy Savings Office Buildings.....	51
Figure 4- 7 PCD Heat rejection In/Out Comparison Office Buildings.....	52
Figure 4- 8 Office Buildings Cash Savings Due to PCD.....	53
Figure 4- 9 Temperature Schedules for Office Buildings.....	54
Figure 4- 10 Max80 Energy Savings for Midrise Apartment Buildings .....	55
Figure 4- 11 Extended Temp PCD Energy Savings Midrise Apartment Buildings .....	56
Figure 4- 12 PCD Heat Rejection In/Out Comparison Midrise Apartment Buildings .....	56
Figure 4- 13 11Mid-rise Apartment Buildings Cash Savings Due to PCD .....	57
Figure 4- 14 Cooling Degree Days vs Price Ratio.....	61
Figure 5- 1 Ball jet nozzle dimensions (Vair-Tech manufacturer catalogue).....	64
Figure 5- 2 Jet discharge velocities vs nozzle diameters .....	65
Figure 5- 3 Jet throw vs centerline velocity for the outlet diameter of 0.105 m.....	66
Figure 5- 4 Center line velocity vs nozzle diameter at 1 m distance .....	67
Figure 5- 5 Center-line temperature vs nozzle diameter at 1 m distance for (a) the cooling mode, and (b) the heating mode.....	67
Figure 5- 6 Human Body Model Simulated Occupant Postures.....	69
Figure 5- 7 PCD Virtual Model .....	70
Figure 5- 8 Virtual Room Models for CFD Study with Seated and Standing Posture .....	70
Figure 5- 9 CFD and PMV Iterative Process .....	75
Figure 5- 10 Sensible Heat loss vs Airflow rate for Different Airflow Rates for Seated and Standing Model.....	77
Figure 5- 11 Seated (a) and Standing (b) Case Cooling Mode 50 cfm.....	78
Figure 5- 12 PCD Air-jet Velocity Flow Field at Different Airflow Rates .....	79
Figure 5- 13 PCD Air-jet Temperature Flow Field at Different Airflow Rates .....	80

Figure 5- 14 PCD Air-jet Temperature Flow Field at Different Airflow Rates .....	81
Figure 5- 15 Percent People Dissatisfied (a) Standing model, and (b) Seated model as a Function of Airflow Rates in Cooling Mode .....	82
Figure 5- 16 PCD Air-jet Velocity Flow Field at Different Airflow Rates .....	83
Figure 5- 17 Percent People Dissatisfied (a) Standing model, and (b) Seated model as a Function of Airflow Rates in Heating Mode.....	85
Figure 6- 1 Human Subject BMI Distribution .....	89
Figure 6- 2 Experimental Room Temperature Profile .....	90
Figure 6- 3 Thermal Sensation and Comfort Survey Scales [52] .....	91
Figure 6- 4 (a) Chamber SetUp, (b) Arduino Based Bracelet Type Data Collection Device.....	93
Figure 6- 5 Distribution of Comfort Responses (a) 10 min before, (b) during, and (c)10 min After Requesting the PCD .....	97
Figure 6- 6 Skin Temperature over 20 minutes before and after Requesting PCD .....	98
Figure 6- 7 Skin Temperature Boxplot Uncomfortable vs Comfortable .....	99
Figure 6- 8 Heart Rate over 20 minutes before and after Requesting PCD.....	100
Figure 6- 9 Heart Rate Boxplot Uncomfortable vs Comfortable.....	101
Figure 6- 10 (a) SDNNA of low variability human subjects (b) SDNNA of high variability human subjects over 20 minutes before and after Requesting PCD.....	103
Figure 6- 11 Standard Deviation of NN Intervals Heart Beat Boxplot Uncomfortable vs Comfortable .....	106
Figure 6- 12 (a) LF/HF Ratio of High Variability Human Subjects (b) LF/HF Ratio of Low Variability Human Subjects over 20 minutes before and after Requesting PCD .....	107
Figure 6- 13 LF/HF Ratio Boxplot Uncomfortable vs Comfortable .....	109
Figure 6- 14 Physiological Variables and Thermal Comfort Relationship.....	111
Figure 6- 15 Distribution of Comfort Responses (a) 10 min before, (b) during, and (c)10 min After Requesting the PCD .....	114
Figure 6- 16 Controlled-group Skin Temperature over 20 minutes before and after Requesting PCD.....	115
Figure 6- 17 Controlled-group SDNNA over 20 minutes before and after Requesting PCD ....	116
Figure 6- 18 Controlled-group LF/HF Ratio over 20 minutes before and after Requesting PCD .....	117
Figure 6- 19 Heat Flux Before and After PCD .....	119

## **Chapter 1**

### **Introduction**

This dissertation presents, in section 1.1, the need to develop a comprehensive analysis, at the building level and the occupant level, when introducing PCDs to the building environment. In addition, this dissertation introduces the possibility of addressing thermal comfort based on the monitoring of physiological variables in a data-driven approach. Section 1.2 presents a summary on the potential benefits on adding PCD to the building environment. Section 1.3 establishes the impact of occupants on the energy consumption of buildings. Section 1.4 addresses the relationship of building energy and occupant's thermal comfort. Lastly, section 1.5 presents the structure of the flowing chapters of this dissertation.

#### **1.1 Statement of the Problem**

The principal function of buildings is to provide humans with a comfortable working and living space and protect them from extreme climate conditions [1]. The build environment has identified the priority to provide comfort with minimal energy possible. Currently, in the U.S. buildings account for almost 40% of the primary energy consumption [2]. The energy associated to conditioning spaces in commercial and residential buildings is 30% and 26%, respectively, of the total energy portfolio in each building type [2]. Based on this information, conditioning spaces is the major energy load in buildings. However, full occupant satisfaction with the environment is seldom achieved [3]. A new generation of distributed Personalized Cooling Devices (PCDs) could provide local thermal microenvironments corresponding to actual thermal comfort preferences of individual building occupants while reducing the energy load on the building [4][5]. Therefore, this study explored the energy consequences of adding PCDs at the building level and the thermal comfort benefits at the occupant level. While at the building level this dissertation conducted

numerical simulation, at the occupant level this dissertation explored numerical simulations and experimental work.

The results of this study could impulse the PCD technology to be utilized in reducing cooling energy and adds a method to measure a PCD impact at the building scale and the occupant scale. In addition, the methodology used on the comfort evaluation of PCD in this study could potentially allow PCD to be driven by individual physiological characteristics and ensure thermal comfort.

### **1.2 Building Energy Consumption and Personalized Cooling Device**

The built environment in the U.S. account for almost 40% of the primary energy consumption [2]. The energy associated with conditioning spaces in commercial and residential buildings is 30% and 26%, respectively, of the total energy in each building type [6]. According to Commercial Building Energy Consumption Survey (CBECS) 2012, the amount of energy used for space cooling and ventilation increased compared to 2003, as shown in Figure 1. Similarly, in 2015 space conditioning, in residential buildings, was 17% of the total electricity consumption [RECS] being the largest energy demand in the residential electrical portfolio. Specifically, the intense energy demand associated to cooling spaces is likely to increase as a consequence of the warmer temperatures due to global warming [7]. Even though buildings allocate a major portion of energy for space conditioning, indoor occupants' thermal satisfaction is seldom achieved. Therefore, an approach to the reduce the energy demand of space conditioning must include tradeoffs between energy reduction and thermal comfort of occupants in buildings. Particularly, the reduction of space cooling could be approached by using PCDs to condition a targeted small volume instead of the entire volume of the room as it is traditionally done. Besides the potential energy savings, PCDs have been associated with electricity peak load shifting, higher thermal comfort, and

occupant productivity [5][8]. Therefore, introducing PCD technology to the building environment has quantifiable energy and comfort benefits.

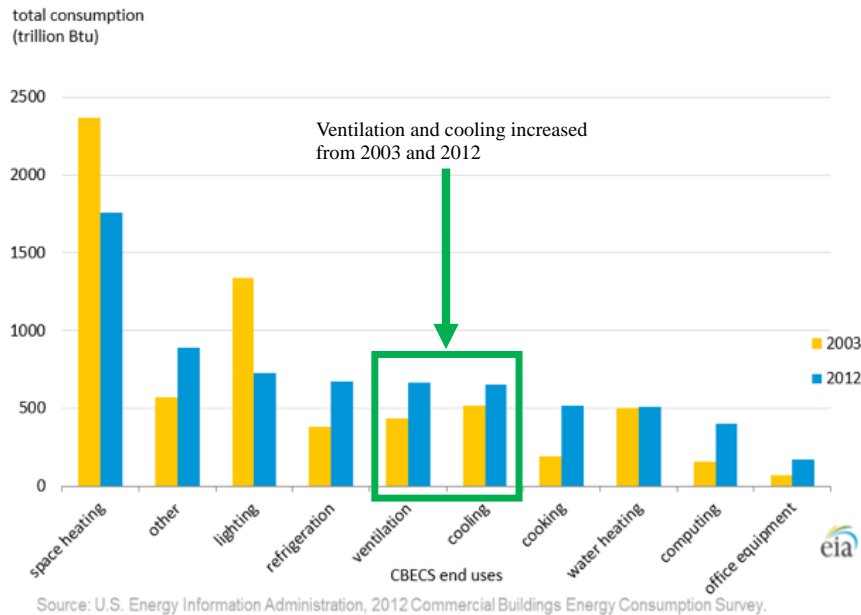


Figure 1- 1 End Use Energy Distribution in Commercial Buildings in 2003 and 2012

### 1.3 Occupants as Energy Consumption Drivers in the Building Environment

The prediction of energy demand in new and old buildings is a common practice in the building sector. The factors that influence energy consumption in buildings are: thermo-physical properties of the building structure, outdoor environment, mechanical systems such as *Heating Ventilation and Air Conditioning System (HVAC)* or lighting system, and the occupant behavior [9][10]. Multiple studies report that there are major differences between predicted and actual energy consumption in buildings [11]–[13]. These studies express that the differences in the predicted and actual energy consumption are consequence of the occupant behavior and their thermal preferences. According to an experimental investigation, occupant’s behavior and preferences could influence the energy up to a factor of three when compared to a predicted baseline [14].

The occupant interaction with the building's mechanical system is driven by their search for comfort [15]. However, due to occupants' fundamental differences such as psychological, physiological, behavioral, economical, and adaptiveness, comfort is not a unique or standard concept. Occupants have the ability to influence the energy consumption on a building by simply opening windows or by using electrical appliances that would disturb the thermal balance of the building or increase the electricity load, respectively. Similarly, by manipulating the temperature setpoint or turning the air conditioning on and off, to reach thermal comfort, occupants impact the energy consumption of the HVAC systems [16]. Particularly, satisfying individual thermal comfort in terms of temperature, humidity, and air cleanness regardless of the outdoor weather condition commonly places a major energy load on the building.

#### **1.4 Building Energy and Indoor Thermal Comfort**

The human desire for control over all aspects of our life is not new to the indoor environmental spaces. Therefore, building occupants push for more interaction with different building systems for health, and comfort purposes [17]. According to a study, occupants interact with building systems to obtain appropriate air quality, perfect acoustical conditions, perfect visual and lighting conditions, and thermal conditions [18]. Allowing occupants to actively interact with building systems to control their comfort highly impact the amount of energy use in the building [19]. A study reported that occupants consider thermal comfort of greater importance compared to visual and acoustic comfort [20]. Thermal comfort is a state of the mind that depends on environmental, physiological, and psychological, which make thermal comfort different for each occupant [18]. Outdoor environmental conditions such as temperature, relative humidity, solar radiation, wind and rain influence the occupant thermal comfort and energy consumption of the HVAC systems. In extreme hot, cold, or humid climates, achieving thermal comfort places an intense energy load



in the HVAC system. Therefore, multiple studies explore the effect of increasing the temperature setpoint during the summer or implementing a varying temperature setpoint that follows the outdoor conditions. However, these energy solutions could negatively impact the thermal comfort of occupants. Therefore, identifying the tradeoffs between energy consumption and thermal comfort could help implementing different energy savings. A study proposes to monitor occupant behavior and occupant interaction with building systems to implement control models that could lead to better utilization of energy within the building [21].

The current industry standard for indoor thermal comfort is based on a heat balance model that assumes a consistent response of thermoregulatory system among all occupants. Specifically, Fanger's models intends to allow HVAC engineers to predict whether indoor spaces are would be thermally comfort for a large group of people [22]. Certainty this model does not account for individual thermal preferences and only allows a narrow temperature range associated with comfort, as shown in Figure 1-2.

Multiple studies suggest that occupant's different physiological response, specifically in skin temperature, heart rate, heart rate variability, and oxygen saturation, are the main cause of different thermal comfort criteria among building occupants [23][24]. Therefore, the constant monitoring of these physiological variables could lead to understanding of thermal comfort as a function of indoor environmental variables, which could push the current operational boundaries recommended by the industry standard.

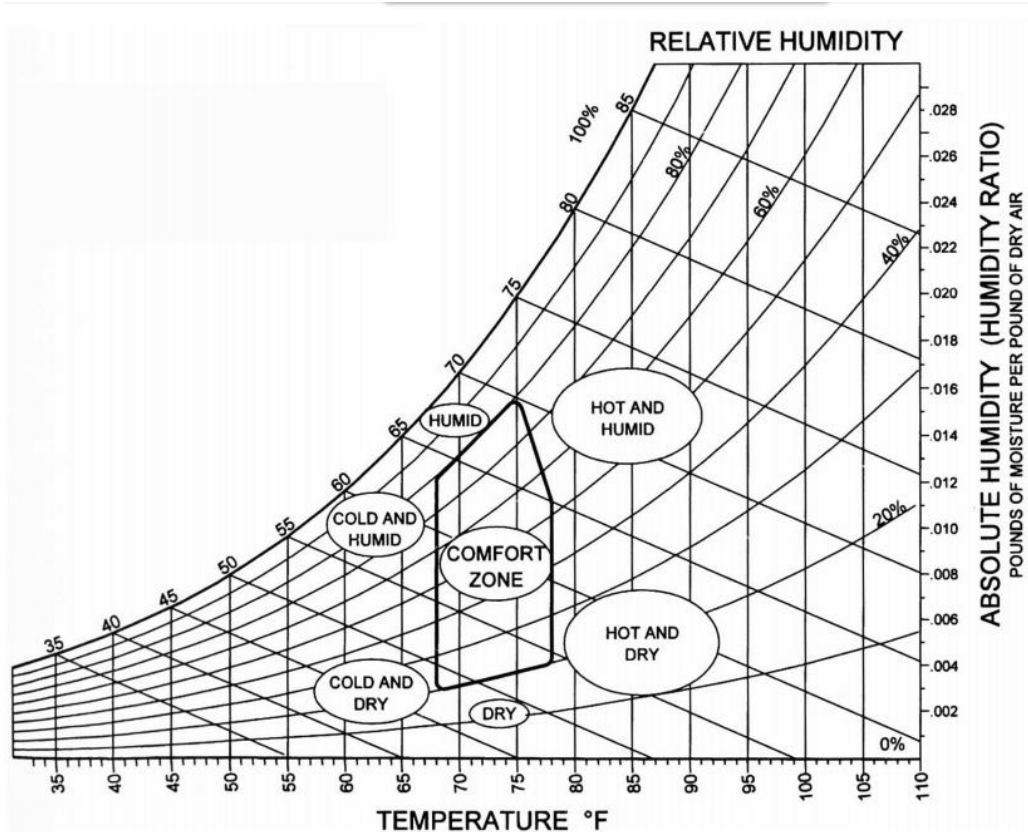


Figure 1- 2 Definition of the thermal comfort boundaries in the psychrometric

### 1.5 Structure of This Dissertation Proposal

Chapter 1 introduces the general information about buildings energy consumption and the effect of occupants on the building energy consumption. In addition, it presents information on the relationship between thermal comfort and its effect on building's energy. Chapter 2 presents the literature review on significant fields that serve as background information for the development of this dissertation. In addition, based on the literature review section this dissertation proposes a methodology to address the knowledge gap. Chapter 3 details the research hypothesis, research objectives and research methodology for this dissertation. Chapter 4 provides the methodology and results of the effect of PCD at the building level. Chapter 5 discusses the numerical methodology and results of the interaction of PCD and the human body. Chapter 6 discusses the

results of the experimental work associated with objective 3 and objective 4. Lastly chapter 7 concludes this dissertation with summary of findings and recommendations for future studies in this field.

## **Chapter 2**

### **Literature Review**

This chapter describes a detail analysis on PCD technology, the potential energy savings in the building sector when using PCD, the analysis of thermal comfort and PCD, and human physiological responses to thermal environments. The literature reviewed in this section allowed this dissertation to identify quantifiable effects of PCD at the building scale, and at the occupant scale, which defines the scope of this dissertation. Section 2.1 defines and classifies PCD technology according to its operational mode. Section 2.2 describes the methodology for potential building energy savings when using PCDs. Section 2.3 establishes the relationship between thermal comfort and PCD. Section 2.4 and section 2.5 shows a numerical and experimental, respectively, analysis of the thermal effect of PCD on the human body. Then, section 2.6 presents a comprehensive analysis on human body physiological responses to different thermal environments. Section 2.7 presents the comparison between two common methods of analysis heart rate variability. Lastly, section 2.8 provides an overview of identified gaps that sets the scope of this dissertation.

#### **2.1 Personalized Cooling Devices (PCD)**

PCD are individually controlled air distribution systems aimed to improve the thermal comfort and air quality of building occupants [25]. PCD are typically used in addition to the general (HVAC) systems in buildings [26]. Yang et al.,[27] separates PCD according to their heat exchange mechanisms, phase change materials (PCM), fluid cooled devices (FCDs), and evaporative devices (ECDs). The PCM technology provides cooling by absorbing heat, which drives a phase change

process of a substance such as frozen water, frozen ice, paraffin wax, etc. The cooling capacity of the PCM depends on the latent heat associated to each substance and the amount of substance available. However, cooling devices using PCM technology have been associated with limited cooling capacity and low portability [28].

FCDs technology is based on cooled fluids circulating through a surface and removing heat from surfaces (human body) attached to the device. FCDs technology uses a conduction-convection heat transfer as the main cooling mechanism since it requires surface contact to provide cooling, commonly using a circuit of plastic tubing around the surface. Devices using FCD technology are rated with cooling capacities between 600 Watts to 1000 Watts [29]. Lastly ECDs cooling technology is based on the latent heat of evaporation of water, 2400 kJ/kg. Commonly, ECDs cools air by passing it through completely water-saturated pads enabling air temperature changes and moisturizing process [30]. This technology is suitable for hot and dry climates since it moistens air to achieve the cooling effect. Table 2-1 shows a summary of the different PCD technologies discussed above; in addition, it describes current products that exhibit each technology and its current market price.

Table 2- 1 Summary of personalized pooling device technology and current products available in the market

<b>Technology</b>	<b>Product name and product description</b>	<b>Price [\$]</b>
PCM	FlexiFreeze Ice Vest [31] Product based on ice as PCM	99.95
	STACOOOL PREMIUM INDUSTRIAL VEST [32] Product based on Thermo Packs (material not disclose)	265.00
	Techkewl Phase Change Hybrid Sport Cooling Vest, Silver/white, Small, 6 Per Case TECHNICHE INTERNATIONAL 4531-SV-S [33] This product combines PCM with evaporative for maximum cooling efficiency	916.69
FCG	LARGE COOLING VEST [34] Product based on water flowing and a pump-cooler (sold additional)	186.31
	Cotton Cool Water Shirt, White, Short Sleeve [35] Product based on water flowing and a pump-cooler (sold additional)	159.00
	Comp cooler Backpack ICE Water Cooling System 2017 [36] Product based on water flowing and a pump-cooler (sold additional)	199.00
ECG	HOLIKE Personal Air Cooler, Portable Mini Air Conditioner Humidifier Desktop Evaporative [36]	29.99
	Portable Evaporative Cooler [37]	199.00
	NewAir AF-1000B Portable Evaporative Cooler [38]	175.99

## 2.2 Personalized Cooling Devices (PCD) and Energy Savings

In the U.S. the mechanical heating ventilation and air conditioning systems (HVAC) account for more than half of the building's total energy consumption [2]. PCDs have the potential to reduce the energy consumption of HVAC systems by reducing the conditioning spaces to specific targets

such as the human body [3]. Multiple studies have investigated the potential energy savings associated with PCD at the building level using energy simulations [39]–[43]. These studies range the potential energy savings between 4 to 60%. According to different studies, it is difficult to compare numerical studies because of the different assumptions regarding HVAC equipment, climate, schedule of operation, and tools behind each study [3]. Nevertheless, these studies use three energy savings approaches when using PCD: 1) Extending the temperature setpoint of the space while maintaining thermal comfort with PCD [44]–[47]. 2) Reducing the outdoor airflow due to PCD higher ventilation effectiveness, assuming PCD are terminal units with physical access to outdoor air such as evaporative cooling PCD [44]. 3) Using PCD based on occupant demand [26], [48], [49]. The majority of studies available to the researcher report that extending temperature setpoints while using PCD is the most viable method to obtain overall energy savings [39]–[41], [43][50], [51]. Figure 2-1 shows the energy savings reported in studies that extended the temperature setpoints between 2K and 6K. The reported energy savings, in Figure 2.1, ranges from 7% to 51%. This large energy savings range could be associated with the assumptions and methodology used during the simulation process. Therefore, there is need for standard methodologies to follow when evaluating the effect of adding PCD as an active part of the building environment. Nevertheless, these studies show the potential energy savings enabled by the adoption of PCD technology.

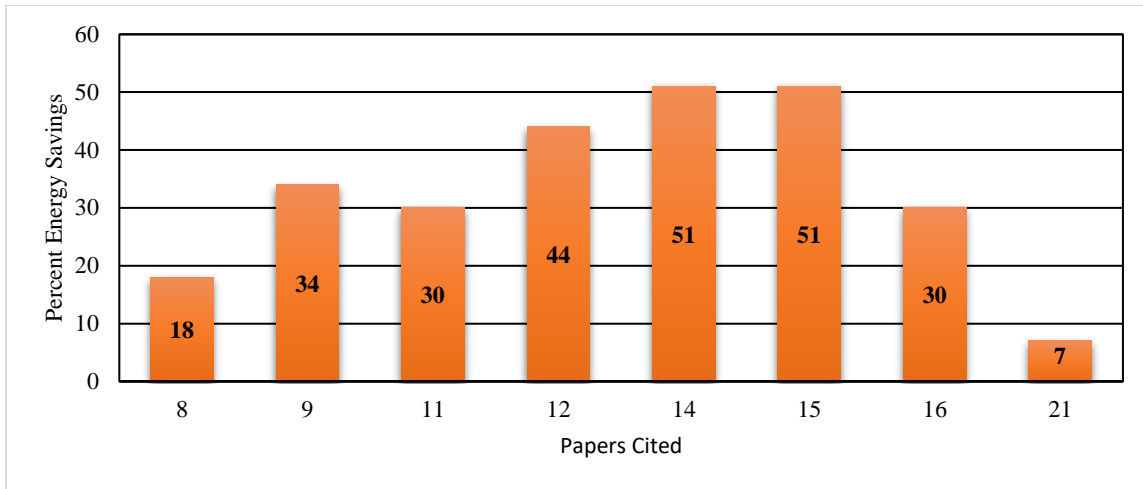


Figure 2- 1 Reported energy savings associated with literature review on extended temperature setpoints while using PCD for thermal comfort

Fewer studies investigate the effect of PCD in the heating mode. According to a study, by extending the temperature setpoint by 3K in the heating mode leads to possible energy savings of approximately 17% [42]. Based on this literature review, multiple studies investigate the influence of PCD in the energy consumption of buildings, but only a limited number of them report the energy penalty associated to the operation of PCD in terms of electricity consumption and the electricity use of HVAC system [8], [9], [40]. A study shows that the use of PCD in buildings might be associated with an energy penalty of 15% in the building electric usage [49]. Therefore, there is a need to develop a comprehensive energy analysis that takes into account the overall energy associated to all the building components that PCD might impact and create a realistic energy savings potential with detail assumptions and descriptive methodology.

### 2.3 Personalized Cooling Devices (PCD) and Thermal Comfort

In the building environment HVAC systems are currently the main method to condition spaces and provide comfortable indoor environments [3]. The goal of HVAC systems is to create uniform and steady state indoor environments to satisfy the majority of people in the space. These uniform



environments are set based on industry standards such as the American Society of Heating, Refrigeration, Air-Conditioning Engineers (ASHRAE 55) [52]. However, in thermal comfort survey in 215 offices only 39% of the responders are thermally satisfied in their indoor working space [53]. The industry standard to evaluate thermal comfort is the Predictive Mean Vote (PMV) model and the Percent People Dissatisfied (PPD) proposed by Fanger et. al [52]. The PMV model is a mathematical expression that combines four environmental variables: air temperature, air relative humidity, air velocity, and local mean temperature; as well as two human factors such as human body heat production, “metabolic rate”, and clothing level. The PMV model uses the environmental and the human factors to predict their thermal sensation in a -3 (cold) to 3 (hot) scale, as shown in Figure 2-2. The PMV model assumes the same human factors for all occupants without considering personal variations [54] In addition, this model ignores physiological adaptation of occupants to different environment as well as changes associated with season of the year. Therefore, allowing occupants to individually control their space according to their individual thermal preferences, could enhance the indoor satisfaction, improve productivity, and health [3].

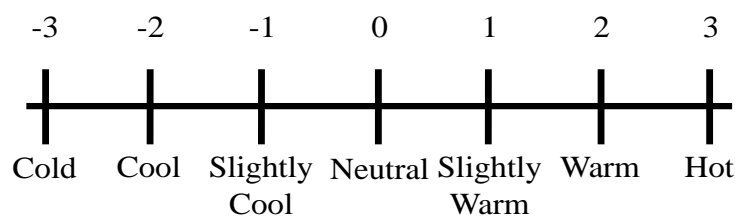


Figure 2- 2 Predicted mean vote model thermal sensation scale

Multiple studies reported that the individual differences between occupants regarding their preferred air temperature or air velocity could vary 10°C in temperature and differ up to four times in velocity [8], [45], [55]–[57]. Current HVAC systems are not designed to address individual

thermal preferences, instead they provide static and uniform environments. The need to address individual thermal comfort have led to the design and implementation of PCD technology [3]. PCD condition a small area around the user Figure 2-3, which improves their thermal comfort and perceived air quality [44],[8],[58]–[60]. In addition, PCDs help reducing the lower sick building syndrome symptoms (SBS) and enhance occupant’s productivity [44]. The primary application of current developing PCD is on cooling effect by air movement in warm environments [8]. According to multiple studies, thermal comfort could be maintained at local temperatures up to 30 °C when using PCD [51], [61], [62]. Melikov et al. claims that PCD associated to air movement are not feasible for heating effect due to the possible risk of draft [8]. The performance evaluations of PCDs regarding thermal comfort are commonly done using numerical and experimental approaches.

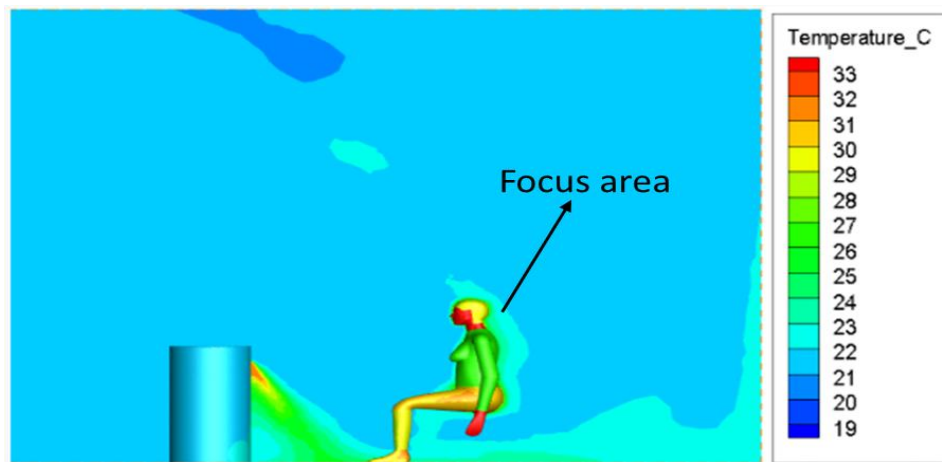


Figure 2- 3 PCD and Human Subject Interaction

#### 2.4 Assessment of Thermal Comfort and PCD using Numerical Approaches

Numerical studies are a less expensive alternative to obtain information about the airflow field and air temperature distribution around human body [63], [64]. Researchers use numerical simulations tools to optimize the design of PCD and their interaction with the human body within the indoor

space [65]. Specially, numerical simulations help to quantify the energy interaction between PCD's air jet and the thermal boundary layer of the human body [66]. In addition, several numerical studies focus on the calculation of convective and radiative heat transfer coefficients, which in most of the cases are later validate by experimental studies [63], [67]. The validation process requires physical measurements of local air temperature, local air velocity, relative humidity, and heat flux at different location around a thermal manikin or a human body.

Numerical investigation of thermal comfort generally coupled computational fluid dynamics (CFD) and thermoregulation models [39], [43], [68]–[70]. A study coupled CFD to thermoregulation a model based on PMV and PPD for the assessment of human thermal comfort when using a two-air terminal PCD [71]. This study investigated the effect of PCD by comparing thermal comfort values calculated by virtual models with and without PCD at a room temperature of 28°C. The calculated PPD values for the model without and the model with PCD were 27.7 % and 16.1 %, respectively. The PPD value for the model without PCD was experimentally validated and reported a value equal to 24.48% [71]. The difference between the experimental and numerical PPD value demonstrated good agreement [71].

Similarly, another study coupled CFD with a thermoregulation model developed by Zhang et al. [72] to assess thermal comfort provided by three different PCD [68]. In the previously mentioned study, the authors calculated parameters such as air temperature, air velocity using CFD and inputted them into the thermoregulation model in an iteratively process. The study predicted thermal comfort values approximately between -1 and 2 when the model included the virtual PCD. The thermal comfort scale in Zhang's model ranges from -4 (very uncomfortable) to 4 (very comfortable), which means numerically the PCD is able to maintain acceptable comfort level. The

numerical results were validated in later experimental studies using Zhang’s model and show good agreement [73]–[75].

Makhoul et al. [39] numerically investigated the performance of an integrated ceiling diffuser and personalized ventilator coaxial nozzle to localize air conditioning and fresh air needs around the occupants. In this study Makhoul used Zhang’s thermoregulation model to investigate the influence of different air local temperatures, PCD supply temperatures, and PCD supply airflow rates on virtual occupants’ thermal comfort. The results indicated that the overall thermal comfort values vary between 1.4 and 1.6 when using each PCD model. Table 2-2 summarized the findings in the studies described in this section. Note that even though these studies use similar parameters in the simulation, the reported thermal comfort values are significantly different. This difference could be associated to the CFD approaches such as solver, turbulence models, grid configuration, etc. Likewise, the difference could be associated to the methods used to couple CFD and the thermoregulation model since a standard test method for PCD evaluation does not exist. Overall, the present investigation found that numerical validation of performance of PCD and thermal comfort is very limited in the literature available to the researcher. In addition, while the majority of this studies reported that PCD enhance thermal comfort, they lack an assessment on human body physiological responses such as human body surface temperature or heat flux that could lead to a deeper assessment of the potential of PCD at the occupant level.

Table 2- 2 Summary of Numerical Studies using PCD and Thermal comfort

PCD (Personal Cooling Devices)	Room Temperature °C	PVS Supply Temperature °C	Airflow Rate cfm	Thermal Comfort
Desk-Edge-Based PC [68]	25	20	7.4	0.50
			10.2	0.50

			13.8	0.55
Movable Panel PC [68]	26	20	10.6	1.0
			21.2	1.2
			31.8	0.8
			42.4	0.4
Chair-Based PC [68]	25	20	1.7	-0.50
			3.4	-0.55
Low-mixing ceiling-mounted PC [39]	26	16	10.6	1.6
	27	20	15.9	1.8
	28	24	21.2	1.4

### 2.5 Assessment of Thermal Comfort and PCD using Experimental Approaches

The majority of the research on PCD and thermal comfort is experimental research [3]. Multiple studies use thermal comfort surveys as the tool for human subjects to evaluate the effect of PCD on thermal comfort [44]. Kaczmarczyk et al., tested the influence of five different PCD and concluded that human subjects reported comfortable values when using PCD with airflow rates between 20 and 30 cfm [74]. Likewise, two investigations demonstrated that a desk mounted PCD with airflow rates between 10 and 30 cfm are associated to neutral comfort levels [44][76]. In a different study, the authors tested the thermal comfort of 16 human subjects while using a PCD for cooling purposes at an environmental temperature of 28°C [27]. The results showed that on average human subject in this experiment needed approximately 23 Watts to lower their thermal sensation to neutral. In addition, Verhaart found that human subjects tolerate air velocities up to 1.6 m/s, which validates the reported results in [77], [78]. A different study tested the performance

of a partition-type fan-coil unit (PFCU) against performance of the main HVAC system [79]. The results of the previously mentioned study showed that PCD is able to provide comfortable environments at 45% less energy than the main HVAC as well as reported reduction of cold drafts. Table 2-3 shows a summary of the different PCD, their working indoor temperature, their supply air temperature, and the reported thermal comfort associated with each PCD.

Table 2- 3 Summary of Experimental Studies using PCD and Thermal Comfort

PCD	Room Temperature °C	PCD Supply Temperature °C	Airflow Rate cfm	Thermal Comfort
Desk Air-terminal [80]	26	20	14.8	0.35
			23.3	0.46
			31.7	0.58
Horizontal and Vertical Desk Grille [81]	26	20	29.6	0.5
Round Movable Panel Air Terminal [81]	26	20	27.5	0.5
Movable Panel Air Terminal [81]	26	20	29.6	0.1
Headset Air terminal [81]	26	20	0.76	0.8

Round Movable Panel Air and Horizontal Desk Grille [81]	26	20	21	0.2
Desk Mounted [76]	26	22	10.6	-0.5
			21	-0.4
Round Panel Air <i>Heating</i> [82]	20	26	26.5	0

The majority of studies reviewed in this section used surveys to assess the thermal comfort effect of PCD. A few studies evaluated the effect of PCD in terms of physiological changes that are representative of thermal comfort [56][8]. An experimental study implements skin temperature and heart rate monitoring in addition to thermal comfort surveys when analyzing the thermal comfort effect of a PCD [56]. The author reported that low heart rate and low and constant skin temperatures when human subjects reported being thermally comfortable. Most of the studies reviewed in this section used thermal comfort surveys to collect data on the performance of PCD, which requires PCD users to actively participate. However, an assessment of thermal comfort with a passive method such as monitoring physiological responses could be a more interesting and accurate approach to quantify the effect of PCD in thermal comfort.

## **2.6 Physiological Responses of the Human Body in Indoor Environments**

### **2.6.1 Thermal Comfort**

The thermal comfort models currently available such as Fanger [22] and Gagge two-node model [83] assess human thermal comfort based on an energy conservation theory. Consequently, these models reflect the average thermal sensation of a large population, but lack explanation on

different people experiencing different thermal comfort sensation in the same environment [84]. Thermal comfort is the condition of the mind that expresses satisfaction with the thermal environment [52]. Thermal comfort depends on environmental and personal factors such as air temperature and humidity, air velocity, activity level, clothing level but more importantly it is influenced by individual's preferences [85]. The thermal interaction of the human body with the environment could be described as a classic heat transfer process that includes radiation, convection, conduction, and evaporation [22]. However, this heat transfer process is a consequence of the human body thermal self-regulation function, which responds to different thermal environments [86]. The self-regulation function includes physiological processes such as vasoconstriction, vasodilatation, shivering, and sweating that control individual's thermal sensation [87]. Therefore, in order to develop a thermal comfort model that explains individual thermal sensation, many researches consider physiological parameters such as skin temperature, heart rate, heart rate variability HRV, and skin conductance [84], [88], [89]. These physiological variables have a direct connection with the human thermoregulatory system. At present, it is possible to merge these traditionally separate data collection processes such as thermal comfort surveys into a comprehensive assessment of occupant preferences, environmental data, and physiological data to evaluate the performance of PCD technology.

### **2.6.2 Skin Temperature Response to Air Local Temperature Changes**

The skin in the human body has a significant number of thermal receptors, which are connected to neurons that respond to the thermal changes in the environment by dilating and constricting blood vessels in the surface of the skin [52]. Therefore, skin temperature is an important component of the human thermoregulation system. Multiple studies, experimentally, develop thermal sensation models that have individual's skin temperature, core temperature and thermal sensation surveys as



the principle input variables [72][89][90][91][92]. Yao et al [89] and Choi et al., [93] develop a regression formula that correlates skin temperatures, at eight different human body points to the response of thermal sensation survey. A study developed by Fiala et al., [91],[94] observed and correlated the temperature changes of body parts such as head, trunk, arms, hands, legs, and feet to transient and uniform thermal conditions in experiments in an environmental chamber.

A study investigated a correlation between human body skin temperatures to thermal sensation in temperatures between 20°C to 30°C [93]. This study found that skin temperature changing rates were consistent with the changing rates reported in thermal sensation survey. Similarly, another study explored the response of skin temperature in environmental temperature between 20°C to 32°C and reported a rapid response of skin temperature when exposed to a step-down temperature (28°C to 24°C), approximately 4 minutes on average, and reaching a final stable skin temperature of 31°C within 10 minutes on average. Humphreys et al., proposed to use the skin temperature of the hands with the temperature of environment to predict thermal comfort [95]. Multiple studies suggested that the dorsal region of the hand is more thermal receptive due to the presence of the main arteries that conduct heat from the inside to the outside of the human body during thermoregulation process [8][51][61]. According to a study, the wrist has main arteries that contain useful information on the human body thermoregulation process [96]. This literature review demonstrates the potential of skin temperature to be an active parameter on the evaluation of thermal comfort. Due to the skin temperature important role in detecting temperature environmental changes, skin temperature could be used to evaluate individual thermal comfort in indoor environments.

### **2.6.3 Heart Rate Response to Air Local Temperature Changes**

Current widely use thermal comfort model such as PMV and standard effective temperature (SET) use metabolic rate as an input variable for determining thermal comfort [97][83]. According to a study, heart rate is significantly correlated to metabolic rate and it has a significant role in the human body thermoregulation process [93]. Temperature changes in the environment are sensed by peripheral and central temperature receptors of the human body located at the skin level. Based on the sensed information the parasympathetic and sympathetic nervous system interact to start the thermoregulation process by controlling organs such as heart, lungs, and vessels [98]. The parasympathetic nervous system serves to slow heart rate in relax states [99]. The sympathetic nervous system releases hormones to increase the heart rate when peripheral sympathetic neurons receive external information such as danger alert, stressful situations, or simple cases such as environmental temperature changes [100]. Multiple studies identified heart rate as a potential indicator of thermal sensation assessment. Choi et al., and Lan et al., observed that heart rates were consistently lower at indoor environmental temperature of 22°C than at indoor environmental temperature of 30°C. [93][101]. However, other studies have reported a lack of significant relationship between heart rate, thermal sensation/comfort, and environmental temperatures [62][80]. A possible explanation for this discrepancy could be due to the low thermal stress produced by the temperature ranges used in the environmental chamber experiments. These relatively large volumes of environmental chambers when compared to the human body size are not the best option for a study of physiological responses to local environments. The literature reviewed in this section suggested that there is a clear relationship between heart rate and thermal sensation at different indoor environmental conditions. However, more research in this field is necessary to understand the influence of indoor thermal environment in the heart rate of individuals. Most of the studies reviewed in this section conducted experiments in uniform and

steady state environments. Therefore, there is a need to investigate potential relationship between heart rate and dynamic thermal environments such as the ones created by PCD.

#### **2.6.4 Heart Rate Variability Response to Air Local Temperature Changes.**

The thermoregulatory process in the human body is specifically controlled by the autonomic nervous system. The autonomic nervous system uses thermoreceptors located in the human skin to detect and regulate the thermoregulatory process according to temperature changes in the environment [8][75][81]. The autonomic nervous system consists of the parasympathetic and the sympathetic nervous systems. In one hand, the parasympathetic nervous system is responsible for the rest/digest activities and one of its function is restoring the thermal balance in the human body. On the other hand, the sympathetic nervous system drives the fight-or-flight response of the human body when exposed to stressful environments such as a warm environment [82]. The balance between the parasympathetic and sympathetic nervous systems is assessed using Heart Rate Variability (HRV) as a non-invasive measurement method [102]. HRV represents the time variation in the beat-to-beat of the heart rate. The analysis of HRV could be done in the time-domain or frequency domain. The time-domain analysis uses statistical techniques to describe the activity of the autonomic nervous system. The most common time-domain variables are *standard deviation of time beats SDNNA*, and *square root of the mean squared differences of successive beats RMSSD*. Information regarding the specific techniques used to evaluate HRV in the time domain could be found in the literature [82]. The frequency domain analysis decomposes the beat-to-beat signal into its fundamental frequencies. There are three power-bands that have been associated with the analysis of HRV: (i) the Very-Low Frequency (VLF) band that ranges from 0 to 0.04 Hz, (ii) the Low Frequency (LF) band ranging from 0.04 to 0.15 Hz, and (iii) the High Frequency (HF) band that ranges from 0.15 to 0.4 Hz. The ratio of LF/HF bands has been

associated with the balance of the autonomic nervous system that controls the thermoregulation process of the human body. Therefore, the LF/HF ratio has the potential to provide an objective measurement of the thermal interaction between a human body, the indoor environment, and more importantly a microclimate created by PCD.

HRV indicates the capacity of human body to adapt and respond to physical changes, such as thermal stress. Multiple studies have reported correlation between environmental temperature and LF/HF and reported significant differences between the LF/HF ratio between comfortable and uncomfortable thermal levels [76][103][104]. A study reported that human subjects under thermal stress and thermally uncomfortable had a LF/HF ratio equal to 2.1 and at a comfortable environment the same human subjects had LF/HF values of 1.3 [52]. In addition, this study showed that human subjects in hot environmental temperatures (28°C to 30°C) have statistically higher LF/HF ratio than the ones in neutral temperatures (24°C to 26°C). Similarly, another study reported LF/HF ratios of 6 human subjects at different environmental temperatures between 22°C and 30°C [76]. This study showed that LF/HF ratios at hot environmental temperature of 30°C and neutral environmental temperature of 26°C are 2.5 and 0.8, respectively. The majority of literature available to the researcher measure HRV using electrocardiogram (ECG), which is the traditional and most common method. However, two studies compared the LF/HF ratios obtained from a traditional electrocardiogram (ECG) and the ratio obtained from a pulse wave sensor detector, such as the ones widely available in wearable devices and showed approximately the same responses between the two types of devices [76] [102]. In study [76] the authors reported higher LF/HF ratios for human subjects in hot environmental temperature of 38°C compared to the ones at a neutral temperature of 25°C. This brings the possibility of using HVR measurements to evaluate individual

thermal comfort by the means of wearable technology even though current commercially available wearable devices only monitor heart rate.

### **2.6.6 Skin Conductance Response to Air Local Temperature Changes**

Sweating is another common physiological response of the human body to warm/hot environments [52][86][105]. The human body dissipates internal heat via sweat evaporation [106]. A recent thermal comfort study found that at thermal uncomfortable environments the sympathetic nervous system activity dominates the thermoregulation process allowing processes such as vasoconstriction and sweating [106][107]. In addition, [108] reports that skin wetness is a good indicator of thermal discomfort at warm conditions. Skin wetness is the ratio between the actual evaporative heat loss (by sweat) and the maximum possible evaporative heat loss for a given environmental condition [109]. A parameter that assesses the presence of sweat in the skin is the galvanic skin conductance (GSC), which reflects the ability of the skin to transmit electrical current based on the presence of sweat [110]. Multiple studies [111][112] demonstrated an increase of GSC before sweat was present at the skin level, which according to [113] reflects the initial activity of the thermoregulatory sweating process and therefore it has the potential to predict thermal discomfort for individuals.

### **2.7 HRV from Electrocardiography (ECG) vs HRV from Photoplethysmography (PPG)**

Traditionally HRV has been determined by spectral analysis using the information of successive inter-beat RR intervals of electrocardiography (ECG) signals [114]. ECG technology measures the electrical activity of the heart generally using electrodes placed on the skin, chest or limbs [115]. Commonly, the electrodes are wire-connected to the equipment that reads, logs, and display the

electrical signals. The wire-connection limits the user's activities and could turn uncomfortable to wear them. Generally, the ECG equipment needs to be operated by certified technicians in the medical field such as nurses and medical doctors [116]. The operation and postprocess of the data obtain from ECG signals makes this technology difficult to be used by the general users. Therefore, photoplethysmography (PPG) technology has been developed in the current market [114]. PPG is a non-invasive optical technique for monitoring beat-to-beat relative to the blood volume circulating through peripheral tissues such as the fingers or the wrist[117]. The idea behind this technology lays in the light absorption as a function of blood flowing through fingers or wrists, more light is absorbed as more blood passes when the heart systoles, and less light is absorbed as less blood passes through the finger or wrists when the heart diastoles [118].

The blood volume circulating through the human body at any time is directly related to the cardiac activity [114]. Therefore, many authors suggested that the physiological information derived from ECG signals could be obtained from PPG signals [119][120]. Figure 2-4 shows a comparison of the beat-to-beat signal obtained from ECG and PPG devices, which is used to estimate HRV. Multiple studies compared the accuracy of HRV calculated from PPG devices to HRV from ECG devices [121][122]. These studies found high accuracy ( $r > 0.7$ ,  $P < 0.001$ ) between the HRV calculated form PPG signals as compared to ECG signals. Therefore, using PPG signals to calculate physiological variables such as HRV is possible with high accuracy. The PPG technology is present in the current market in wearable devices, specifically, for heart rate calculation for fitness purposes. However, the estimation of the HRV for diagnostic purposes is gaining more attention from wearable technology manufacturing such as Apple.Inc.

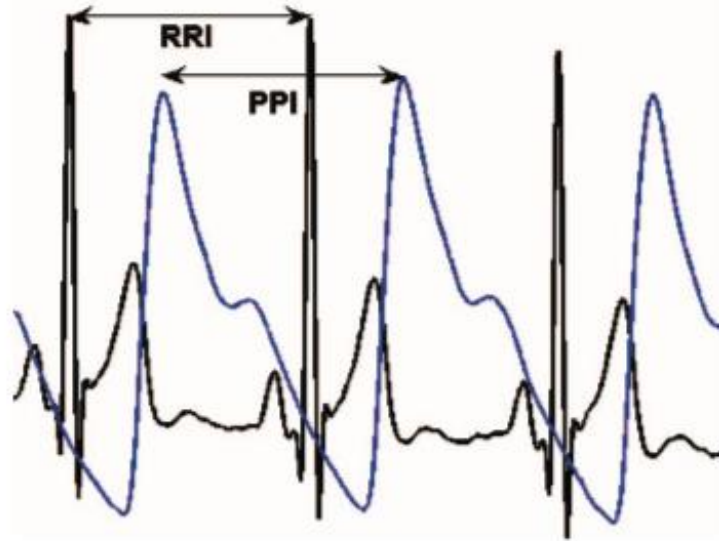


Figure 2- 4 Comparison of ECG (RRI) and PPG (PPI) signals from a cardiac test taken simultaneously [114]

## 2.8 Summary

This section summarizes the key findings identified in the literature available to the researcher.

Based on these findings, this dissertation elaborated its hypothesis and researcher objectives.

The following list states the key findings and a possible method to address each finding.

1. Studies do not present an overall energy effect of PCD at the building level.

The existing studies investigate the influence of PCD in the energy consumption of buildings, but only a limited number of them report the energy penalty associated to the operation of PCD in terms of electricity consumption and the electricity use of HVAC system. This dissertation proposes an overall energy analysis of at the building level to quantify the effect of introducing a PCD for thermal comfort while increasing the indoor temperature setpoint by 2.6°C during the peak hours of the day. This analysis focuses on the end-use energy such as electricity consumption, cooling energy, heating energy, and HVAC fan energy. In addition, this

dissertation links the electricity effect of PCD and higher indoor temperature setpoint to a cost analysis based on electricity price of each city.

2. Numerical studies do not quantify the tradeoff between thermal comfort and energy associated with PCD.

This dissertation proposes a numerical assessment of thermal comfort based on the operational features of PCD. The features that are part of this investigation are airflow rates supply by PCD, air temperature supply by PCD, energy capacity of PCD, and the amount of sensible energy remove from the human body by PCD.

3. Experimental studies evaluate the performance of PCD based on comfort surveys.

Most of the studies reviewed in this section used thermal comfort surveys to collect data on the performance of PCD, which requires PCD users to actively participate. However, an assessment of thermal comfort with a passive method such as monitoring physiological responses could be a more interesting and accurate approach to quantify the effect of PCD in thermal comfort. This dissertation considers that it is possible to merge these traditionally separate data collection processes such as thermal comfort surveys into a comprehensive assessment of occupant preferences, environmental data, and physiological data to evaluate the performance of PCD technology.



## **Chapter 3**

### **Dissertation Hypothesis, Objectives and Methodology**

The objective of this investigation is to quantify the tradeoffs between thermal comfort and energy saved by PCD at the building level and occupant level. Section 3.1 presents the research hypothesis for this dissertation. Section 3.2 details the research objectives to fulfill the research hypothesis. Section 3.3 describes the methodology to identify the effect of PCD in the building environment and at the occupant level. Section 3.4 enlists the tasks for each objective in this dissertation. Lastly, section 3.5 has a summarizes the critical parts for the success of this research.

#### **3.1 Research Hypothesis**

The problem statement and the literature review presented in Chapter 2 delineated the research hypothesis for this dissertation, as shown in Table 3-1. The applications of this hypothesis could advance the development and future adoption of PCD as part of the building environment to ensure thermal comfort at the lowest possible energy cost. This dissertation assesses the impact, at the building level and at the occupant level, of adding a PCD as an additional equipment in the building environment. In addition, this dissertation explores the impact of PCD on physiological variables that are responsible for the human thermoregulation process in the interest of quantifying the interaction of occupants and PCD. The results of this thesis could be used in the Robotic Personal Conditioning Device (RoCo) that is being developed in collaboration with the Cluster for Sustainability in the Built Environment at the University of Maryland (CITY@UMD), the Center for Environmental Energy Engineering University of Maryland (CEEE) and Oak Ridge National Lab. This research was sponsored by the Department of Energy of the United States (DOE) (ARPA-E DEAR000530).

Table 3- 1 Proposed Research Hypothesis

<b>Research Hypothesis:</b>	Utilizing an automated occupant thermal comfort assessment combined with a Personalized Cooling Device could yield an overall system level energy savings while satisfying the individual comfort preferences.
-----------------------------	--

### 3.2 Dissertation Objectives

This dissertation identifies four objectives to prove the hypothesis, as shown in Table 3-2. The first objective numerically evaluates the energy savings associated with extending the temperature setpoint while using PCD in office, and mid-rise apartment buildings constructed pre-1980 and post 2004. The second objective numerically explores the heat flux of the human body when using PCD at different operational modes. The third objective studies the effect of PCD on human subjects experimentally, specifically during this dissertation monitors physiological variables as well as comfort surveys to evaluate the performance of PCD. The last objective explores the relationship between physiological variables and thermal comfort in the interest of developing a data-driven thermal comfort assessment of building occupants.

Table 3- 2 Proposed Research Objectives

<b>Research Objectives:</b>	1- Evaluate the potential energy saved by Personalized Cooling Device and extended temperature setpoints in commercial buildings.
	2- Quantify the tradeoffs between energy savings and thermal comfort.
	3- Experimentally examine influence of PCD on personal thermal comfort.
	4- Establish a method to assess thermal comfort using a data-driven approach.

### 3.3 Effect of PCD in the Overall Building Energy Analysis

The literature available for this researcher does not present an overall energy analysis, numerical or experimental at the building level, of the effect of extending temperature setpoints during the summer months while introducing the PCD to control thermal comfort at different climates across the U.S. Furthermore, numerical studies in this field do not discuss the potential effect of extending temperature setpoints in terms of monetary cost savings of adding a PCD in the building environment. Therefore, this dissertation considers the effect of extending the temperature setpoints during the summer months for different cities in the U.S. and makes an overall energy analysis the impact of introducing PCD in the building environment. In addition, this dissertation considers the electricity cost at different cities to estimate the monetary savings of extending temperature setpoints in the summer while adding PCDs to the building. The results of this study

could offer an initial understanding of potential profitable markets for the PCD industry based on the location climate and electricity price.

This dissertation uses office and midrise apartment buildings to perform the numerical energy analysis of the tradeoffs between extending the temperature setpoints and introducing PCD devices for thermal comfort. Office buildings historically are internal-load dominated buildings. This suggest that the energy consumption of office buildings is driven primarily by internal equipment, occupancy level, and occupancy and lighting schedules [123]. The outdoor conditions dictate a small portion of the energy consumption in internal dominated buildings. On the other hand, mid-rise apartments are external-load dominated buildings. The energy consumption of external-dominated buildings is driven by the outdoor conditions and the type of HVAC system [123]. These two building types are great candidates for adopting PCD technology for potential energy savings by extending setpoints and higher thermal comfort by allowing occupants to control their microenvironment. Figure 3-1 shows the energy modeling process that this study proposes to produce an accurate and overall energy assessment at the building scale.

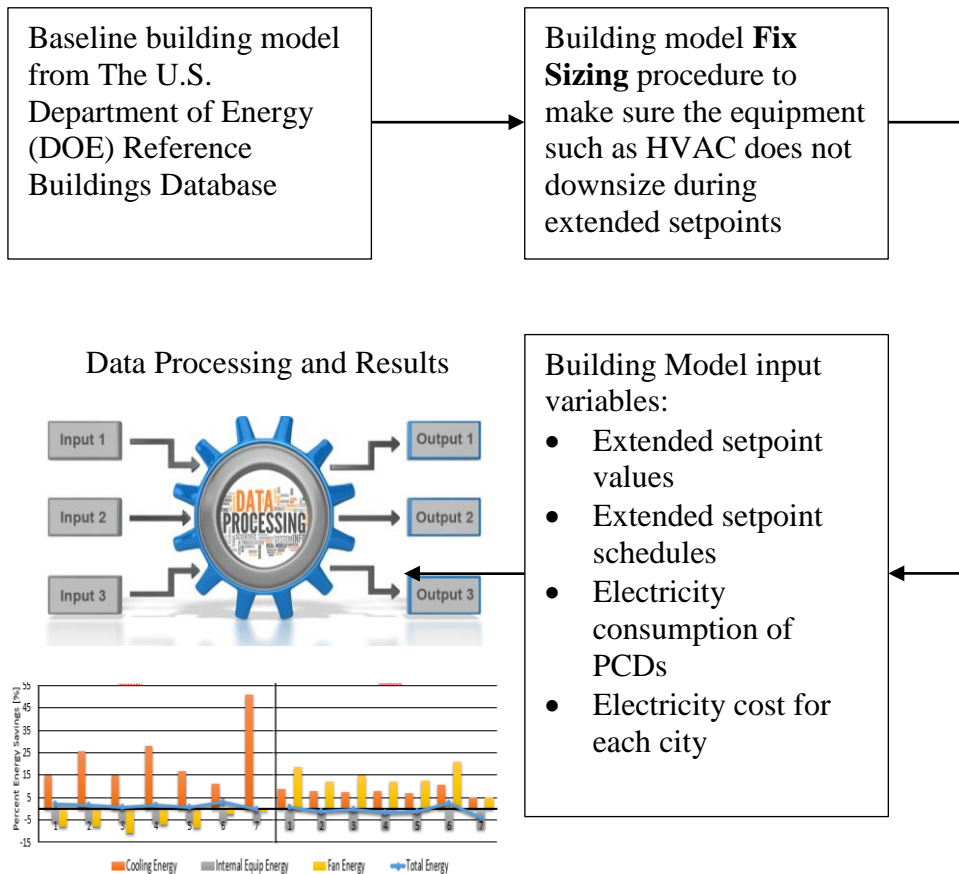


Figure 3- 1 Energy Modeling Process

At the occupant level this thesis evaluates the performance of the PCD as a function of heat removed from the human body and the cooling capacity of the PCD. Similarly, it uses the PMV method to estimate thermal comfort of the virtual model when using the PCD. This thesis uses a validated Computational Fluid Dynamic (CFD) model coupled with PMV thermoregulation model to calculate the heat removed from the human body and the thermal sensation of the virtual model. Figure 3-2 illustrates the iterative process of the coupling CFD and the PMV thermoregulation model. The coupled simulations process enables frequent updates to the temperature boundary condition at each surface mesh of the virtual human body model. These frequent updates allow the calculation of heat removed from the virtual model of human body. The cooling efficiency of the

PCD was evaluated based on Equation 3-1. This equation is the ratio between the total sensible heat loss of the human induced by PCD and the cooling capacity of the PCD. The total sensible heat loss induced by PCD is the difference between total sensible heat loss of human model when using PCD ( $Q_{sPCD}$ ) and the total sensible heat loss of human when not using PCD ( $Q_s$ ). This method to evaluate the performance of PCD allows a quantitative evaluation of PCD.

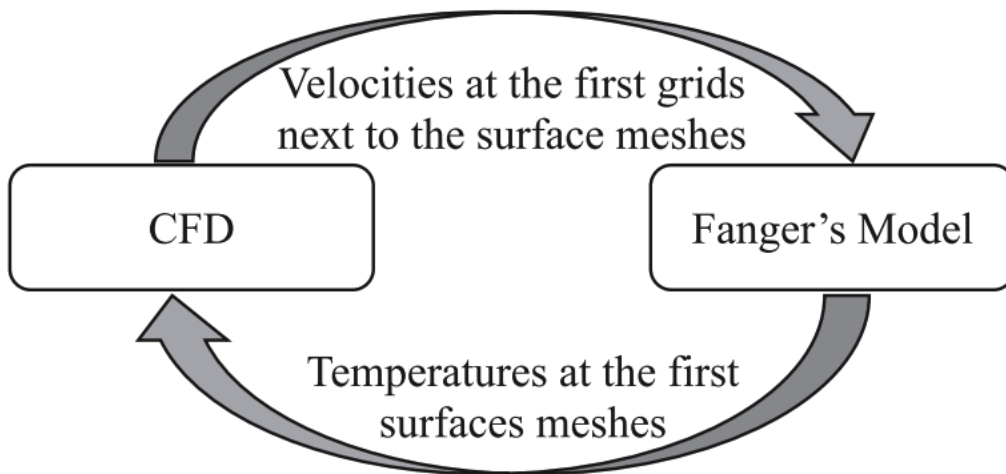


Figure 3- 2 CFD and PMV Iterative Process

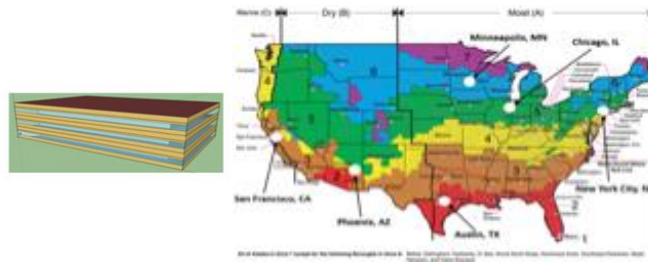
$$\text{Cooling Efficiency} = \frac{Q_{sPCD} - Q_s}{\text{PCD Cooling Capacity}} \quad (\text{Equation 3-1})$$

### 3.4 Tasks Overview for each Objective

This dissertation identifies critical tasks that ensure the accomplishment of each objective. Figure 3-3 shows a broad view of the objectives and tasks in this thesis. This dissertation evaluates the effect of using PCD at building level and at the occupant level and quantifies the tradeoffs between overall energy performance and thermal comfort, which are the main goals of PCDs. In addition, this dissertation explores the energy performance of buildings using PCD across the U.S. climate

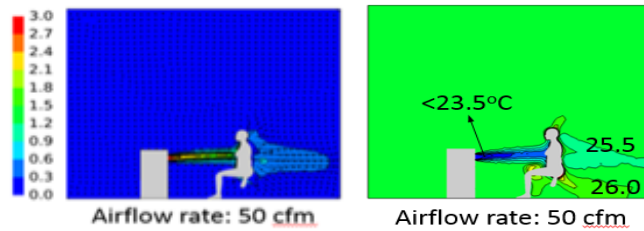
conditions and the electricity costs in order to have a costs analysis of PCD. The results of this study are part of the marketing approach for the RoCo project.

**Objective 1**  
Energy Savings at the building level



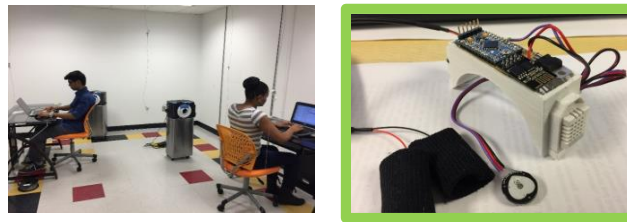
Evaluate the overall energy and monetary savings of PCD in office and midrise apartment buildings across the U.S.

**Objective 2**  
Quantify the tradeoff between energy savings and thermal comfort



Identify the cooling capacity and the temperature and airflow range of operation of PCD for thermal comfort

**Objective 3**  
Human subject experiments with PCD



Test the performance of PCD with human subjects and monitor their physiological response before, during, and after using PCD

**Objective 4**  
deploy personal physiological responses for a data-driven assessment of thermal comfort.



Process physiological data to quantify the effect of PCD on the human subject's thermal comfort

Figure 3- 3 Objectives and Main Task Overview

The objective 1 of this dissertation studies the effect of PCD in the energy consumption of office and mi-rise apartment building models for buildings constructed pre-1980 and post 2004. This dissertation explores the climate effect on the building energy consumption of building using PCD while extending their temperature setpoints from 24°C to 26.6°C during the peak hours of the day (13:00 to 17:00). In addition, this dissertation quantifies the monetary savings at building level by

estimating the price in electricity bill when not using and when using PCD. Table 3-3 details the identified tasks for the accomplishment of the first research objective.

Table 3- 3 Tasks Associated with Research Objective 1

Tasks associated with research objective 1	1-1	Create the building energy models for the proposed office and midrise apartments buildings
	1-2	Find TMY3 data for each city
	1-3	Collect electricity rates for each city
	1-3	Create baseline and PCD Building models for each building type
	1-3	Analyze the simulation results for each building type
	1-4	Identify potential market for PCDs.
	1-5	Explores the energy effect of PCD in small density occupant building such as warehouse building

The objective 2 of this dissertation focuses on the interaction of PCD and the human body. This research uses CFD to quantify the heat removal from the human body while using PCD and the thermal comfort, based on PMV thermoregulation model, produce by PCD. This part of the research couples CFD with the PMV thermoregulation model to continuously update the temperature boundary condition at the surface mesh of the human body model. Based on the heat flux removed from the human body and the calculated thermal comfort this dissertation proposes the cooling capacity for the PCD and the possible size for the discharge nozzle as well as the possible operating airflow rates to prevent risk of draft. Table 3-4 presents the tasks associated with the second research objective of this dissertation.



Table 3- 4 Tasks Associated with Research Objective 2

Tasks associated with research objective 2	2-1	Numerical analysis of the microenvironment created by PCD in cooling mode
	2-2	Numerical analysis of the microenvironment created by PCD in heating mode
	2-3	Numerical analysis of heat removal from the human body by PCD
	2-4	Numerical analysis of thermal comfort when using PCD
	2-5	Quantify the performance of PCD based on human model heat removal

Table 3-5 shows the tasks associated with the human subject experiments, which is objective 3. This research develops a data collection device monitor physiological variables during the PCD experiments. Current commercially available devices have limitation on physiological data access and have low sampling rates, which is key for the HRV. The data collection device is a bracelet type device based on commercially available heart rate, temperature, galvanic response sensor. The experimental protocol as well as all the instruments use in the experiments are approved by The University of Maryland Institution Review Board (IRB) protocol [655690-7]. The experiments test the ability of the PCD to maintain thermal comfort of human subjects at environmental temperature between  $27 \pm 1$  °C and  $29 \pm 1$  °C. Throughout each experiment this research monitors physiological variables such as skin temperature, heart rate, and conducts thermal comfort surveys to correlate physiological changes with thermal comfort and assess the ability of PCD to influence these physiological variables.

Table 3- 5 Tasks Associated with Research Objective 3

Tasks associated with research objective 3	3-1	Develop physiological data collection device
	3-2	Conduct 40 human subject experiments to test the performance of PCD
	3-4	Process experiment data for analysis

The last objective of this research uses the physiological data and the survey comfort data to find correlations associated with using PCD. Using this data, this dissertation evaluates the ability of PCD to influence human physiology. The research approach in this section is to apply machine learning, specifically, classifications algorithms. Table 3-6 shows the tasks to accomplish the research objective.

Table 3- 6 Tasks Associated with Research Objective 4

Tasks associated with research objective 4	4-1	Correlate thermal comfort and physiological variables
	4-2	Present a data-driven thermal comfort assessment when using personalized cooling device

### 3.5 Summary

This chapter evaluates the possible end-use energy savings associated with PCD in office and midrise apartment buildings. The investigation initially explores the potential energy savings by extending the temperature setpoint from 24 °C to 26.7 °C and by adding a PCDs to the overall energy consumption of the building. The second objective is to numerically investigate the tradeoffs between thermal comfort, using Fanger’s PMV and PPD approach, and the energy

associated with PCD. Furthermore, this dissertation conducts experimental analysis on the ability of PCD to regulate or maintain thermal comfort of human subjects under warm and hot indoor environmental temperatures, validate the numerical results and complement the overall research with actual human subject's inputs on their thermal comfort and thermal comfort. During the thermal comfort experiments the human subjects use a bracelet-type device that monitors their physiological parameters. This information enables this research to understand the human body responds to different thermal environments and the ability of PCD to influence physiological changes associated with thermal comfort. Furthermore, this dissertation develops a data-driven thermal comfort approach based on the subjective (surveys) and physiological data being monitored during the experiments.

## **Chapter 4**

### **Personalized Cooling as an Energy Efficiency Technology in Commercial Buildings**

This chapter shows the results of the building energy simulation study on the energy effect of PCD in commercial buildings such as office, and midrise apartments buildings constructed Pre-1980 and Post 2004. In addition, this chapter presents a discussion section on low occupancy-density building such warehouse and manufacturing buildings. Section 4.1 details the overall framework for the building energy simulations and PCD. Section 4.2 presents the background information for energy simulations and PCD. Section 4.3 shows parameters and details for the energy simulation models. Section 4.4 demonstrate the results of the energy analysis for office and midrise apartment buildings. Section 4.5 presents a discussion on buildings with low-occupancy density such as warehouse and manufacturing buildings. Section 4.6 shows a comprehensive cost analysis for the electricity savings for each city. Lastly, section 4.7 summarizes the results and the discussion of this research.

#### **4.1 Building Energy Simulations and PCD**

The first objective is to evaluate the potential energy savings by extending temperature setpoints while using PCD in commercial buildings at different representative climates in the U.S. The investigation of the effect of different climates will develop benchmarking criteria to evaluate the potential benefits of adding PCD as a building equipment device. This analysis aims to locate potential markets (cities) based on climate and electricity rates where PCD could provide energy and monetary savings. Additionally, this investigation will implement a second benchmarking criteria associated with building types such as office, and mid-rise apartments in terms of energy

response to the implementation of PCD. The goal of this benchmarking analysis is to observe the effect on PCD on different building types specifically in the energy consumption patterns.

#### 4.2 Building Energy Simulations Background Information

Building energy models account for a total heat balance on both internal and external building enclosure surfaces, heat transfer through a building enclosure, and heat sources /sinks such as internal loads generated by equipment, occupants and lighting. This modeling is governed by heat transfer equations for both the outside and inside surfaces of the building, as shown in Table 4-1, which are solved simultaneously. In order to determine an annual rate of energy consumption, EnergyPlus solves the governing equations iteratively with an hourly time step over the duration of a year. The internal boundary conditions used an indoor air temperature setpoint, and the external boundary conditions used hourly weather data for a Typical Meteorological Year [“NSRDB: 1991- 2005 Update: TMY3,” Wind Energy Resource Atlas of the United State. [Online]. Available: [https://rredc.nrel.gov/solar/old\\_data/nsrdb/1991-2005/tmy3/](https://rredc.nrel.gov/solar/old_data/nsrdb/1991-2005/tmy3/)]. Figure 4-1 and Figure 4-2 shows the external and internal wall heat balance use in EnergyPlus for each building geometry.

Table 4- 1 Outside and Inside Heat Balance Equations

Outside Surface Heat Balance	Inside Surface Heat Balance
$q''_{\alpha sol} + q''_{LWR} + q''_{conv} - q''_{ko} = 0$ <p>where:</p> <p><math>q''_{\alpha sol}</math> = Absorbed direct and diffuse solar (short wavelength) radiation heat flux.</p> <p><math>q''_{LWR}</math> = Net long wavelength (thermal) radiation flux exchange with the air and surroundings (including sky).</p> <p><math>q''_{conv}</math> = Convective flux exchange with outside air.</p>	$q''_{LWX} + q''_{SW} + q''_{LWS} + q''_{ki} + q''_{sol} + q''_{conv} = 0$ <p>where:</p> <p><math>q''_{LWX}</math> = Net longwave radiant exchange flux between zone surfaces.</p> <p><math>q''_{SW}</math> = Net short-wave radiation flux to surface from lights.</p> <p><math>q''_{LWS}</math> = Longwave radiation flux from equipment in zone.</p> <p><math>q''_{ki}</math> = Conduction flux through the wall.</p> <p><math>q''_{sol}</math> = Transmitted solar radiation flux absorbed at surface.</p>

$q''_{ko}$ = Conduction heat flux ( $q/A$ ) into the wall.	$q''_{conv}$ = Convective heat flux to zone air.*
--	---

\*Note: the  $q''_{conv}$  term uses a system of equations for transient convective heat transfer to the air volume in each building zone defined by bulk air properties and heat sources from internal loads, wall surfaces, and the air conditioning system.

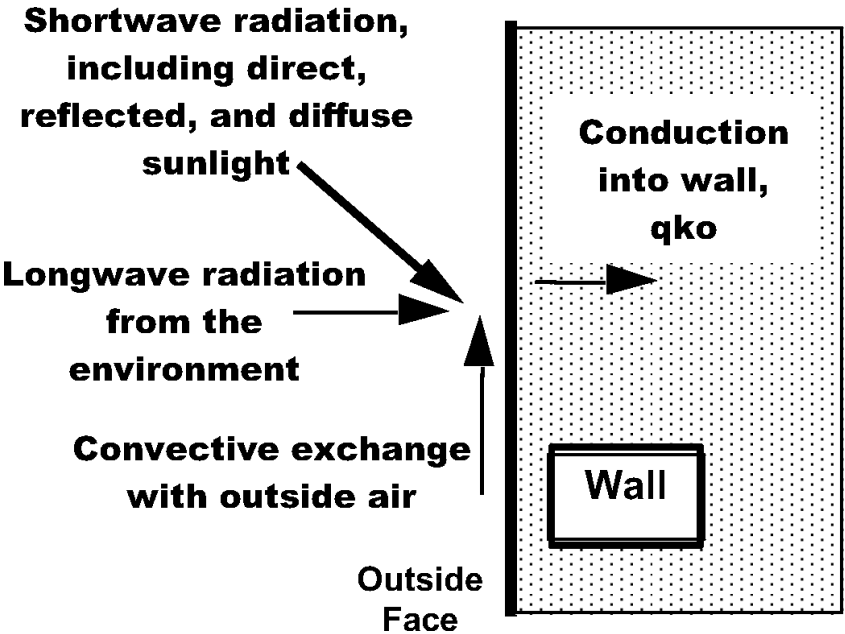


Figure 4- 1 External Wall Heat Balance

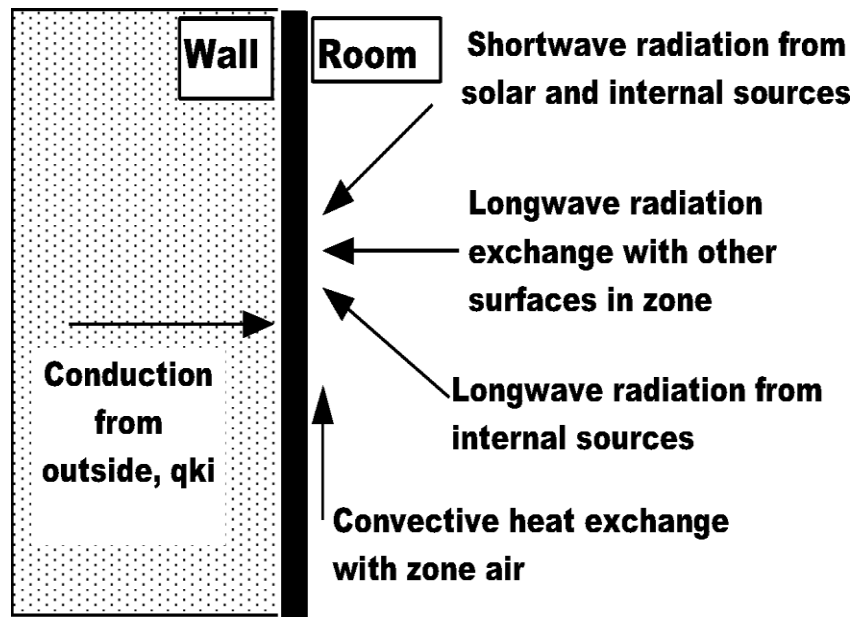
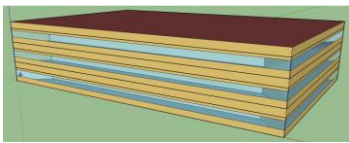
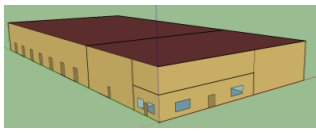


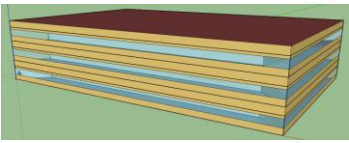
Figure 4- 2 Internal Wall Heat Balance

The building energy analysis in this investigation uses EnergyPlus V 7.0 as a computational tool to simulate three primary commercial building types and one residential building type. The building models are shown in Figure 4-3. This analysis explores the effect of climate in seven different cities across the U.S., as shown in Table 4-2. In addition, Table 4-2 shows the cooling degree days for each city. According to the Commercial Building Energy Consumption Survey (CBECS), office and warehouse buildings account for 18.8% and 14.8% of the total building spaces in the U.S., respectively, and represent more than 33% of the commercial building space in the country. While the office and manufacturing buildings require constant space conditioning, the warehouse buildings have limited access to air-conditioning in the occupied space. Similarly, the total floor area of residential buildings is consistently increasing from 87 million square feet in 1970 to 211 million in 2011 [124]. These different scenarios allow this investigation to perform a broad analysis on the overall energy effect of PCD in the building environment.

This investigation considers buildings constructed with codes and regulation Pre-1980 [125] and buildings constructed with codes and regulations Post 2004 [125] in the energy assessment. This approach allows to perform a broad investigation on the effect of different construction materials and different mechanical equipment associated to each building during extending temperature setpoints while using PCD technology.

### Commercial Building Models

<p><b>Office Building</b> Area = 4892 m<sup>2</sup> (50,000 ft<sup>2</sup>) People = 268</p> 	<p><b>Warehouse Building</b> Area = 4835 m<sup>2</sup> (52,043 ft<sup>2</sup>) People = 5</p> 
--	--

<p><b>Manufacturing Building</b> Area = 4892 m<sup>2</sup> (50,000 ft<sup>2</sup>) People = 102</p> 
---

### Residential Building Model


<p><b>Midrise Apt Building</b> Area = 2029.75 m<sup>2</sup> (21,848 ft<sup>2</sup>) People = 58</p> 
---



Table 4- 2 Selected Cities and Climates

	<b>City</b>	<b>Climate</b>
1	Austin, TX	Climate Zone 2A: Hot – Humid <b>CDD18°C= 441</b>
2	Chicago, IL	Climate Zone 5A: Cool– Humid <b>CDD18°C= 199</b>
3	Honolulu, HI	Climate Zone 1A: Very Hot/Humid <b>CDD18°C= 408</b>
4	Minneapolis, MN	Climate Zone 6A: Cold – Humid <b>CDD18°C= 185</b>
5	New York City, NY	Climate Zone 4A: Mixed – Humid <b>CDD18°C= 243</b>
6	Phoenix, AZ	Climate Zone 2B: Dry <b>CDD18°C= 744</b>
7	San Francisco, CA	Climate Zone 3C: Warm – Marine <b>CDD18°C= 30</b>

### **4.3 Building Energy Simulations Procedure**

The first task is to create a baseline model for each building type for each of the selected cities.

The energy simulation inputs for the baseline model are obtained from the DOE Reference

Building [125]. This investigation uses the results of the building energy simulations to summarize the potential savings of adopting a PCD technology across the U.S.. Additionally, the baseline model provides the necessary inputs for the HVAC system, such as system capacity, airflow rate, and ducts size, to be later used in the simulations models with extended setpoints temperatures and PCD. Fixing the HVAC system inputs in the models prevents EnergyPlus from downgrading/upgrading the building's HVAC system when extending temperatures or adding/removing energy loads with the PCD. Ensuring the same building characteristics and mechanical equipment between the baseline and subsequent energy models allows a clean comparison among all the energy models.

Following the baseline models, this study explores the potential energy savings associated to extending temperature setpoints in each building space. These results of this step target the potential energy savings associated with the central temperature setpoint in the building. Furthermore, the results of models with extended temperature setpoints help to understand, and later quantify the energy impact when introducing PCD to the building space. This means that, any distributed heat rejection systems such as PCDs, would need to account for energy penalties associated with internal equipment and heat rejection/absorption, which includes the amount of heat rejection into the space, amount of electricity consumption, and building's HVAC power to increase/decrease temperature setpoints.

This investigation uses the following operation characteristics for the PCD [126].

- Operates 4 hours
- Removes 165 W from the space
- Consumes 70 W electric load to recharge electric battery

- Electrical battery recharges from 22:00 to 4:00 (6 hours)
- Requires 10 W fan power to recharge Phase Change Material (PCM) or thermal battery
- PCM recharges from 22:00 to 2:00 (4 hours)
- Rejects PCM heat outside the building space
- Rejects PCM heat inside the building space

These parameters are obtained from the Prototype Y2V1 Ice RoCo , which is a PCD created by researchers in the University of Maryland under the Delta Program sponsored by DOE.

This investigation uses the energy balance equation (*Equation 4-1*) to include the effects of RoCo in the building energy balance. Using the operational schedules, thermal energy is subtracted from the space during the PCD's operational hours and energy is added to the building space during the PCD's non-operational hours. The adding and subtracting of energy follow the operation characteristics of the PCD and the occupancy schedule associated with each building type.

$$C_z \frac{dT_z}{dt} = \sum_{i=1}^{N_{sl}} \dot{Q}_i + \sum_{i=1}^{N_{surface}} h_i A_i (T_{si} - T_z) + \sum_{i=1}^{N_{zones}} \dot{m}_i C_p (T_{zi} - T_z) + \dot{m}_{inf} C_p (T_{\infty} - T_z) + \dot{Q}_{sys} \quad (\text{Equation 4-1})$$

where  $C_z \frac{dT_z}{dt}$  represents the energy store in the air as a function of time

$\sum_{i=1}^{N_{sl}} \dot{Q}_i$  is the sum of convective heat loads

$\sum_{i=1}^{N_{surface}} h_i A_i (T_{si} - T_z)$  is the convective heat transfer from the zone surfaces

$\sum_{i=1}^{N_{zones}} \dot{m}_i C_p (T_{zi} - T_z)$  is the heat transfer due to inner zone air mixing

$\dot{m}_{inf} C_p (T_{\infty} - T_z)$  is the heat transfer due to infiltration

$\dot{Q}_{sys}$  is the air system energy output

## 4.4 Building Energy Models and Results

### 4.4.1 Office building model

The baseline model for this building space assumes a gross floor area of 4,892 m<sup>2</sup>, and 268 occupants. The energy simulation estimates that the cooling season expands from May 15 to September 15 for the old and new office models. The main differences between the old and new office models are construction materials and HVAC systems. Specifically, the new office model has Variable Air Volume (VAV), while the old office model has a Constant Air Volume (CAV). This study considered three different temperature schedules, shown in Figure 4-4 a-c, for each model to compare the building energy consumption. The first temperature schedule is the baseline, where the room temperature is 24°C from 6:00 to 22:00 and 26.7 °C from 22:00 to 6:00 of the following day.

The second temperature schedule (MAX<sub>80</sub>) follows the extended setpoint temperature required by the DOE - DELTA program, where the room temperature is 26.7°C (Max<sub>80</sub>) throughout the day. The third temperature schedule is a combination of the baseline and Max<sub>80</sub> schedules, where the temperature setpoint from 6:00 to 13:00 is 24°C and 26.7 °C from 13:00 to 6:00 of the following day. This study assumes that PCD operates between 13:00 to 17:00 hours every day to provide cooling during the extended setpoint. According to preliminary results, increasing the day-time (6:00 to 22:00) temperature further than 26.7°C increases the fan energy consumption; in addition, based on experience, building managers would not operate buildings at temperatures higher than 26.7°C to avoid occupant discomfort. The building's fan increases the energy consumption in order to satisfy the temperature changes in the space.

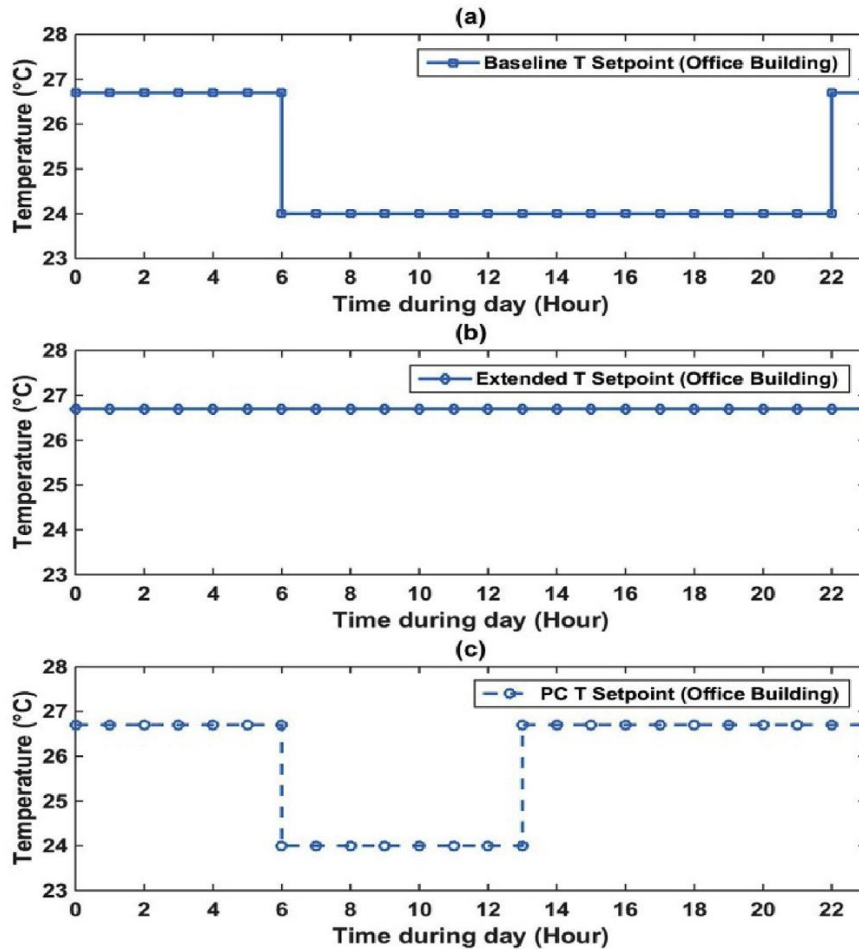


Figure 4- 4 Temperature Schedules for Office Buildings

#### 4.4.2 Office Model Results

The simulation results demonstrate that by extending the temperature setpoint to 26.6°C the energy required to cool the building approximately reduces 20% to 38% for old office models and 7% to 11% for new office models, as shown in Figure 4-5. San Francisco and Chicago are associated to low cooling degree-days where cooling is a minor portion of the total energy of the building. Therefore, by extending the temperature setpoint to 26.6°C in old offices, significantly reduces cooling energy by 38% for Chicago and 64% for San Francisco, but it does not impact the building's total energy consumption. The results indicate an increase in the fan energy

consumption in the old offices, which limits the total energy savings to 4% to 5% percent since fan energy represents approximately 17% of the total energy in the building.

The energy increase is a characteristic of constant volume systems where the fan operates for longer periods to benefit from free cooling and maintain the desired temperature setpoint of 26.7°C. In contrast, the results for new offices buildings indicate potential savings in the fan energy ranging from 7% to 32%; however, the fan energy is only 3% of the total energy in the building, which has a negligible impact on the overall energy consumption of the building. The simulation results indicate that the potential savings for cooling energy using the extended setpoint temperature of 26.7°C are approximately 10%, which represent depending on the city, approximately 1% to 3% of the total energy in the building. For both models, the internal equipment is the same since no additional equipment have been added to the space. An important difference between the old and new building models is the internal equipment energy, which represents 22% and 38%, respectively, of the total energy in the buildings.

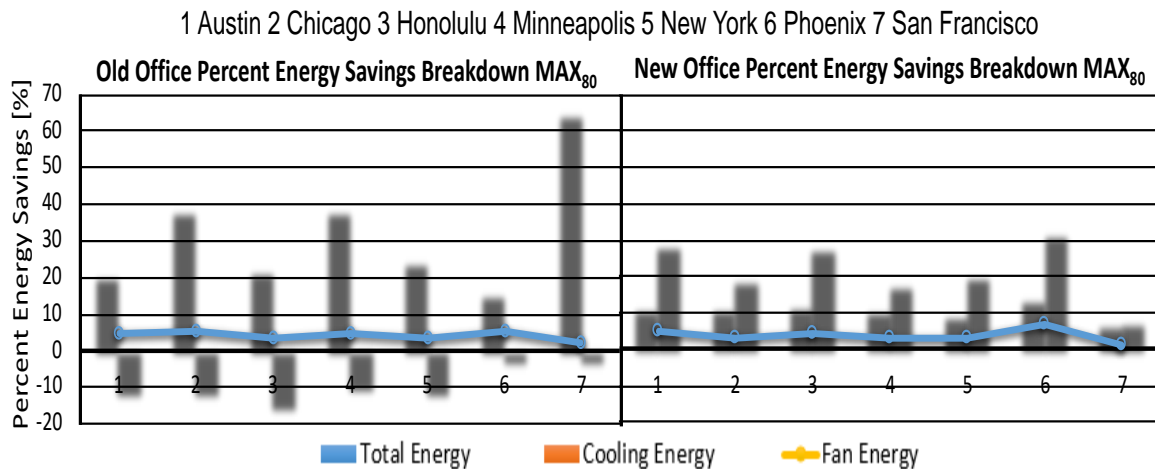


Figure 4- 5 Max80 Energy Savings for Office Buildings

Introducing PCD to the building environment increases the internal equipment energy by 9%. However, operating PCD in old offices enables savings in cooling energy that range from 11%

(Phoenix) to 51 % (San Francisco), as shown in Figure 4-6. However, as the previous case the fan energy in old offices indicate an increase of approximately 8%, which combined with the internal equipment energy limit the total energy savings to 2%, as presented in Figure 4-6. The results for old office buildings show that on average 20% of cooling energy savings depending on the city. The results for the new office models show cooling energy savings range from 11% (Phoenix) to 5% (San Francisco). In addition, the results indicate potential savings for the fan energy, but as explained in the previous section, it does not contribute to the total energy of the building. For this building model the total energy does not change compare to the baseline model since the increase in interior equipment counterbalance the savings in cooling energy. In addition, these results assume that the PCD does not have to reject heat or that the heat is rejected outdoors, which could bring an extra penalty for moving the PCD outdoor.

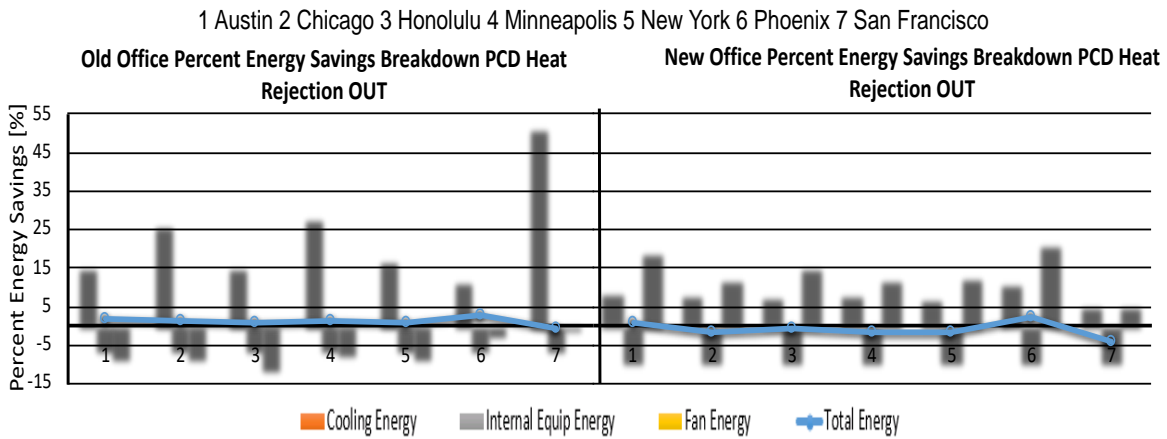


Figure 4- 6 Extended Temp PCD Energy Savings Office Buildings

To demonstrate a more realistic effect of adding a PCD into the building environment, this investigation conducts energy simulations with PCD rejecting the absorbed heat inside the building. This research is interest in effect of absorbing and rejecting heat on each end-use energy component of the building. Figure 4-7 shows data comparing the cooling energy and fan energy

for the model cases when PCD rejects heat inside the building space and when PCD rejects heat outside the building space (ideally). The results indicate that the cooling energy savings reduce approximately 3 %, when rejecting heat inside for old and new buildings. Likewise, in the old buildings, the fan energy increases 7 % since it needs to remove more heat from the space during PCD’s heat rejection process. The fan energy for new office buildings is a small part of the total energy; therefore, its change is negligible. The cooling energy for the city of San Francisco stays the same for both heat rejection processes. The overall energy savings in the building reduces approximately 2% when heat is rejected inside.

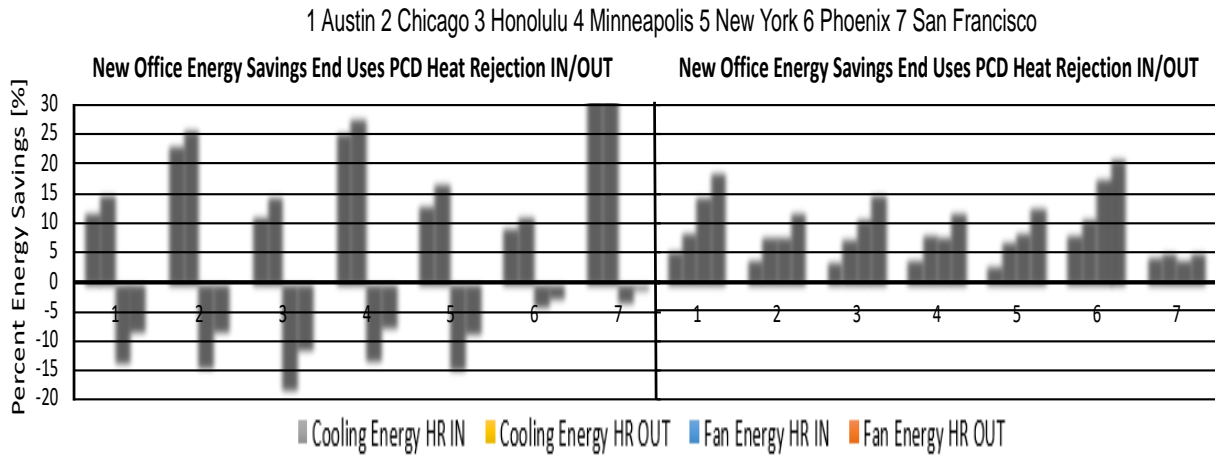


Figure 4- 7 PCD Heat rejection In/Out Comparison Office Buildings

The cost analysis of office buildings reveals higher potential cash savings in the old building compared to the new buildings. Figure 4-8 shows the breakdown cost savings for each city and each case. The city of Phoenix has the major savings associated to MAX<sub>80</sub>, PCD (heat rejection outside), PCD (heat rejection inside), which escalate up to \$3,200. Cities such as Chicago, Honolulu, and San Francisco have limit cash savings potential due to the combination of low-price ratio and low cooling degree days. The cash savings for new office buildings are lower than the old office due to the high internal energy, which offsets the cash savings associated to cooling



energy. By rejecting heat inside, the cash savings are limited due to a slight increase in cooling energy added by this process.

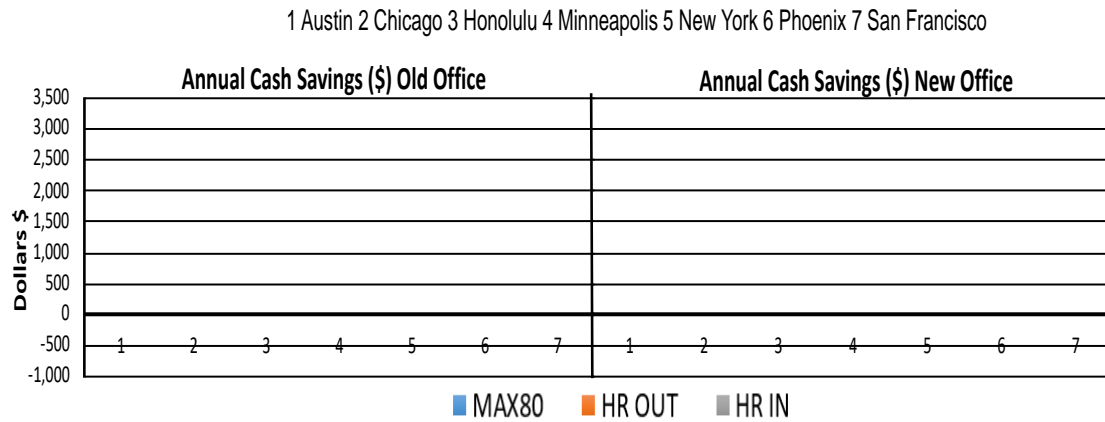


Figure 4- 8 Office Buildings Cash Savings Due to PCD

#### 4.4.3 Mid-rise Apartment building model

The baseline model for the midrise apartment building has two main space types, which include an apartment space type and an office space type. These two spaces have a gross floor area equal to 2030 m<sup>2</sup> and 88.25 m<sup>2</sup>, respectively. According to DOE reference building [1], the total number of people for the apartment space type is 58 people and for the office space type is 2 people. Similar to the office building model, this study compares the energy performance of midrise apartment based on three temperature setpoint schedules Figure 4-9 d-f. The baseline temperature schedule sets the temperature in the apartment space to 24°C throughout the day. The office space follows the same temperature schedule as the office building models, presented in Figure 4-4.

The second temperature schedule (MAX<sub>80</sub>) drives the apartment temperature to 26.7°C throughout the day, which is in accordance with the DOE - DELTA project requirements. The third temperature schedule assumes that PCD operates from 13:00 to 16:00 in the apartment environment and PCD is available for 50% of the total number of occupants, where the temperature setpoint is 25°C from 6:00 to 16:00 and 24°C for the rest of the hours in the day. Extending the

temperature setpoint by 1 degree Celsius during the day targets potential energy savings while providing a reasonable thermal environment for possible occupancy during those hours. This study assumes that between 6:00 to 16:00 the occupancy level in the space is limited.

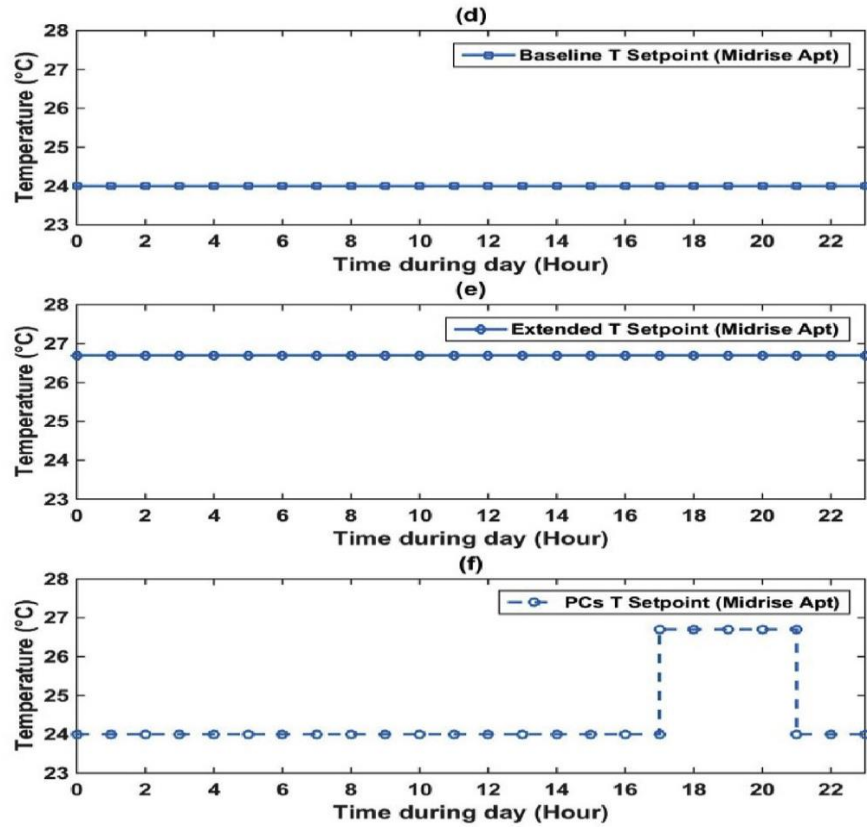


Figure 4- 9 Temperature Schedules for Office Buildings

#### 4.4.4 Mid-rise Apartment Model Results

The mid-rise apartment model energy simulation results demonstrate potential savings in cooling energy, fan energy, and total energy, when the temperature setpoint is extended from 24°C to 26.7°C for old and new mid-rise apartment models, as shown in Figure 4-10. The cooling energy savings range from 26% to 85% for old building models and 6% to 15% for new building models. The fan energy savings range from 25% to 50% for old and new midrise apartment models. The

potential reduction in cooling and fan energy allows savings in total energy that range from 10% to 20% depending on the city.

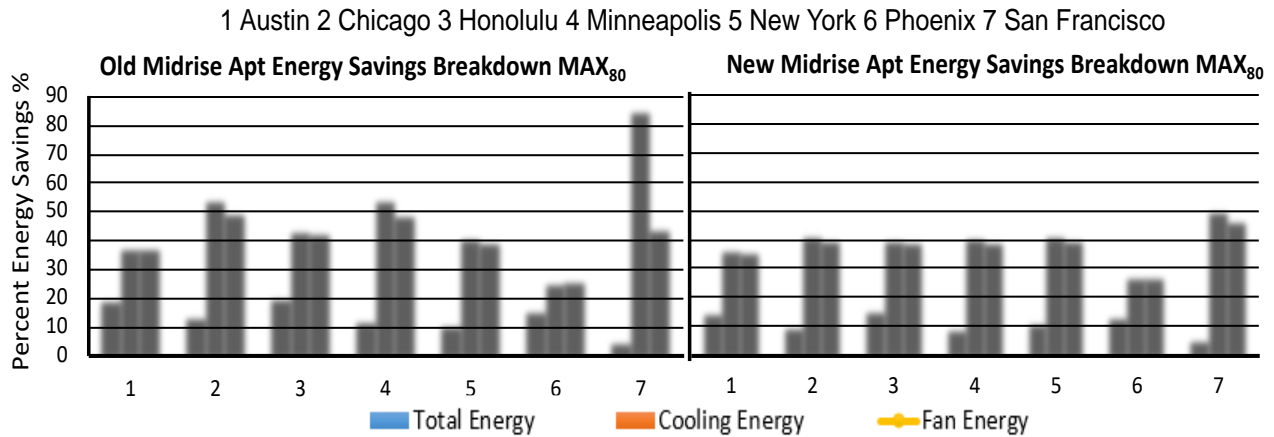


Figure 4- 10 Max80 Energy Savings for Midrise Apartment Buildings

Figure 4-11 shows the percent energy difference between the baseline model and the model that includes a PCD. The results indicate that the potential savings for cooling and fan energy escalate up to 25% and 21%, for the old and new building models, respectively. Introducing a PCD to the building environment increases the internal equipment energy by 5%, when compared to the baseline model. The internal equipment energy represents approximately 25% of the total energy in the building while cooling energy and fan energy represent approximately 30% and 8%, respectively. Consequently, the 5% increase in internal equipment energy counterbalances the cooling energy savings, which at the end has a negative effect in the total energy savings. In addition, this energy model assumes that the PCD device does not reject the absorbed heat to the indoor building space. Lastly as expected, the city of San Francisco is the outlier in the cooling energy savings due to its low cooling degree-days.

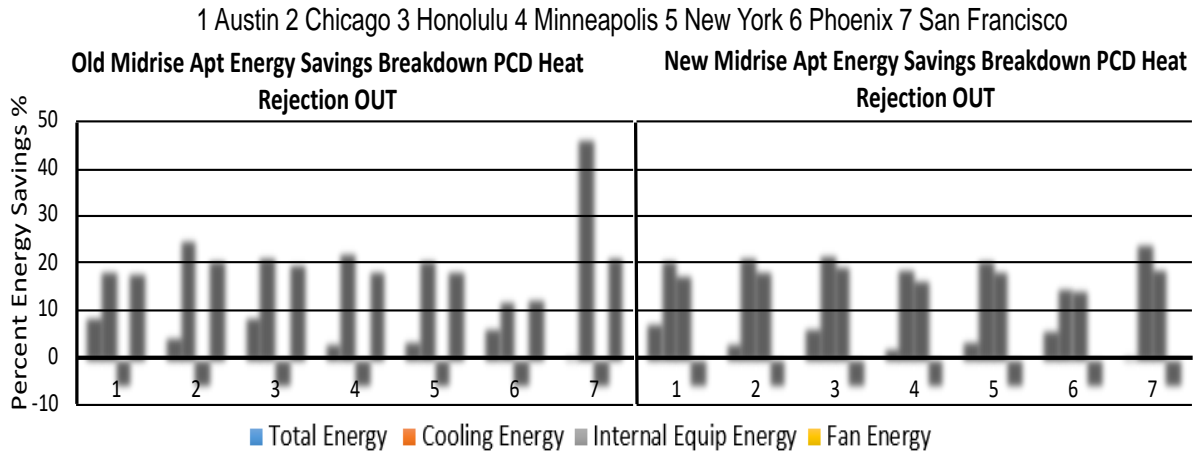


Figure 4- 11 Extended Temp PCD Energy Savings Midrise Apartment Buildings

Figure 4-12 shows a comparison of cooling and fan energy for models where the PCD rejects heat inside the building space and when PCD rejects heat outside the building space. The results indicate that the cooling energy savings reduce approximately 3%, when rejecting heat inside for old and new buildings. The savings reduction in the fan energy for this building type is a small part of the total energy; therefore, its change does not affect the overall energy savings of the building. The overall energy savings does not change whether heat is rejected inside or outside of this building type.

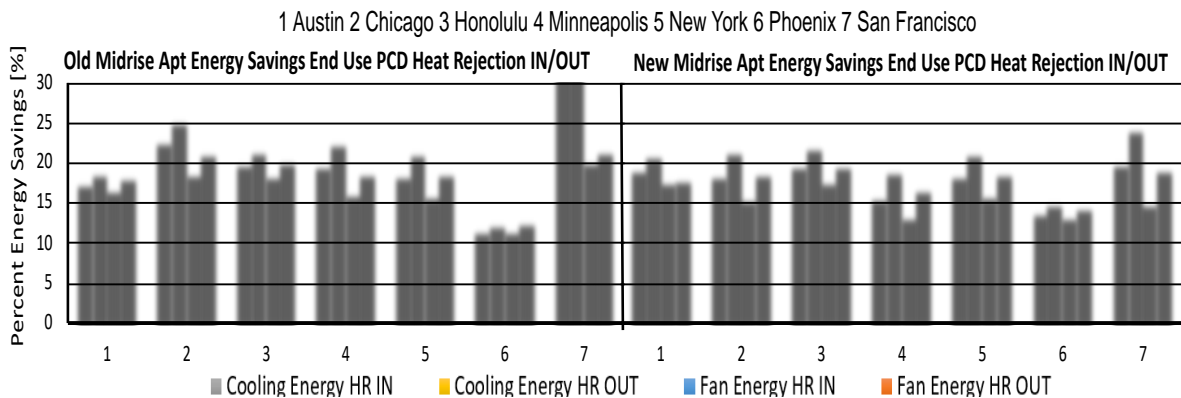


Figure 4- 12 PCD Heat Rejection In/Out Comparison Midrise Apartment Buildings

Figure 4-13 shows the breakdown of cash savings for midrise apartment buildings. The cash savings potential in this building type range from \$1,000 (Minneapolis) to approximately \$7,500 (Honolulu) in the MAX<sub>80</sub>. As expected, Chicago, and San Francisco have low cash savings due to the low-price ratio and low cooling degree-days. This building type has the highest cash savings among all the studied building types. These high savings are a result of the significant cooling energy savings. Figure 4-13 also shows that the heat rejection process, inside or outside, has a negligible effect in the cost savings, which suggest that this building type has important profit potential as a market place for PCD technology.

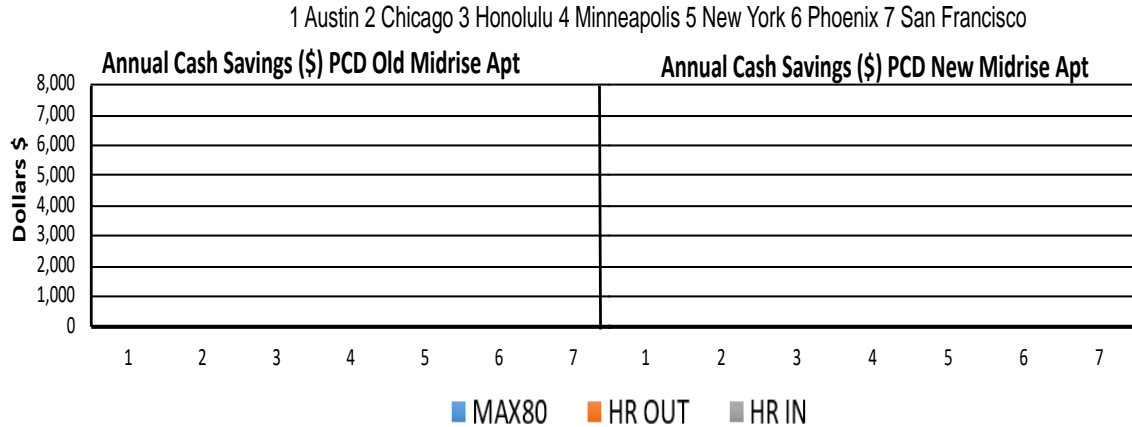


Figure 4- 13 11Mid-rise Apartment Buildings Cash Savings Due to PCD

#### 4.5 Discussion on Manufacturing and Warehouse Buildings

The main differences among the building types in this study are the number of people and the energy loads associated to each of the buildings. The results for the other two building type, manufacturing and warehouse, show a similar response as the office building when expanding the temperature from 24°C to 26°C and introducing PCD to the building environment. As described in the office building results, the cooling energy decreases when extending temperature setpoints with an energy penalty associated to the HVAC fan in the old building models. Additionally,

adopting the PCD in the environment slightly increases the internal energy for both building type models. While increasing temperature setpoints during the hot season lead to cooling savings, the total energy savings in the both building types are approximately less than 2 %. Likewise, the maximum costs savings associated to the manufacturing and warehouse are \$1,600 and \$250, respectively. The large difference between the costs savings lays in the number of people associated to each building. The analysis suggests that the energy and costs savings in the manufacturing and warehouse buildings are small compare to the office case. However, improving thermal comfort is an important benefit that brings value to PCD technology.

#### **4.6 Cost Savings Analysis**

An important aspect of adopting PCD technology in the building environment is the potential cost savings due to the peak shifting. The integration of PCD could save HVAC energy consumption during the day when the electricity cost is at a peak rate. Many cities offer different programs that commercial buildings can enroll to save energy and money. The most common program is the Time of the Use program that entails off-Peak, mid-Peak, and Peak hours with associated electricity rates. The most expensive time frame is the peak hours, followed by the mid-Peak, and lastly the off-Peak hours. Table 4-3 and Table 4-4 show the electricity rates for the commercial buildings and the respective time schedule. Commonly, during the weekends and holidays, the electricity rate falls into the off-peak price. For the case of Chicago, the only information publicly available is the flat rate for both commercial and residential buildings. Therefore, the models for the city of Chicago assume a constant electricity rate.

Table 4- 3 Commercial Buildings Electricity Rate in cents/kWh

City	Off-Peak	Mid-Peak	On-Peak
<b>Austin, TX</b>	0.067	3.91	6.54
<b>Chicago, IL</b>	6.24	N/A	6.24
<b>Honolulu, HI</b>	16	16.9	16.9
<b>Minneapolis, MN</b>	3.02	N/A	15.13
<b>New York City, NY</b>	1.34	N/A	18.99
<b>Phoenix, AZ *</b>	5.48 / 5.15	10.5 / 10.7	15.41 / 16.48
<b>San Francisco, CA</b>	20.7	23.4	25.8

\*Phoenix summer/Phoenix Summer Peak

Table 4- 4 Time of Use Program for Commercial Buildings

City	Off-Peak Hours	Mid-Peak Hours	On-Peak Hours
<b>Austin, TX</b>	10:00 pm-6:00 am	6:00 am-2:00 pm 8:00 pm-10:00 pm 6:00 am-10:00 pm	2:00 pm- 8:00 pm
<b>Minnesota, MN</b>	9:00 pm-9:00 am	NA	9:00 am- 9:00 pm
<b>Honolulu, HI</b>	9:00 pm-7:00 am	7:00 am-5:00 pm	5:00 pm- 9:00 pm
<b>New York City, NY</b>	12:00 am-8:00 am	NA	8:00 am-12:00 am
<b>Chicago, IL</b>	NA	NA	NA
<b>San Francisco, CA</b>	9:30 pm-8:30 am	8:30 am-12:00 pm 6:00 pm- 9:30 pm	12:00 pm-6:00 pm
<b>Phoenix, AR</b>	7:00 pm-12:00 pm	NA	12:00pm-7:00 pm

This investigation initially found that the potential costs savings associated to extended setpoints and the adoption of PCD are a combination of electricity prices and cooling degree-days CDD18°C. This study normalizes the electricity price of each city as a ratio between the off-peak to the on-peak price using *Equation 4-2*. This equation is the ratio between on-peak electricity price and off-peak electricity price, where unity is subtracted to sort each city in an ascending order, as shown in Figure 4-14. This normalization reveals potential profitable markets for PCD technology. This study proposes that cities with electricity price ratio (*Equation 4-2*)  $\geq 0.3$  and CDD18°C higher than 400 could be the highest profitable markets for PCD. Cities such as Austin, Minneapolis, New York, and Phoenix have high cooling degree days and high electricity price ratio between off-peak and on-peak, which makes them a suitable market for systems such the one being used in this investigation. On the other hand, cities such as Chicago and San Francisco have low cooling requirements and low-price ratio, which prevents potential cash savings associated to extending temperatures setpoints and PCDs. Similarly, the city of Honolulu may not be a potential market for PCD technology due to the small price ratio for the electricity rate. Nevertheless, due to its hot and humid climate, PCD could have a positive impact in terms of comfort.

$$Price\ Ratio\ deff = 1 - \frac{off\ peak\ price}{on\ peak\ price}$$



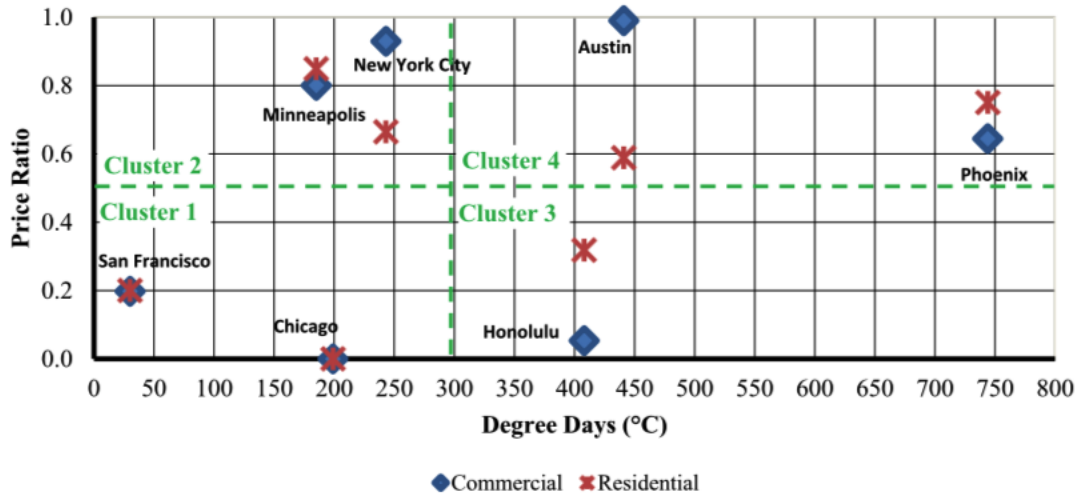


Figure 4- 14 Cooling Degree Days vs Price Ratio

#### 4.7 Summary

This chapter presents the energy analysis of deploying a PCD based on a phase-change material on pre-1980 (old) and post-2004 (new) buildings. This study focuses on two building types: office building and mid-rise apartment building. Additionally, this study includes a discussion section on the effect of PCD on low occupancy density buildings such as warehouse and manufacturing buildings. The effect of PCD in each building model is characterized by the difference in end-use energy between baseline models and models that have PCD included. In addition, this study calculates the electricity cost savings associated with models that include PCDs.

The results of study show that increasing the temperature setpoint by 2.6°C during the peak hours of the day in the summer season could lead to energy savings between 10% to 70%, depending on the city. In addition, the results show costs savings associated with electricity. Midrise apartment buildings present the highest cost savings annually with \$130 per person for the city of Honolulu. These cost savings are the consequence of increasing the temperature setpoints during the electricity peak hours of the day when the electricity cost is highest while using PCDs to address thermal comfort of occupants. These cost savings are cities' dependent. This study proposes a

method to identified potential cities that could benefit from adopting PCD technology based on cooling degree days and electricity rate. Cities with cooling degree days higher than 300 and the ratio of peak versus off-peak electricity price of 0.5 or higher, have the potential to show energy and cost savings. Overall the adoption of PCD has the potential decrease the cooling energy in the building while reducing expenses on electricity bill.

## **Chapter 5**

### **Numerical Analysis of Thermal Comfort with PCD**

This chapter focuses on the numerical analysis on the interaction between the human body and PCD. Section 5.1 shows a preliminary analysis of centerline velocities as a function of nozzle diameter. Section 5.2 describes the CFD models and background information on the approach taken in this dissertation. Section 5.3 presents the results of the numerical analysis of the interaction between PCD and the human model in cooling mode. Section 5.4 presents the results of the numerical analysis of the interaction between PCD and the human model in heating mode. Lastly, section 5.5 has a summary of the main findings of this section.

#### **5.1 Theoretical Analysis of Air-jet Centerline Velocity and Temperature as a Function of Nozzle Diameter**

##### **5.1.1 Selection of PCD Air-Nozzle**

The objective of this task is to select an adequate discharge air nozzle for the PCD that fulfils the project parameters specified by the sponsor agency (DOE). The criteria for the selection of air nozzles includes momentum loss, jet throw distances, and discharge velocities and temperature.

This dissertation implements appropriate jet formulae to model the behavior of air jet. In addition, the selection of nozzles considers weight, and pressure drops as part of the analysis to select the appropriate nozzle for the PCD. The results of this section are implemented in the design process of the RoCo device and in the numerical analysis in the flowing section.

Based on the nozzle selection criteria, this study selected a ball jet type nozzle. This nozzle is currently available in the market and among its design characteristics it has small pressure drop compared to different types of air nozzles. The low-pressure drop allows the PCD fan to operate with relatively low power requirements. Table 5-1 shows the estimated pressure drops for different exit velocities representing different airflow rates ranging between 50 cfm to 100 cfm (24 L/s to 47 L/s). The theoretical analysis, in this section, targets three different air nozzles with outlet diameters ranging from 80 mm to 128 mm. The dimensions of the selected nozzles vary according to the size of the inlet diameter (D4) and the outlet diameter (D2) shown in Figure 5-1.

Table 5- 1 Pressure drops for nozzles of different diameters and flowrates

	Initial Velocities [m/s]			
	3	5	7	10
Pressure Drop [Pa]				
Nozzle Diameters [m]	4.9	17	30	64
0.08				
0.09				
0.105				
0.115				
0.128				

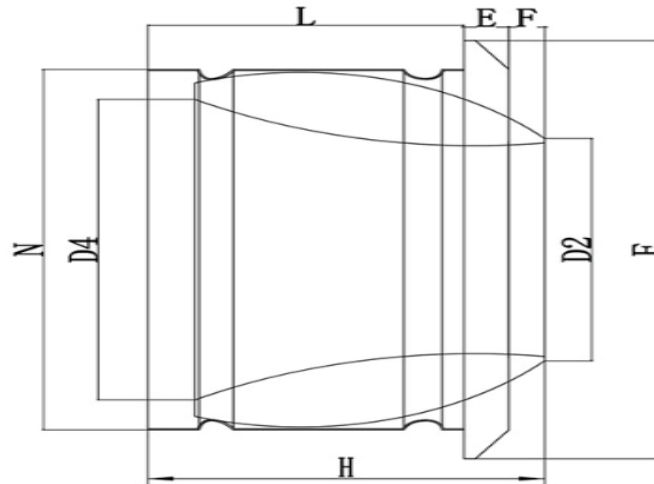


Figure 5- 1 Ball jet nozzle dimensions (Vair-Tech manufacturer catalogue)

### 5.1.2 Analysis of Discharge and Centerline Velocity-Temperature

This dissertation analyses the air discharge velocities as a function of PCD's nozzle diameter. The discharge velocities are calculated using the conservation of mass as follows:

$$V = \frac{Q}{A_o} \quad (\text{Equation 5-1})$$

where Q is the flowrate,  $A_o$  is the nozzle area for the jet discharge diameter (D2), and V is the discharge velocity. The discharge velocities are based on the PCD specification parameters that allow airflow rates ranging between 50 cfm to 100 cfm (23.6 L/s to 47 L/s). As it is expected bigger flowrates with smaller areas have higher pressure drops, which increase the discharge velocities. Figure 5-2 shows the expected discharge velocities as a function of the outlet diameter.

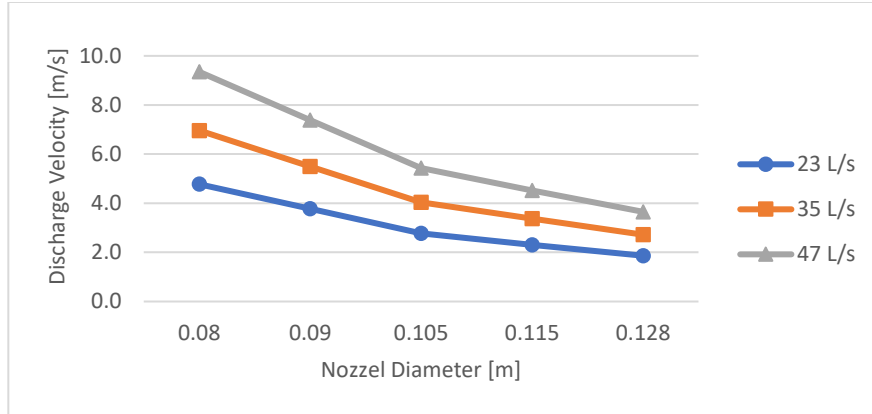


Figure 5- 2 Jet discharge velocities vs nozzle diameters

The jet-throw is the distance from the center of the nozzle to a point where the air-stream velocity is reduced to a user’s specified value [127]. The jet-throw curves in Figure 5-3 show how the center-line velocity changes as a function of the distance for an air nozzle diameter equal to 105 mm. According to the literature, jet-throw can be estimated using Equation 5-2 when the jet is in the fully established turbulent zone (main zone):

$$V_x = V_o * K * \frac{\sqrt{A_o}}{x} \quad (\text{Equation 5-2})$$

where  $V_x$  is the center-line velocity in m/s at a certain distance,  $V_o$  is the outlet velocity in m/s,  $K$  is the constant of proportionality, which for free-jets has a value of 6 according to the literature.  $A_o$  is the area in  $m^2$  around the initial diameter, and  $x$  is the distance of interest in m. For a diameter of 105 mm (0.34 in) at a terminal velocity of 1.5 m/s (295 ft/min) and flow rate of 23 L/s (50 cfm) the jet throw is approximately 1 m (3.2 ft).

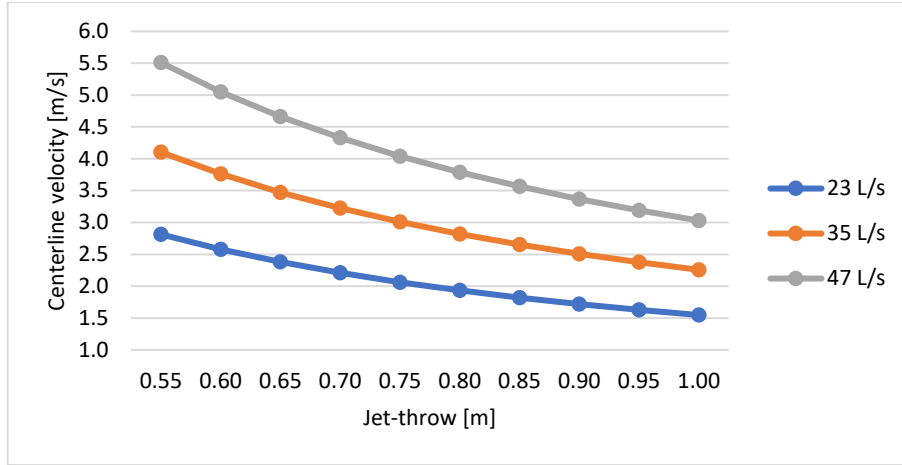


Figure 5- 3 Jet throw vs centerline velocity for the outlet diameter of 0.105 m

This dissertation follows the expected distance between the occupant and PPCD is 1 m (3.2 ft), which DOE specified in the project requirements. Therefore, initial calculation of center-line velocity and center-line temperature predict the velocity and temperature at the given distance as function of nozzle diameters. The center-line temperature is calculated using Equation 5-3, where  $\Delta t_x$  is the difference between the local air-stream temperature and the room temperature,  $\Delta t_o$  is the difference between the outlet air temperature and the room temperature. Notice that the center-line velocity and temperature equations, best model the jet behavior when it is in the fully established turbulent zone. Figure 5-4 and 5-5 show the calculated center-line velocity and temperature, respectively, as a function of the outlet diameter at the target distance of 1 m. Figure 5-5 (a) shows the cooling mode center-line air temperatures, and Figure 5-5 (b) shows the heating mode center-line air temperatures.

$$\Delta t_x = 0.8 \Delta t_o * \frac{V_x}{V_o} \quad (\text{Equation 5-2})$$

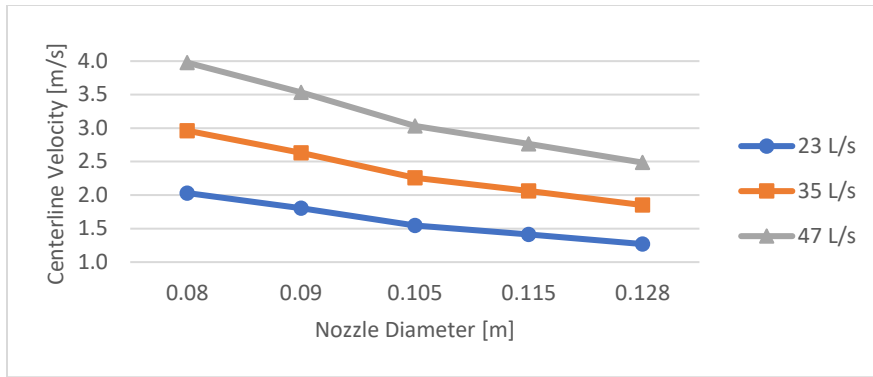
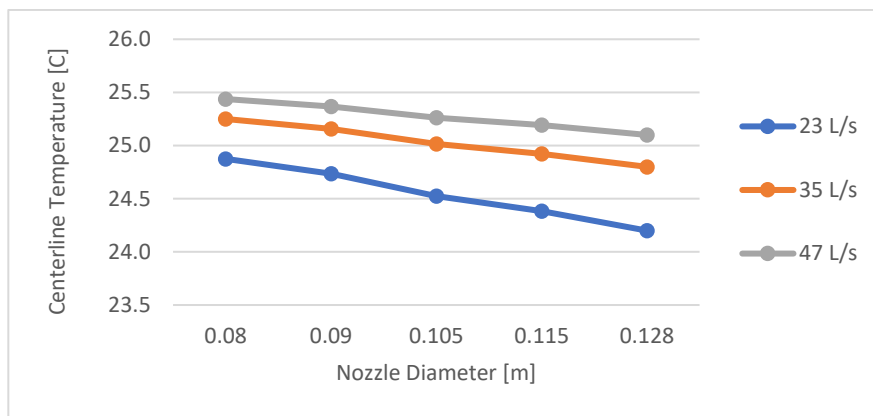
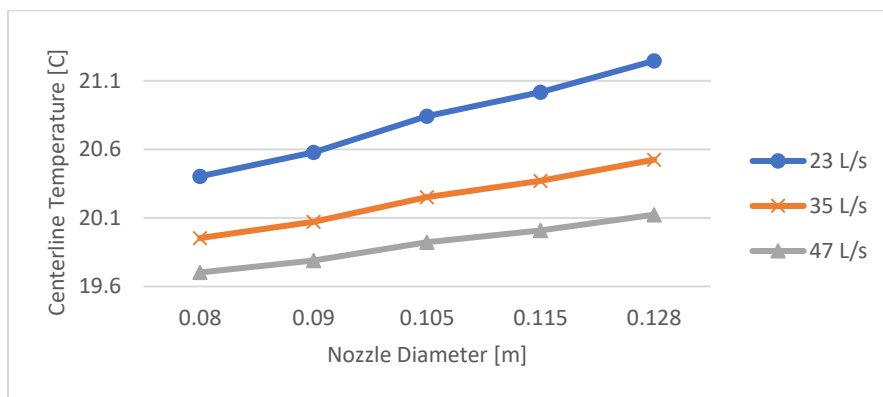


Figure 5- 4 Center line velocity vs nozzle diameter at 1 m distance



(a)



(b)

Figure 5- 5 Center-line temperature vs nozzle diameter at 1 m distance for (a) the cooling mode, and (b) the heating mode

The outlet diameter needs to have the sufficient area to allow airflow rates that have enough momentum to reach the human subject and remove heat from the human body. According to the calculated velocities, an air nozzle with diameter less than 0.105 mm (0.34 in), and a flow rate of 23 L/s (50 cfm) seem to meet the requirements for both the cooling and heating regimes. Numerical simulations with CFD and physical testing are the next step to test the selected nozzle diameters and the calculated air-jet center-line velocity and temperature. In addition, CFD provides perception of thermal comfort expressed by the PMV and PPD thermoregulation model, and the amount of heat removed from the human model. Overall, the selected nozzle type has promising characteristics to be further investigated with CFD and physical testing.

## **5.2 Thermal Comfort Numerical Simulations Models**

While the first research objective explores potential energy savings associated to extended temperature setpoints and PCD, the second objective aims to quantify the tradeoffs between energy savings and thermal comfort. This section numerically explores, using ANSYS Fluent CFD software, the thermal comfort of human subjects exposed to increased and decreased indoor temperature setpoints while using PCD for cooling and heating. Additionally, the second task in this section is to explore the influence in thermal comfort of different PCD's air nozzle diameters and airflow rates. This investigation explores thermal comfort with two common postures of occupants in office buildings, seated and standing, as shown in Figure 5-6. The model for the PCD consists of a cylinder with height equal to 0.9 m, a base diameter equal to 40 cm, and three different nozzle diameters 0.08 m, 0.10 m, and 0.13 m, as presented in Figure 5-7. The models of human body and PCD are located at the center of a virtual room at a 1 m distance from each other, as shown in Figure 5-8. The virtual model of the space consists of a room with dimensions equal to  $x = 4.5\text{m}$ ,  $y = 4\text{m}$  and  $z = 3.5\text{m}$  and a mechanical ventilation that provides approximately 3 air



changes per hour (ACH). The indoor temperatures selected for this investigation are between 24 °C to 30 °C in the cooling mode and 19 °C to 21 °C in the heating mode. This investigation explores the effect of three nozzle diameters that supply five different airflow rates, as shown in Table 5-2. The PCD being modeled in this study has a 100 Watts cooling capacity; consequently, the air temperature supply increases as the airflow rate increases. Furthermore, this study aims the air-jet towards the chest of the human model. Therefore, the air-jet orientation had to be upward at different angles, especially for the standing model. Table 5-2 shows the discharge air velocity, orientation angles, and air temperature for each airflow rate.



Figure 5- 6 Human Body Model Simulated Occupant Postures

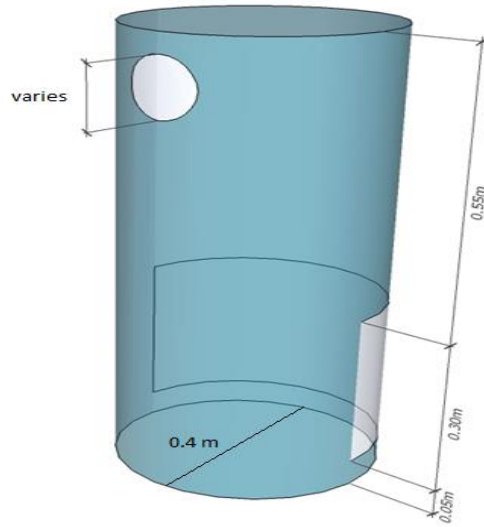


Figure 5- 7 PCD Virtual Model

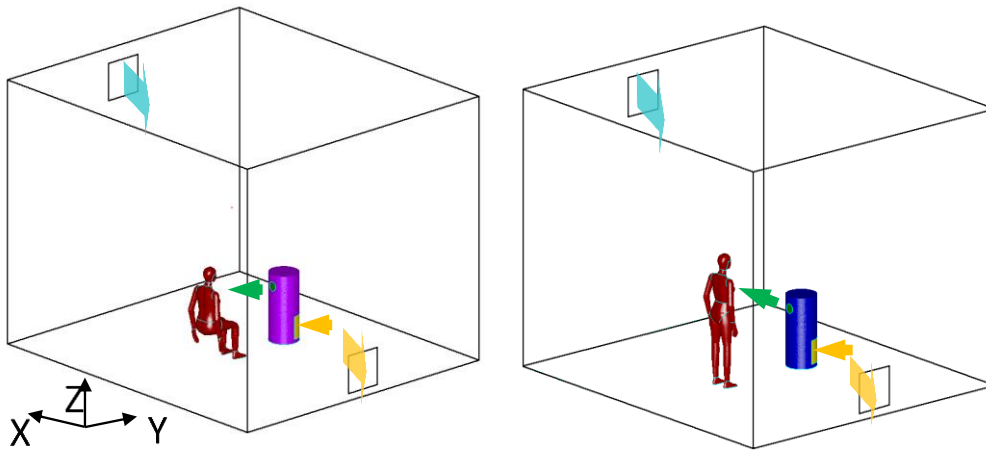


Figure 5- 8 Virtual Room Models for CFD Study with Seated and Standing Posture

Table 5- 2 Discharge Air Velocity and Temperature for each Airflow rate

<b>Seated (Front, Back) Cooling mode</b>								
Case	Ambient ventilation parameters			Discharge RoCo Parameters				
	[ACH]	Air velocity [m/s]	Air temperature	Airflow rate [cfm]	Flow Direction (angle of discharge) [°]	Velocity Discharge [m/s]		Air temp [°C]
						y	z	
0.47 clo-100 Watts-1m distance	3	0.21	26	25	4	2.36	0.17	19
				50	4	4.72	0.33	22.5
				75	4	7.09	0.5	23.6
				100	4	9.44	0.66	24.2
				125	4	11.81	0.83	24.6
<b>Standing (Front, Back) Cooling mode</b>								
Case	Ambient ventilation parameters			Discharge RoCo Parameters				
	[ACH]	Air velocity [m/s]	Air temperature	Airflow rate [cfm]	Flow Direction (angle of discharge) [°]	Velocity Discharge [m/s]		Air temp [°C]
						y	z	
0.47 clo-100 Watts-1m distance	3	0.21	26	25	20	2.36	0.86	19
				50	20	4.72	1.72	22.5
				75	20	7.09	2.58	23.6
				100	20	9.44	3.44	24.2
				125	20	11.81	4.3	24.6

The human body model for both cases, seated and standing, is divided into 17 parts with a total surface area of  $1.5 \text{ m}^2$ . This investigation assigns individual thermal resistance cloth values as recommended in ASHARE 55 [46], except to face and hands, which are assumed to be naked. The clothing level considered in this study are a bra (0.001 clo), panties (0.03), long sleeve dress shirt (0.25 clo), thin straight trousers (0.15 clo), athletic socks (0.02 clo), and shoes (0.02 clo). In addition, this investigation provides individual human body parts with convective and radiative heat transfer coefficients according to Table 5-3 for the seated model and Table 5-4 for the standing model [107]. The convective and radiative heat transfer coefficients come from empirical formulas based on experimental data. These convective and radiative correlations are suitable for velocities that are within and actual PCD provide [126]. In addition, these coefficients substitute the ones calculated by ANSYS Fluent, which tend to overestimate these coefficients due to wall functions.

Table 5- 3 Convective and Radiative Heat Transfer Coefficient and Thermal Resistances for  
Seated Model

Body Part	Convective heat transfer coefficient $h_{c,i}$ [w/m <sup>2</sup> K]		Radiative heat transfer coefficient $h_{R,i}$ [w/m <sup>2</sup> K]	Thermal resistance of cloth/w ig [w/m <sup>2</sup> K]
	V < 0.1 m/s	V > 0.1 m/s		
Face	3.7	$4.9V^{0.73}$	3.9	0
Head		$4.9V^{0.73}$		0.089
Chest	3	$9.1V^{0.59}$	3.4	0.04
Back	2.6	$8.9V^{0.63}$	4.6	0.039
Pelvis	2.8	$8.2V^{0.65}$	4.8	0.028
L. Foot	4.2	$12.8V^{0.55}$	4.2	0.006
R. Foot		$13.0V^{0.54}$		
L. Low er Leg	4	$12.9V^{0.56}$	5.4	0.023
R. Low er Leg		$13.4V^{0.58}$		
L. Thigh	3.7	$8.9V^{0.60}$	4.6	0.023
R. Thigh		$8.9V^{0.60}$		
L. Hand	4.5	$14.3V^{0.60}$	3.9	0
R. Hand		$12.6V^{0.60}$		
L. Forearm	3.8	$11.6V^{0.62}$	5.2	0.039
R. Forearm		$11.9V^{0.63}$		
L. Upperarm	3.4	$11.2V^{0.62}$	4.8	0.039
R. Upperarm		$11.6V^{0.66}$		

Table 5- 4 Convective and Radiative Heat Transfer Coefficient and Thermal Resistances for  
Standing Model

Body part	Convective heat transfer coefficients $h_{c,i}$ [W/m <sup>2</sup> K]		Radiative heat transfer coefficients $h_{r,i}$ [W/m <sup>2</sup> K]	Thermal resistance of cloth/wig [m <sup>2</sup> K/W]
	$V^* < 0.1$ m/s	$V^* \geq 0.1$ m/s		
Face	3.6	$3.2V^{0.97}$	4.1	0
Head		$3.2V^{0.97}$		0.089
Chest	3.0	$7.5V^{0.66}$	4.5	0.040
Back	2.9	$7.7V^{0.63}$	4.4	0.039
Pelvis	3.4	$8.8V^{0.59}$	4.2	0.028
L. Foot	5.1	$11.9V^{0.50}$	3.9	0.006
R. Foot		$12.1V^{0.49}$		
L. Lower leg	4.1	$12.7V^{0.50}$	5.3	0.023
R. Lower leg		$13.1V^{0.51}$		
L. Thigh	4.1	$10.1V^{0.52}$	4.3	0.023
R. Thigh		$10.1V^{0.52}$		
L. Hand	4.1	$15.4V^{0.51}$	4.1	0
R. Hand		$13.4V^{0.60}$		
L. Forearm	3.7	$12.7V^{0.53}$	4.9	0.039
R. Forearm		$12.4V^{0.55}$		
L. Upper arm	2.9	$9.9V^{0.61}$	5.2	0.039
R. Upper arm		$10.2V^{0.64}$		

The grid configuration used for the CFD models has approximately one million cells and a  $Y^+$  around the human model that varies between 2.0 and 4.0. Likewise, the aspect ratio for the grid configuration varies between 1 and 5. Air movement in indoor environments is mainly associated to forced convection and natural convection. In this investigation the force convection part is associated to the room's ventilation system and the air jet from PCD. On the other hand the natural convection is associated to the natural thermal plume generated by the human body. In order to model the air flow effects in the space, the mass (equation 5-3), momentum (equation 5-4), and energy (equation 5-5) conservation equation are solve simultaneously using the finite volume method. In order to include the buoyancy effects of air (natural ventilation) the Boussinesq approximation was used. Likewise, the RNG k- $\epsilon$  turbulent model was used in this investigation.

The boundary conditions for the solution of these equations are: no slip adiabatic conditions for walls and surfaces, velocity inlet for room air supply and PCD air supply/suction opening, pressure outlet for the room air outlet opening, and no slip, temperature surface for each body part, which is calculated using Fanger's thermoregulation model applied in a User Define Function (UDF).

$$\frac{\partial \rho}{\partial t} + \frac{\partial}{\partial x_k} (\rho u_k) = 0$$

*Equation 5-3 Mass Conservation*

where  $\rho$  is the air density and  $u$  is the air velocity

$$\frac{\partial}{\partial t} (\rho u_j) + \frac{\partial}{\partial x_k} (\rho u_k u_j) = -\frac{\partial p}{\partial x_j} + g_i + \frac{\partial}{\partial x_k} \left( \mu_{eff} \frac{\partial u_j}{\partial x_k} + \mu_{eff} \frac{\partial u_k}{\partial x_j} - \frac{2}{3} \left( \mu_{eff} \delta_{kj} \frac{\partial u_i}{\partial x_i} \right) \right)$$

*Equation 5-4 Momentum Conservation*

where  $\mu_{eff}$  is the effective viscosity,  $p$  is the hydrostatic pressure,  $g_i$  is the body force, and  $\delta_{kj} = 1$  if  $k=j$  and  $= 0$  if  $k \neq j$ . The subscripts  $i, k, j$  are associated to the coordinates directions.

$$\frac{\partial}{\partial t} (\rho E) + \nabla \cdot (\vec{u}(\rho E + p)) = \nabla \cdot \left( k_{eff} \nabla T - \sum_j h_j \vec{J}_j + (\tau_{eff} \cdot \vec{u}) \right)$$

*Equation 5-5 Energy Conservation*

where  $k_{eff}$  is thermal conductivity of air,  $J_j$  is the diffusion flux,  $E$  is the air enthalpy, kinetic energy, and potential energy.

This thesis uses a validated Computational Fluid Dynamic (CFD) model coupled with PMV thermoregulation model to calculate the heat removed from the human body and the thermal sensation of the virtual model. Figure 5-9 illustrates the iterative process of the coupling CFD and the PMV thermoregulation model. The coupled simulations process enables frequent updates to

the temperature boundary condition at each surface mesh of the virtual human body model. These frequent updates on the human body surface mesh allow the calculation of heat removed associated with the virtual PCD model. This study accounted for the human model heat loss driven by radiation and convection only with and without using the PCD device. The difference between the PMV with PCD and without PCD is the overall thermal sensation associated with PCD. Equation 5-6 shows the mathematical model for the PMV associated with PCD.

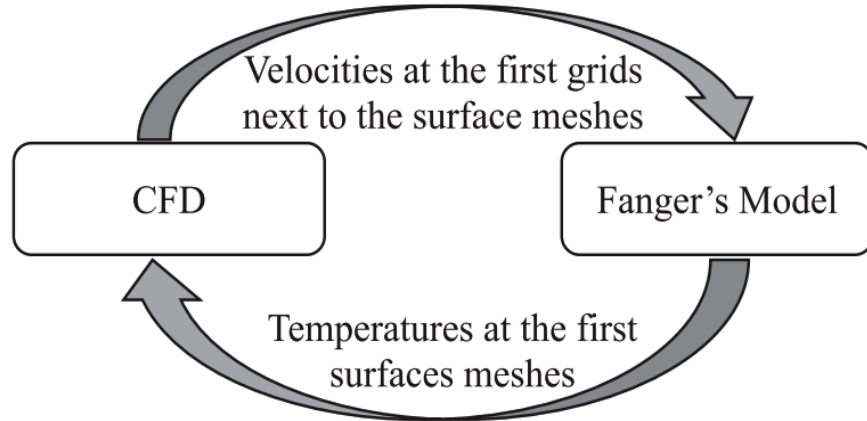


Figure 5- 9 CFD and PMV Iterative Process

$$\Delta PMV = PMV_{withPCD} - PMV_{withNOPCD}$$

$$\Delta PMV = -[0.303 e^{-0.036M} + 0.028] * (Q_s - Q_{sPCD})$$

Where:

$M$  is the metabolic rate of the human body.

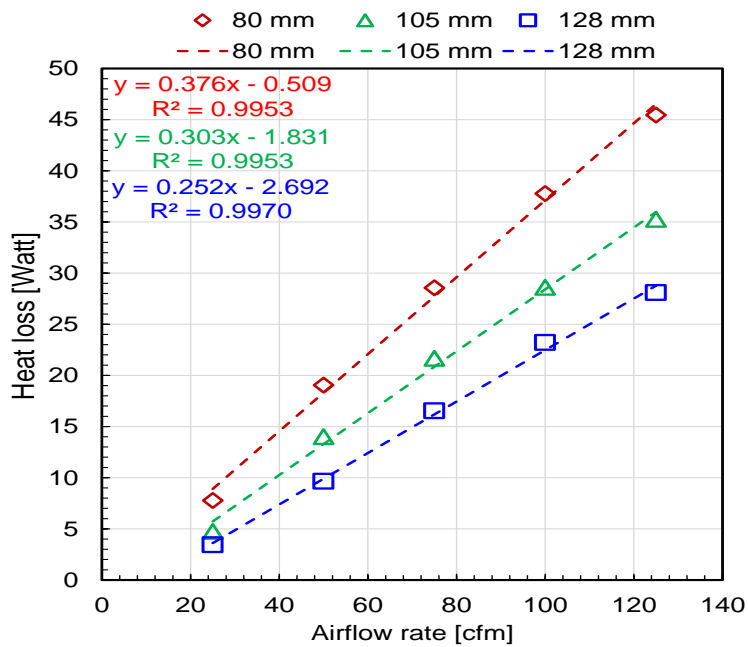
$Q_s$  is the sensible heat rejected from the human body with no PCD

$Q_{sPCD}$  is the sensible heat rejected from the human body with PCD

### 5.3 Results of Numerical Analysis of Cooling Mode

This study focuses on the air-jet velocity magnitude distribution, air-jet temperature distribution, surface mesh temperature distribution for the human body, and the heat fluxes from the human body. An operational objective during the cooling mode for the PCD is to remove approximately 23Watts of sensible heat from the human body. The CFD results for seated and standing models indicate that approximately 23 Watts of heat are lost to the environment when using a 0.08 m and 0.10 m nozzle diameter at airflow rates equal to 35 L/s (100 cfm) and 47 L/s (75 cfm), respectively as shown in Figure 5-10. Therefore, this investigation chooses to continue study using 0.08 m nozzle diameter to test the effect of different airflow rates.

Sitting Model



Standing Model



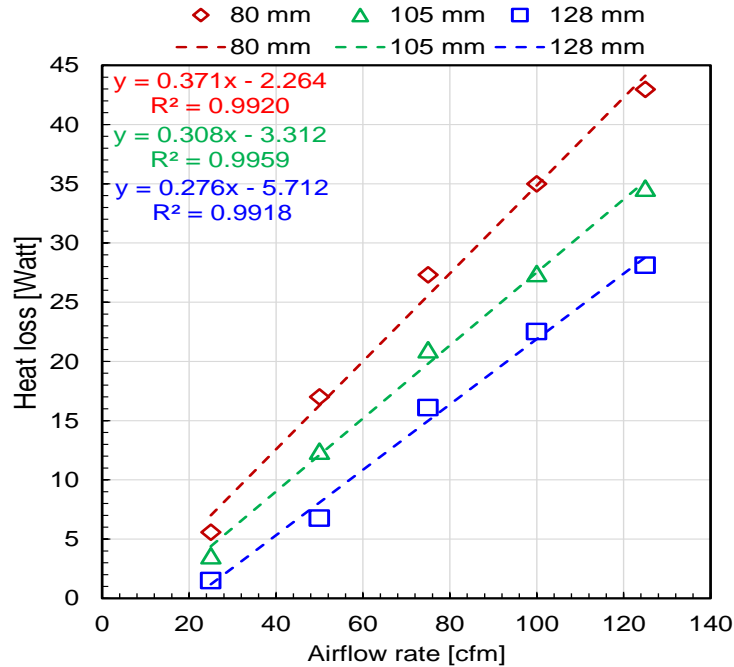
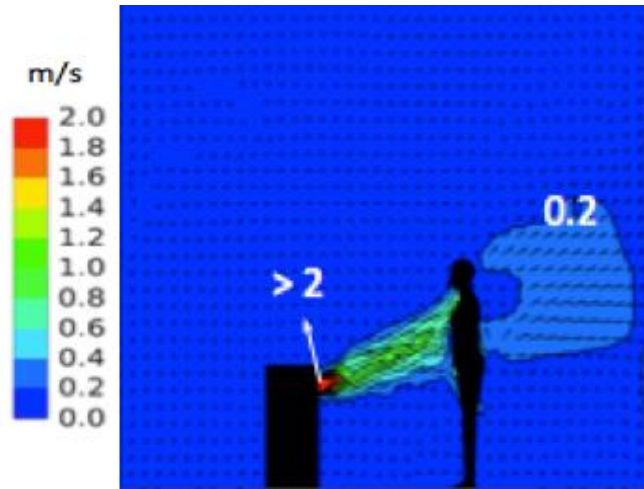
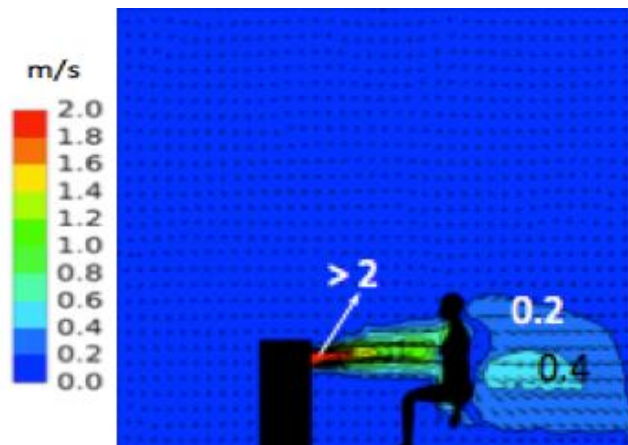


Figure 5- 10 Sensible Heat loss vs Airflow rate for Different Airflow Rates for Seated and Standing Model

During cooling operation the PCD provides cooling by working against the natural thermal plume of the human body. For this case, the air jet could target the torso, back, or side of the human body, which enhance heat transfer due to the available surface area. For the standing occupant, Figure 5-11 (a) shows the air jet leaving the PCD at an angle of approximately 20° to reach the occupant's torso. Similarly, for the seated model, Figure 5-11 (b) shows the air jet traveling in a straight line to reach the occupant. These figures show the air-jet supplied by PCD great speed drop from the center-line to the surroundings. The dissipation of the air-jet velocity carries out behind the human mode.



(a)



(b)

Figure 5- 11 Seated (a) and Standing (b) Case Cooling Mode 50 cfm

Figure 5-12 shows the velocity flow field of various airflow rates associated with PCD. A convective flow field around the human body is present when not using PCD (0 cfm). This convective flow field is dominated by natural convection around the human body. As the PCD starts operating, the convective flow field around the human body disappears due to the higher momentum of the air-jet being supplied from the PCD. The spreading of the air-jet velocity at low cfm (25 cfm) suggest a fast degeneracy of the cooling capacity of the air-jet. As the airflow rates increase, the air-jet velocity profile does not spread to the environment due to higher momentum. This increase velocity delivers more air-jet cooling capacity to the human body but it could have a negative effect related to risk of draft.

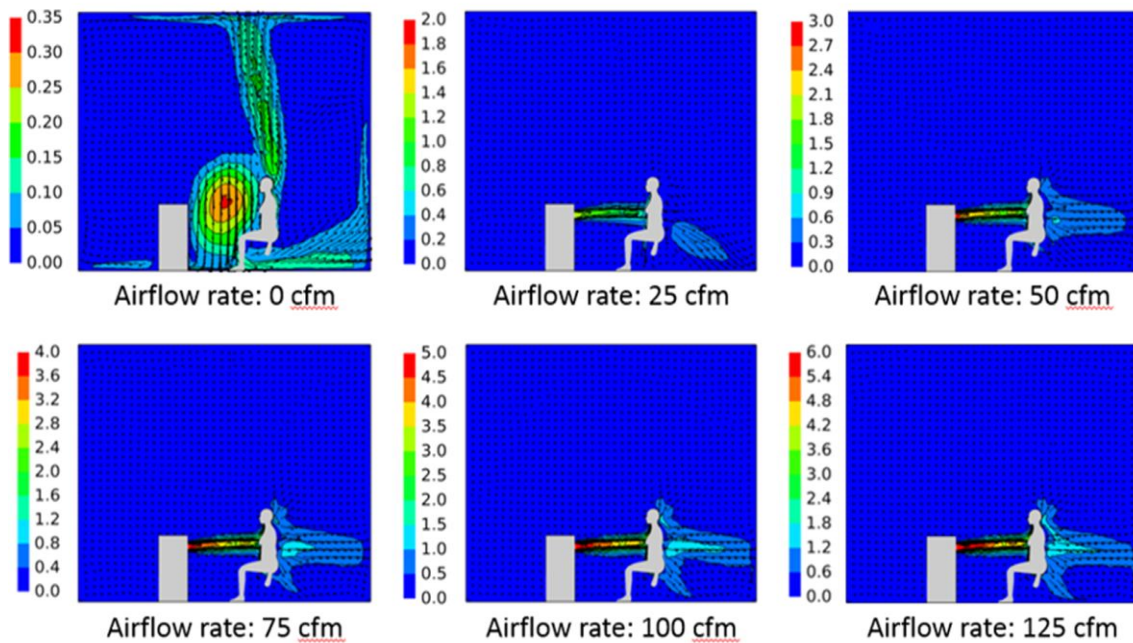


Figure 5- 12 PCD Air-jet Velocity Flow Field at Different Airflow Rates

Figure 5-13 shows a contour map of the temperature field for the CFD models in cooling mode. The temperature profile for the model with no PCD shows a consistent temperature of 26.5°C in the room and a temperature of 27.5°C for the air around the human body, which is the effect of

natural thermal plume of the human body. As the PCD starts supplying cooled air, it pushes away the natural thermal plume. In addition, as the airflow rates increase the air-jet temperature increases due to the fixed cooling capacity. However, higher airflow rates allow more uniform temperature around the torso of the human body, as shown in Figure 5-14. Similar effect is observed in the standing model.

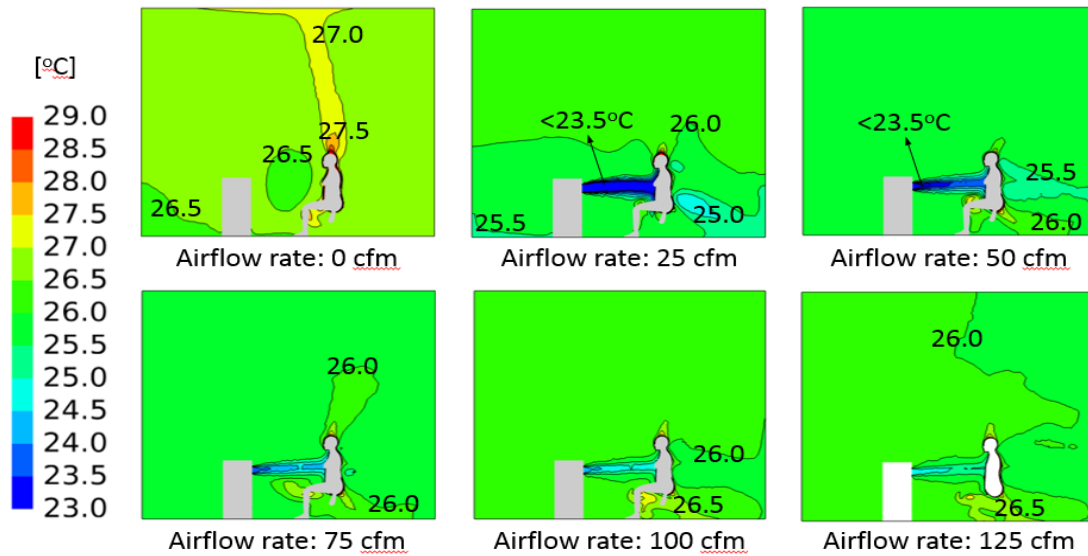


Figure 5- 13 PCD Air-jet Temperature Flow Field at Different Airflow Rates

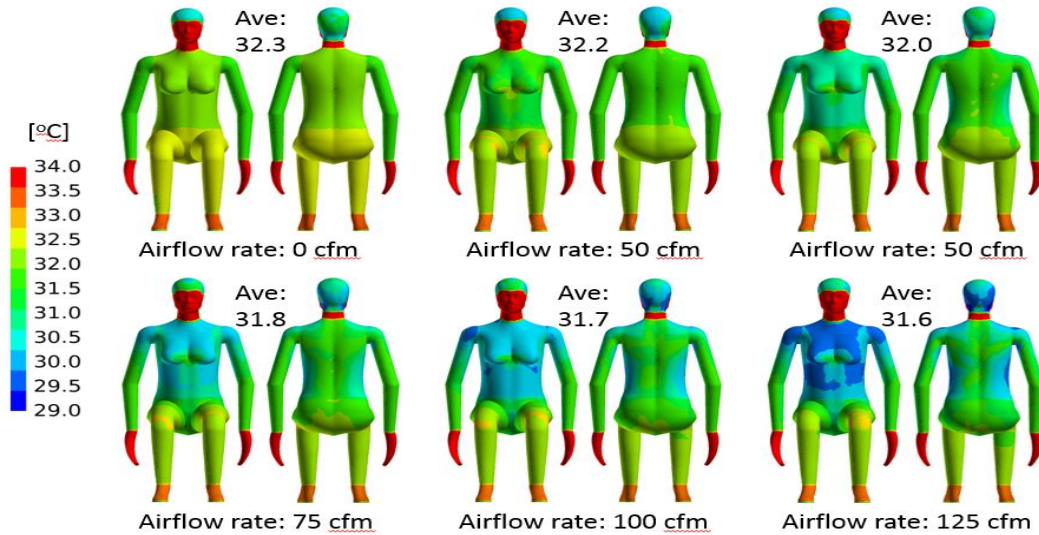
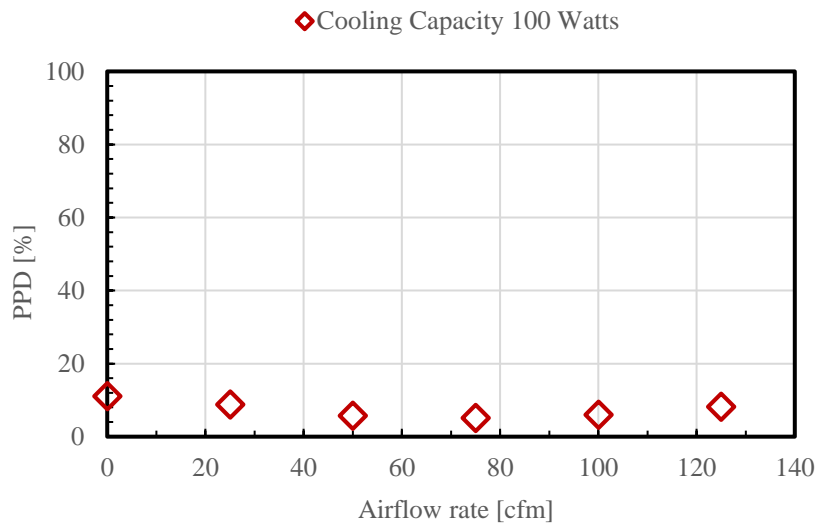


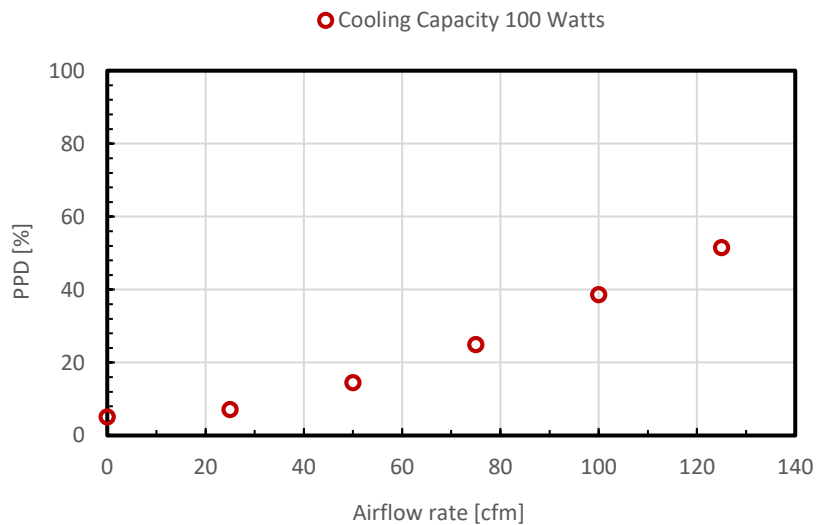
Figure 5- 14 PCD Air-jet Temperature Flow Field at Different Airflow Rates

The analysis of thermal comfort in this study is approached by the PMV and PPD thermoregulation model. The baseline model for comparison purposes simulates an environment with a local air temperature at 26.7 °C without PCD where PMV and PPD values are calculated iteratively. The results indicate that the baseline model for the standing case has a PPD equal to 11%, and the body heat loss equals to 70.4 Watts. Similarly, the base model for the seated case has a PPD value equal to 5.1 percent, and the body heat loss equals to 71.5 Watts. The PPD for both cases technically indicates that the environment is already comfortable without the need of PCD. However, these thermoregulation models do not account for human thermal preferences and physiology that drive thermal sensation and comfort. Adding PCD to the environment slightly increases PPD values for the standing case and dramatically increases PPD values for the seated case, as shown in Figure 5-15 (a) and (b). PPD increases because the room temperature lies inside the thermal comfort zone defined by ASHRAE 55. Therefore, these results suggest the potential to further increase of building's temperature setpoints outside the thermal comfort zone during the summer condition. While PPDs for the standing case increase between 5 % and 10 % for the airflow rate

tested, the PPD values for the seated case increase from 7 % to 48 %. The difference in PPD between these two cases is mainly due to the different metabolic rate for each case (1.6 met standing and 1.2 met seated). In the standing case the human body generates enough heat to be removed by the PCD. On the hand, the seated case generates lower energy, which causes the high discomfort values when operating the PCD.



(a)



(b)

Figure 5- 15 Percent People Dissatisfied (a) Standing model, and (b) Seated model as a Function of Airflow Rates in Cooling Mode

## 5.4 Results of Numerical Analysis of Heating Mode

In the heating mode the idea is to enhance the formation of the natural thermal plume of the human body. Therefore, this investigation oriented the PCD's air-jet towards the floor to reduce its momentum and allow it to mix with the human thermal plume. Similar to the cooling mode, the heating mode analyses a seated and standing case. Figure 5-16 shows the air-jet velocity profile for the seated case model. This investigation used low airflow rates to limit force convection and allow the formation of natural convection as a consequence of the warm air supplied by the PCD. Table 5-5 shows the airflow rates and air discharge temperature tested in this investigation. In addition, this investigation explored the effect of varying the distance-position of the device relative to the human body, and different clothing level. Three clothing levels were tested in the analysis, 0.97 clo, 1.2 clo, and 1.5 clo. According to ASHRAE Standard 55 [46], a clothing level of 1.0 clo typically represents a complete business suit and increasing the clothing level represents adding an additional layer of clothing under the suit such as a sweater. Lastly, the local air temperature in the room was 19 °C.

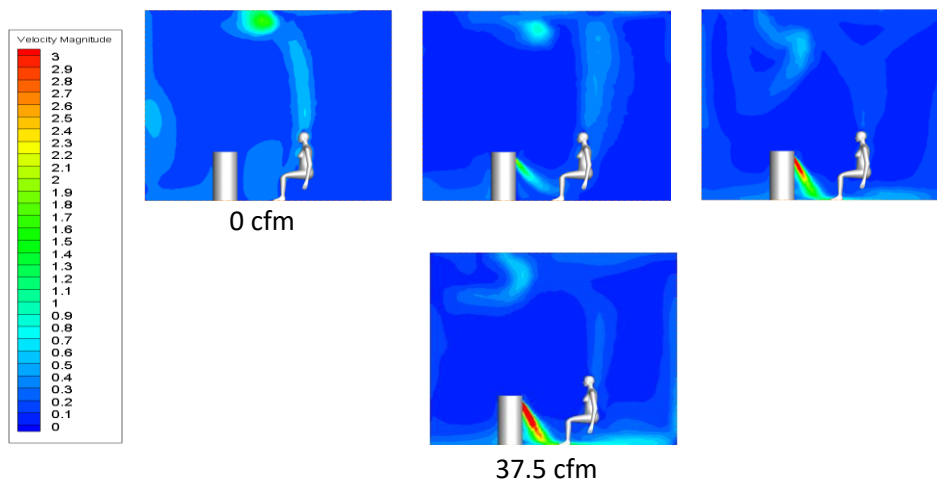


Figure 5- 16 PCD Air-jet Velocity Flow Field at Different Airflow Rates

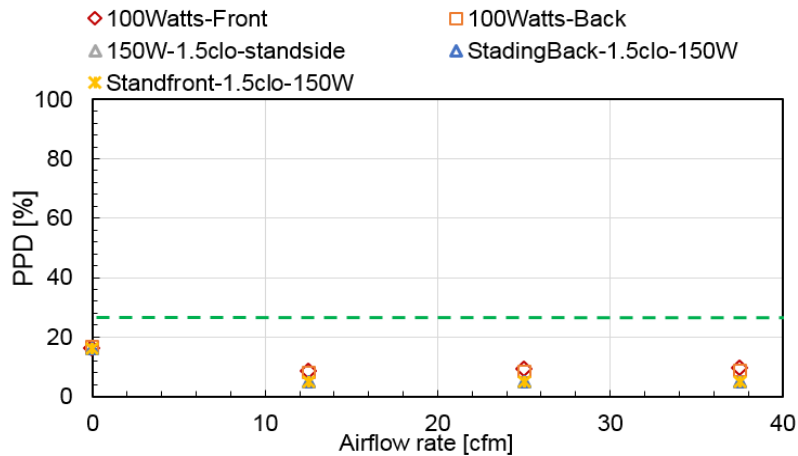
Table 5- 5 Airflow Rates and Air Discharge Temperature

Air Flowrate [L/s]	5.9 (12.5 cfm)	12 (25 cfm)	17.7 (37.5 cfm)
Air temperature [°C] (100 Watts)	33°C (91°F)	26°C (79°F)	23°C (73°F)
Air temperature [°C] (150 Watts)	42°C (108°F)	32°C (90°F)	28.6°C (83°F)

Similar to the cooling analyses, this investigation created a baseline model with a local air temperature at 19 °C and without using a PCD. The results indicate that the PPD value for the seated base model is 61 % and 16 % for the standing base model. The difference in PPD for the standing and seated cases is due to the human body energy generation associated to each case. Figure 5-17 (a) and (b) show the PPD results for the seated and standing cases, respectively. According to these results, the system is able to reduce PPD values of the seated case from 61 % to a range of 40 to 50 %, depending on the airflow rate, with a heating capacity of 100 Watts. However, increasing the heat capacity of the device to 150 Watts allows PPD values for the same case to fall to a range of 31±2 %. Further reduction of PPD is observed when clothing level is increase from 0.97 clo to 1.2 clo and subsequently to 1.5 clo, where PPD values fall below 25 %. In addition, reducing the distance between the user and the device also report low PPD values. The PPD values for the standing case also decrease to a range of 5±0.5 %, which means the overall environment improves. However, due to technical and financial limitations the project does not pursue the implementation of the heating mode as a feature of the PCD design.

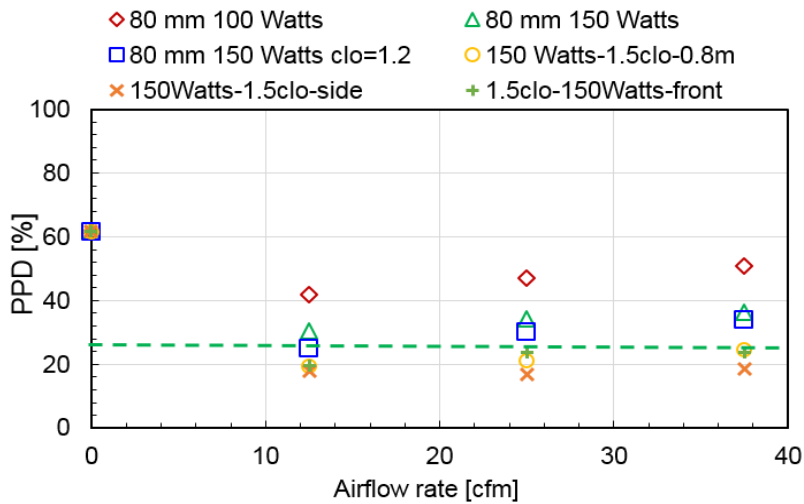


### • Standing Case



(a)

### • Seated Case



(b)

Figure 5- 17 Percent People Dissatisfied (a) Standing model, and (b) Seated model as a Function of Airflow Rates in Heating Mode

## 5.5 Summary

The numerical analysis of the micro-environment created by PCD demonstrates that it is possible to remove approximately 23 Watts of sensible heat from the human body using an air nozzle of diameter equal to 8.0 cm, an airflow rate equal to 35 L/s (75 cfm), and 100 Watts cooling capacity.

In addition, the results show a linear relationship between airflow rate and sensible heat removed

from the human body. Airflow rates higher than 75 cfm more than 25 Watts of heat is removed from the human body. This indicates that the device is performing as intended and meets the required heat removal from the project specifications. In addition, the PPD calculations show a 26% dissatisfaction for seated model and a 5% dissatisfaction for standing model, which is under required PPD of 20% set by industry standards (ASHRAE) and the sponsoring agency Department of Energy (DOE). The results also indicate that PCD creates an uncomfortable environment for the seated model and a comfortable environment for the standing model. This discrepancy is associated with the amount of heat that the human body is set to generate under the two conditions, where the standing model generates more heat than the seated model. This specific result allows the study to propose higher operative room temperatures since the current room temperature is still within the comfort zone defined by ASHRAE55.

In heating mode, this study analyses parameters such as two heating capacities (100 Watts and 150 Watts), the device's position and distance with respect to the human body, and clothing level to determine their effect on the thermal comfort calculations. In the heating mode, this study oriented the air nozzle towards the floor with the intend to reduce its momentum and use natural convection to create a warm microenvironment around the human body. Increasing the heating capacity of the from 100 Watts to 150 Watts reduces the PPD for the seated and standing model. The increase heating capacity reduces the PPD values lower than 20%, which is the target for this study. Further reduction in PPD values are possible when increasing the clothing level set to the human models. The difference in position, and small difference in distance does not significantly change the PPD values. In the heating the airflow rates range between 12.5 cfm to 38 cfm in order to limit force convection. Based on the technical limitation of the real PCD, small airflow rates are technically difficult to maintain reliably; additionally, financially a heating PCD using phase-change material

will not be able to compete with current heating devices. Therefore, further research with heating mode of operation was not conducted.

## **Chapter 6**

### **Experimental Analysis of Thermal Comfort with Data-Driven Approach with PCD**

This chapter provides an experimental analysis of the influence of PCD on the thermal comfort of human subjects. This study correlates physiological variables to the subjective responses of human subjects regarding their thermal comfort experience. Section 6.1 describes the experimental objective and variables of interest. Section 6.2 details the physiological information of the human subjects that participated in the study. Section 6.3 details the experimental protocol. Section 6.4 describes the physiological variables being monitored in these experiments. The data analysis applied in this study is in section 6.5. Section 6.6 presents the results of the study in terms of subjective responses and the response of each physiological variable of interest. Section 6.7 presents a discussion on the results of controlled-experiments that are part of this study. Lastly, section 6.8 summarizes the key findings of this study.

#### **6.1 Experimental Assessment of Thermal Comfort**

The third objective is to experimentally examine the influence of PCD on personal thermal comfort. The experiments replicated the setups of the numerical analyses described the previous section. Forty human subjects were exposed to different environmental temperatures with access to a PCD. The metrics for the evaluation of the thermal effect of PCD were thermal comfort survey and the monitoring of physiological variables related to human body thermoregulation process. Human characteristics such as gender, body mass index, activity level, and clothing level have a strong influence on thermal comfort, so this study made note of these factors for the thermal comfort evaluation of PCD. The relationship between physiological variables and thermal comfort

opens the opportunity to objectively explore individual thermal comfort under the influence of PCDs in different building environments. This study used physical variables of human subject, the experimental procedure, and the instrumentation that lead to the development and execution of the experiment. This study monitored skin temperature, heart rate, and heart rate variability (HRV) to capture changes associated with thermal comfort while using PCDs.

As this study did not collect any samples from occupants, the experimental protocol belongs to the social science subclass and the University of Maryland (UMD) IRB office has approved and issued the required IRB approval documents. The collected occupant information and feedback is analyzed, using statistical methods, to find patterns or trends that correlate physiological response to the thermal comfort and local air temperature provided by the PCD. These patterns or trends could be used to assess individual thermal comfort and enable a new path to automate a data-driven evaluation of thermal comfort.

## **6.2 Information on human subjects**

Overall 40 human subjects participated in the experiment, which include 20 males and 20 females. The recruitment process takes place via email with the target audience being the University of Maryland (UMD) student population. Students who volunteer to participate will receive a compensation of \$10/hour. In every experiment, each human subject provides information regarding their physical conditions such as body weight, height, age, and gender. According to their body mass index (BMI), most of the human subjects in the experiment are classified as normal weight (18.5 – 24.9) and overweight (25 – 29.9) as shown in Figure 6.1. Similarly, the age distribution of the human subjects ranges from 20 to 29 years old, with an outlier of 43 years old. Most of the human subject are students at the university of Maryland College Park. As part of the experiment, each human subject is required to wear office type clothing (pants, shirt, and closed-

shoes), which limits the clothing level variable to approximately 1.0 clo. The selection criteria for human subjects specifies healthy adults with no ongoing fever, cold/flu symptoms, or chronic diseases that could potentially affect the physiological variables being monitored. Among the 40 human subjects, 10 were discarded due to invalid data provided by the human subject regarding their comfort level or faulty functioning of the data collection device. In addition, 6 human subjects (4 women and 2 men) reported comfortable values throughout the experiment and did not request the PCD; therefore, they were discarded from the analysis. From 10 human subjects this study was only able to obtain heart rate and skin temperature. Therefore, the major results in this paper that includes skin temperature, heart rate, and HRV are presented for 14 human subjects.

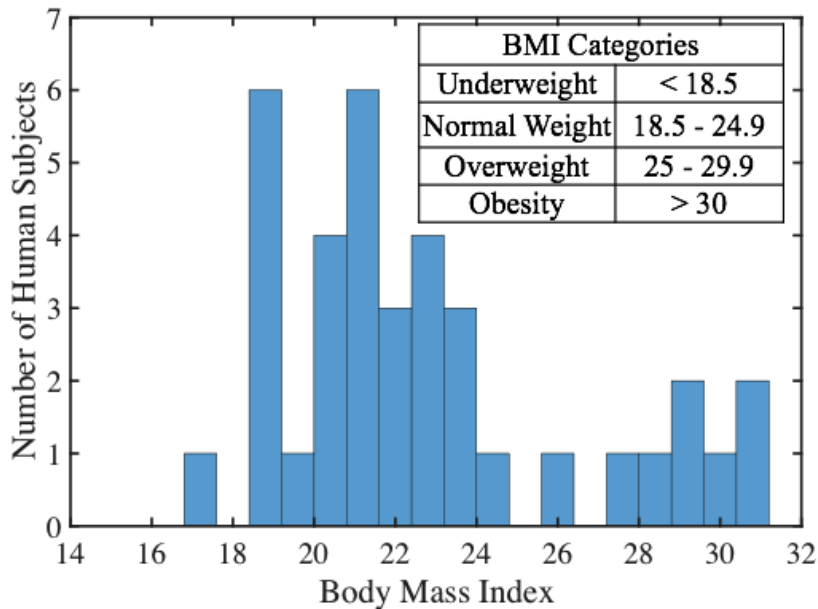


Figure 6- 1 Human Subject BMI Distribution

### 6.3 Experimental Procedure

Each of the experiments lasted for two hours. The initial room temperature was  $27 \pm 1^\circ\text{C}$  at the point of arrival of human subjects. This temperature was maintained during the first 50 minutes of each experiment. Then, the room temperature was increased and maintained at  $29 \pm 1^\circ\text{C}$  during

the second hour of the experiment, as shown in Figure 6-2. These temperatures are generally experienced by building occupants in indoor spaces, and they are at upper limit of the recommended operating temperatures in ASHARE 55 [52]. During the time of the experiment, human subjects reported their thermal sensation and comfort level based on a 7-point scale and 3-point scale [52], as shown in Figure 6-3. In addition, they wore a bracelet type data collection device that monitored their heart rate, heart rate variability, skin temperature, and galvanic response. Similarly, 20 out of 40 human subjects wore heat flux sensors and temperature sensors around the torso area to determine the actual heat flux of their bodies. Throughout the experiment each human subject had the option to request, deny, or stop the use of the PCD at any point of time. The majority of human subjects requested the PCD during the second hour of the experiment at a room temperature of  $29 \pm 1^\circ\text{C}$ . The PCD was located to the left or right of the human subject at approximately  $1 \pm 0.5$  meter distance. The PCD supplied cooled air towards the upper body, specifically torso and face. The PCD had a consistent temperature differential of  $5^\circ\text{C}$  when compared to the room temperature and airflow rates between  $18.8 \pm 5$  L/s to  $28.3 \pm 5$  L/s. Although the PCD could provide higher flowrates, they were not used due to risk of draft associated to high air velocities.

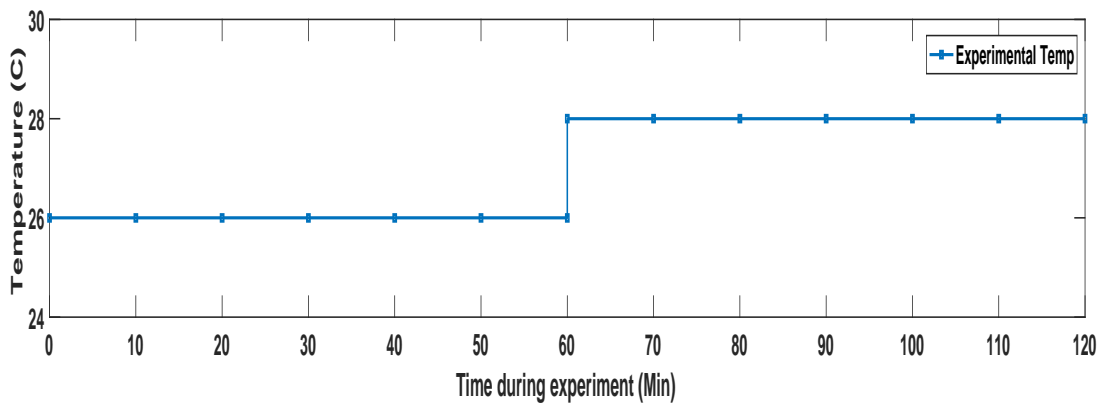


Figure 6- 2 Experimental Room Temperature Profile

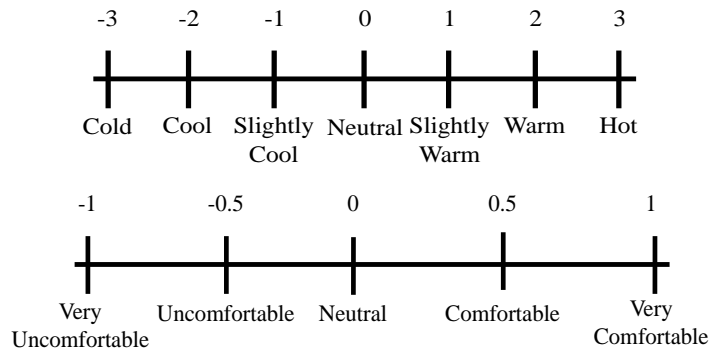


Figure 6- 3 Thermal Sensation and Comfort Survey Scales [52]

#### 6.4 Physiological Measurements

The heart rate was measured based on the photoplethysmography (PPG) principle, which estimates the heart rate based on the light intensity reflected from the blood vessels located in the fingertip. Similarly, the data obtained from the PPG sensor was used to estimate HRV in the time domain and frequency domain. The sampling frequency used by the PPG sensor was set to 330 Hz. The HRV measured with PPG sensors show the same trend and respond characteristics as the HRV measured from an electrocardiogram (ECG), especially the LF/HF ratio and the time domain variables such as the SDNNA, under different environmental temperatures [128]. Furthermore, the non-intrusive functionality of the PPG sensor allows the development of a wearable data collection device shown in Figure 6-4 (a). The skin temperature is monitored on the upper wrists part of the non-dominant hand. Multiple studies suggest that the dorsal region of the hand is more thermal receptive due to the presence of the main arteries that conduct heat from the inside to the outside of the human body during thermoregulation process [129] [112] [130]. The skin conductance

correlates to the sweat glands that are an essential part of the thermoregulation process of the human body [131]. However, the range of air temperature used in this study did not challenge the human body to activate sweat responses. Additionally, according to a study, sweat is the last stage of the thermoregulation process consequently it does not offer temporal interpretation of the thermoregulatory process [106]. In addition, the presence of the PCD mitigated the presence of sweat since its air supply helps the human body to remove excess heat.

## **6.2 Environmental Chamber Setup and Instrumentation**

The environmental chamber setup replicates an office space with two desks and two computers for the experiment, as presented in Figure 6-4 (b). The environmental chamber allows environmental temperature and air supply control. Each subject had a computer where they performed office type activities such as reading, writing, and typing. This study built a bracelet type device for skin temperature, heart rate, HRV, and environmental air temperature and humidity using commercially available sensors that are supported by Arduino devices. The technical details of each sensor are shown in Table 6-1. The sensors used in this study were connected to a micro-controller Arduino pro-mini 5V and packaged in a 3D printed bracelet-type device, as shown in Figure 6-4 (b). This micro-controller was programmed in-house to collect the analog signals at 2 Hz and 330 Hz for the skin temperature and heart rate, respectively. A DHT-22 sensor was used to monitor the ambient temperature and relative humidity of air in the proximity of the human body. All the data was sent, stored, and analyzed in a server located *in-house*. The PCD device used in this study is the Prototype Y2V1 Ice RoCo, technical details of this device-technology are specified in the literature [132][126]. Overall, this PCD has the capacity to output a temperature differential of 5°C when compared to the room temperature and airflow rates between  $18.8 \pm 5$  L/s to  $28.3 \pm 5$  L/s for approximately 2 hours.



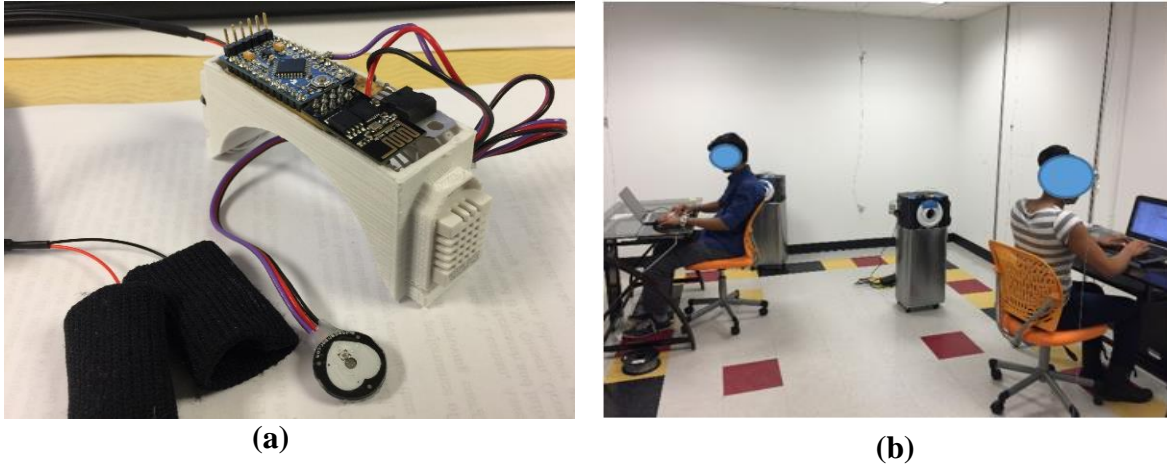


Figure 6- 4 (a) Chamber SetUp, (b) Arduino Based Bracelet Type Data Collection Device

Table 6- 1 Technical Description of Sensors Used in the Experiment

Sensors	Technical Information
<i>Arduino Pro Mini</i>	ATmega 328 chip, 5 Volts, 16 MHZ
<i>Pulse Sensors Amped</i>	5 Volts
<i>DHT22 Temperature and Humidity</i>	5 Volts, 2-5% humidity resolution, $\pm 0.5$ Temperature resolution
<i>DS18B20 Skin Temperature</i>	%, $\pm 0.5$ Temperature resolution
<i>GSR sensor Module</i>	5 Volts

### 6.5 Data Analysis

All the collected data was processed off-line using Matlab 2017a. The raw data from the PPG sensor was processed using an *in-house* developed software to calculate heart rate and heart rate variability (HRV). After extracting the pulse-to-pulse time interval of the heart from the heart rate data, HRV was calculated in the time and frequency domain using standard deviation tools and the power spectral density of the time series, respectively. While the heart rate was calculated in a minute-based interval, HRV parameters were calculated in a 5 minutes interval as suggested in the

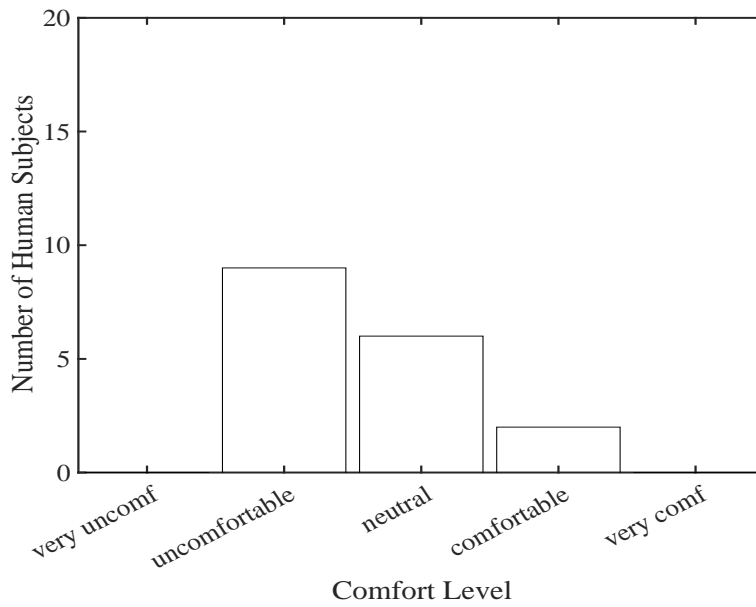
literature [133]. The data analysis concentrated on significant differences in physiological values caused by the PCD. Since the PCD device was the only external change during the experiments, all significant differences are attributed to it. Therefore, a one-way ANOVA was implemented as the analysis method to show the statistical difference in skin temperature, heart rate, and HRV, for scenarios before and after starting the use of the PCD device. This study used a 95% confidence interval in the ANOVA analysis.

## **6.6 Experimental Results**

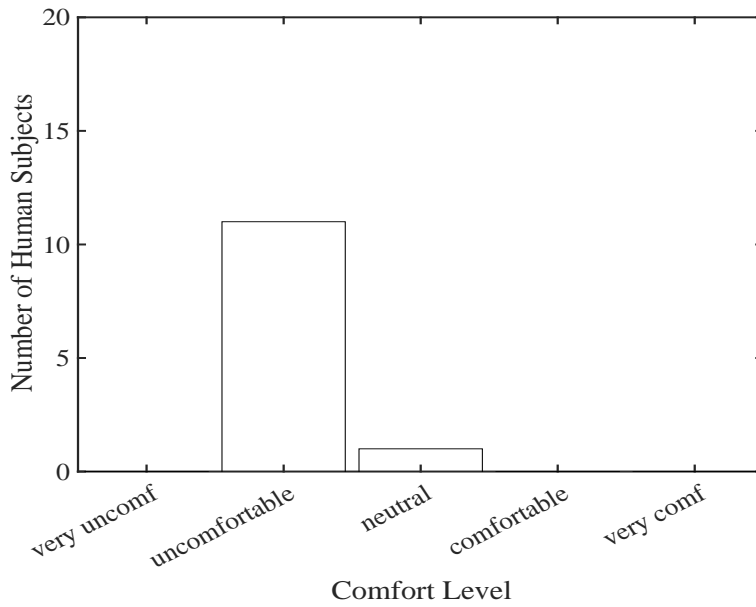
This study evaluated the effect of PCD on the human body. Each human subject reported their comfort level every 10 minutes. In addition, the skin temperature, heart rate, and heart rate variability were monitored during the experiments and these variables were correlated with the comfort level reported by human subjects in a survey. The population sample size of human subjects is relatively small, but representative as indicated in the literature of thermal comfort studies [76][103][104]. The results in our experiments demonstrated that the PCD has a positive subjective as well as a physiological effect on thermal comfort that could be monitored and measured with a bracelet-type device detailed in the previous section.

During the experiments, human subjects reported different thermal comfort levels under the same environmental conditions. However, the subjective comfort data reported by most of the human subjects during the experiments showed a consistent pattern of *very uncomfortable*, *uncomfortable*, and *neutral* comfort levels before requesting the PCD. After requesting the PCD, the thermal comfort values reported by human subject vary from *neutral*, *comfortable* and *very comfortable*, as shown in Figure 6-5. This figure shows a histogram distribution of the comfort responses 10 minutes before requesting the PCD, at the moment of requesting the PDC, and 10 minutes after requesting the PCD. The thermal comfort values 20 minutes before and 20 minutes after requesting

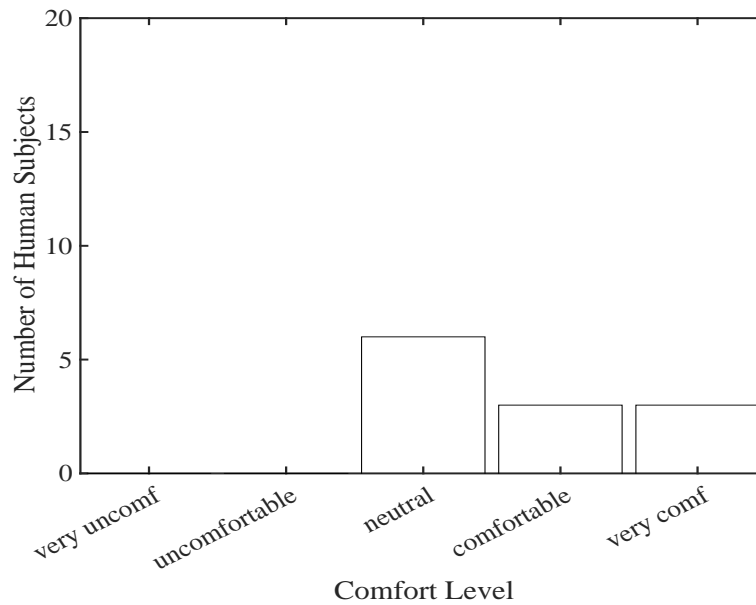
the PCD looked almost identical to the distribution presented in Figure 6-5 (a) and Figure 6-5 (c), respectively; therefore, they were not included in this section. The fact that human subjects reported the same thermal comfort values after requesting PCD suggested that the PCD is able to maintain a comfortable environment for the human subjects. Besides these subjective data, this study also explored the physiological responses due to the PCD's presence, such as the response of skin temperature, heart rate, and heart rate variability (time domain and frequency domain). The results present statistical analysis of these variables during "uncomfortable" state before requesting the PCD and "comfortable" state after requesting the PCD. Furthermore, the results show a relationship between each physiological variable and the comfort state reported during the experiments. Due to the individual differences in thermal comfort and thermal sensation, the timing for requesting the PCD varies among human subjects. Therefore, to have a consistent comparison among human subjects, the results present a time frame of 20 minutes before and after requesting the PCD. Lastly, the experiments were divided into two stages, the first stage monitored heart rate and skin temperature, and the second stage also included measurements of heart rate variability.



(a) Subjective Responses 10 min before Requesting PCD



(b) Subjective Responses when Requesting PCD



(c) Subjective Responses 10 min After Requesting the PCD

Figure 6- 5 Distribution of Comfort Responses (a) 10 min before, (b) during, and (c)10 min After Requesting the PCD

### 6.6.1 Skin Temperature

The individual differences and characteristics of each human subject manifested in the skin temperature response during the experiments. The skin temperature values for human subjects during the experiments ranged from 29°C to 35.5°C. Even though the skin temperature magnitude was different among human subjects, they all shared similar response pattern for skin temperatures that increased during the beginning of the experiment until the human body and the environment reached thermal balance. This balance was maintained until each human subject reported being thermally uncomfortable and requested the PCD for local cooling. At that time, the skin temperature started decreasing until, again, it reached a steady state value based on a new thermal balance between the human body and cool air jet provided by the PCD. Figure 6-6 shows the skin temperature data for time span of 20 minutes before and 20 minutes after requesting the PCD. The

variability in skin temperature values among human subjects indicates the differences in thermoregulatory system of each person.

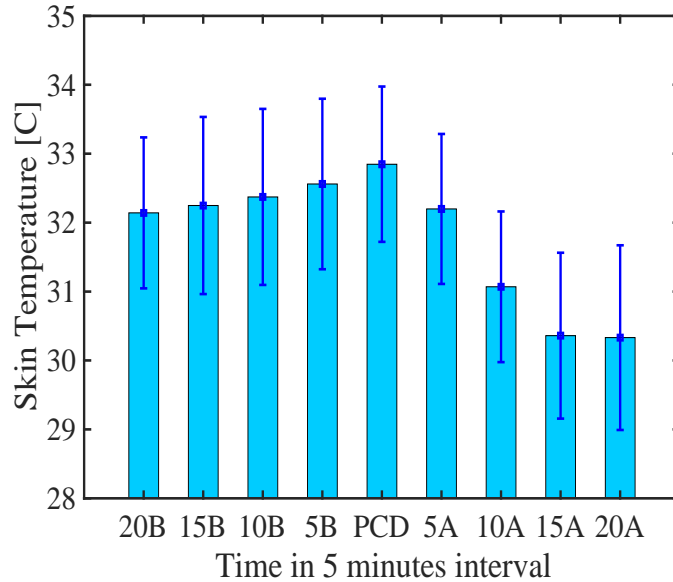


Figure 6- 6 Skin Temperature over 20 minutes before and after Requesting PCD

Table 6-2 shows the results of an ANOVA test with the statistical difference,  $P$ -value  $<0.0001$ , between the skin temperature before and after requesting the PCD. The results presented in this section correspond to data obtained before and after human subjects requested the PCD. It is important to note that the majority of human subjects reported being thermally uncomfortable or uncomfortable before requesting the PCD. Figure 6-7 shows the box plot of the aggregated skin temperature data for all the human subjects. Since the mean skin temperature values for uncomfortable and comfortable conditions do not overlap, the conclusion, with a 95% confidence, is that the true medians for the uncomfortable and comfortable cases differ. The overlap of the whiskers in the box plot, besides indicating extreme data points, they also indicate a fairly high variability of the skin temperature values among human subjects. These temperature values decreased by  $2^{\circ}\text{C}$  on average in response to the microclimate created by PCD. Specifically, within

10 to 15 minutes, the majority of human subjects reach steady-state for their skin temperature. The difference in time required to reach steady-state is a consequence of the individual thermoregulatory system of human subjects. Nonetheless, the significant difference in skin temperature is a consequence of the presence of the PCD since it is the only changing condition during the experiments.

Table 6- 2 Results of ANOVA test with Skin Temperature Data Between Uncomfortable and Comfortable Conditions

ANOVA Results Uncomfortable vs Comfortable Skin Temperature ( <i>p</i> -value < 0.001)			
	N. of Human Subjects	Mean [°C]	STD [°C]
Uncomfortable	11	32.6	1.3
Comfortable	11	30.5	1.5

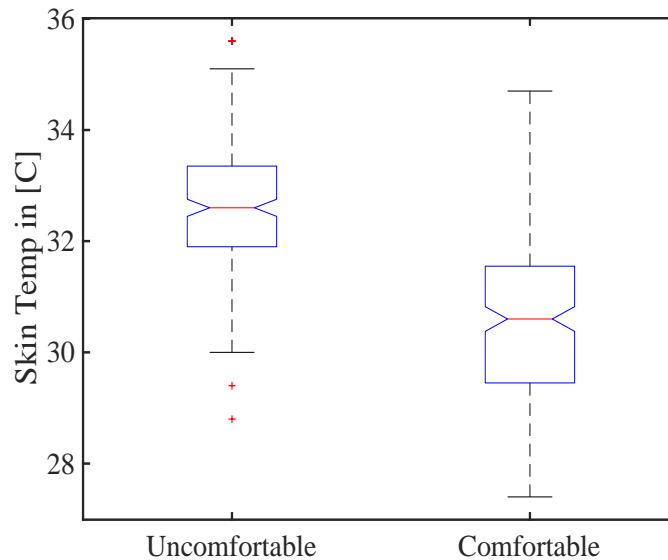


Figure 6- 7 Skin Temperature Boxplot Uncomfortable vs Comfortable

### 6.6.2 Heart Rate Response

During the experiments all human subjects performed an office work activity and were exposed to

the same temperature changes. Nonetheless, heart rates were different among all the human subjects. Figure 6-8 shows the average heart rate for human subjects in the 20 minutes time period before and 20 minutes after requesting the PC device. The heart rates of each human subject showed slight changes during the experiments, with decreasing values for most of the human subject after requesting the PCD for local cooling. The heart rate changes observed in the experiments are not significant since the human body was not subject to a drastic temperature change that could lead to a significant change in heart rate. These results are consistent with the results found in the literature, where the heart rate of 14 human subjects showed no significant differences in similar operative indoor temperatures [93]. However, there is a trend of slightly higher heart rate just before the human subjects requested the PCD, indicating the activation of the thermoregulatory process of the human body.

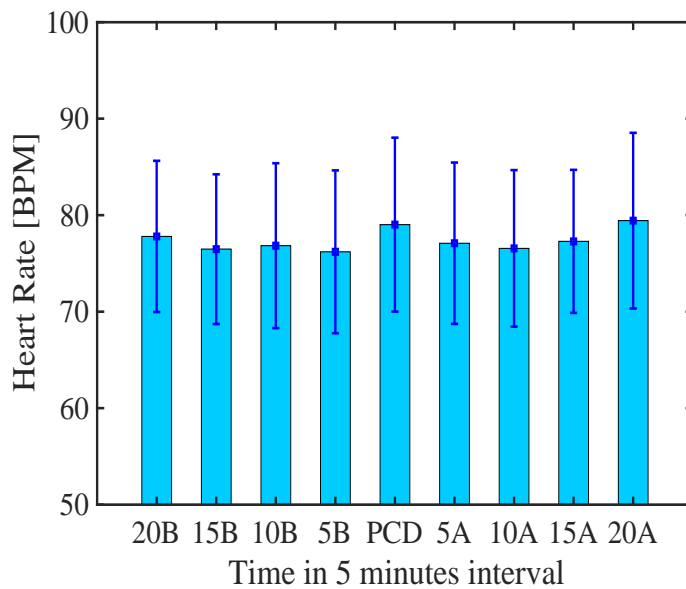


Figure 6- 8 Heart Rate over 20 minutes before and after Requesting PCD

The ANOVA analysis of the comparison of heart rates before and after requesting the PCD are shown in Table 6-3. This analysis specifically focused on the difference in heart rate when the



human subject reported being thermally uncomfortable and comfortable. The results of the ANOVA test demonstrated a lack of statistical difference,  $P\text{-value} > 0.5$ , in heart rates before and after using the PCD. The lack of statistical difference could be attributed to the high deviation in the heart rate data shown in Figure 6-9. Even though there is no statistical difference in heart rates before and after requesting the PCD, there is a decreasing trend in heart rates by 5 bpm (beats per minute) on average, as shown in Figure 8. The decreasing trend of heart rates is a sign that the thermoregulation system of the human body is less active when using PCD.

Table 6- 3 Results of ANOVA test with Heart Rate Data Between Uncomfortable and Comfortable Conditions

ANOVA Results Uncomfortable vs Comfortable Heart Rate ( $p\text{-value} > 0.05$ )			
	N. of Human Subjects	Mean [BPM]	STD [BPM]
Uncomfortable	11	77.4	9.4
Comfortable	11	75.1	8.2

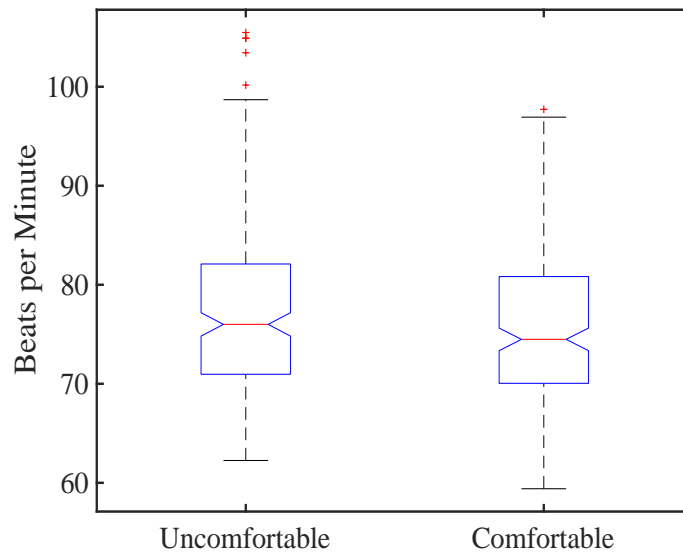


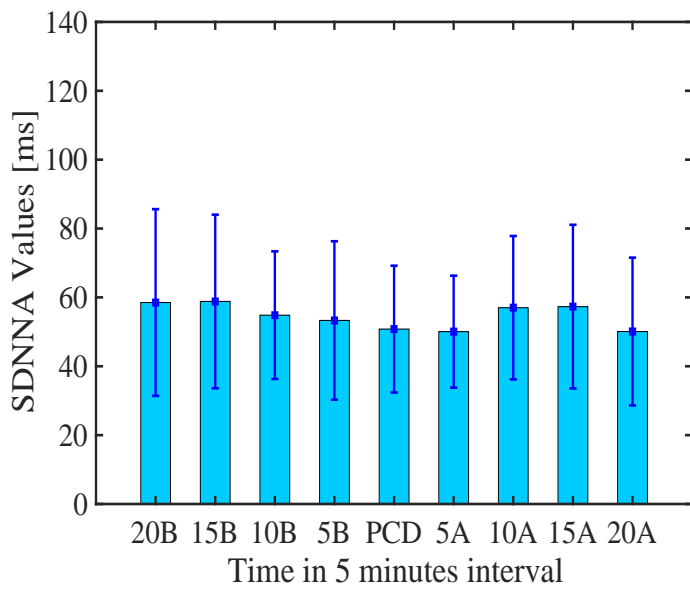
Figure 6- 9 Heart Rate Boxplot Uncomfortable vs Comfortable

### 6.6.3 Heart Rate Variability (Time Domain)

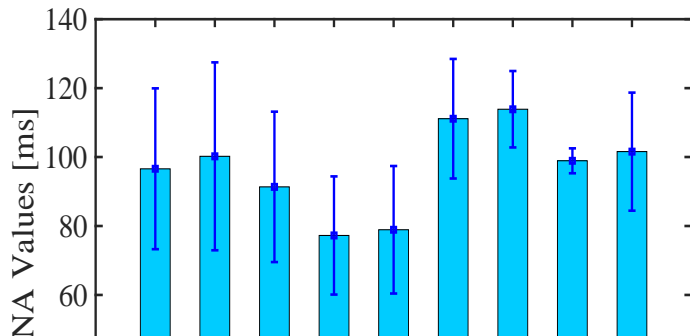
The SDNNA values over time, *the standard deviation of time beats*, showed a time-dependent variation that is individual for each human subject and represented by the deviation bars in Figures 6-10 (a) and 6-10 (b). The low individual SDNNA values correspond to uncomfortable conditions, and the high individual SDNNA values correspond to comfortable conditions in the experiments. This response of SDNNA values is consistent with the SDNNA patterns reported in the literature by *Kim et.al* [134]. The variation of SDNNA values was due to temperature changes. In general, as human subjects became thermally uncomfortable, SDNNA values consistently decreased until the PCD is requested for local cooling. After requesting the PCD, SDNNA values increased and human subjects reported being thermally comfortable. The results observed in this study are similar to results supported in the literature, where higher SDNNA values are observed in comfortable (less stress) scenarios [128][135].

Our experiments indicate two distinct groups of human subjects with respect to the SDNNA variations in response to temperature changes. Specifically, the first group of human subjects had a low-individual SDNNA variation of approximately 60 ms, and the second group of human subjects had a high-individual SDNNA variation of approximately 100 ms based on the observed responses. The results for human subject with low SDNNA variation values are shown in Figure 6-10 (a). This group of human subjects seemed to tolerate higher temperatures as they requested the PCD device during the environmental temperature equal to  $29 \pm 1^\circ\text{C}$ , which corresponds to the second hour of the experiment. In contrast, human subjects with high SDNNA variation values, shown in Figure 6-10 (b), requested PCD earlier in the experiments. This group of human subjects seemed to have lower tolerance to high temperatures since they requested the PCD device at the environmental temperature equal to  $26 \pm 1^\circ\text{C}$  that corresponds to the first 50 minutes of the experiment. The individual variation of SDNNA values could be an indicator of the

thermoregulatory system activity for each human subject. These SDNNA values could be used to objectively evaluate the thermal comfort effect of PCD at an individual level for human subjects.



(a)



The ANOVA analysis of SDNNA values before and after human subjects requested PCD indicates that there exists a statistical difference with  $p\text{-value} < 0.001$ , as shown in Table 6-4. These SDNNA values also correspond to human subjects reporting being thermally uncomfortable and comfortable. The statistical difference found in this section must be attributed to the microclimate created by the PCD, with a 95% confidence interval. The difference in SDNNA values before and after requesting PCD suggest the ability of PCD in delivering a comfortable microclimate to each human subject. Specifically, the warm temperatures lead to consistent time between heart-beats to activate the thermoregulatory processes, such as vasodilation for heat rejection. The microclimate created by the PCD enhanced the heat removal from the human body, leading to less consistent time between heart-beats that increased the SDNNA values. The less consistent time between heart-beats is a natural response of the human body in rest.

Table 6- 4 Results of ANOVA test with Heart Rate Data Between Uncomfortable and Comfortable Conditions

ANOVA Results Uncomfortable vs Comfortable Stand. Deviation of NN time intervals ( <i>p-value</i> < 0.001)			
	N. of Human Subjects	Mean [msec]	STD [msec]
Uncomfortable	11	63.4	24.3
Comfortable	11	80.9	33.7

Figure 6-11 shows the box plot of the aggregated SDNNA data for all human subjects. The mean SDNNA values for comfortable and uncomfortable thermal states do not overall, which indicates at a 95% confidence interval, the statistical difference between the two cases. The overlap of the box and whiskers indicate the high variability in the data that corresponding to different human subjects. This result suggests that while SDNNA values could be high for some human subjects, the same set of SDNNA values could be low for other human subjects. Overall, the results in Figure 6-11 show the increasing trend of SDNNA values when human subjects reported being comfortable due to the intervention with PCD.

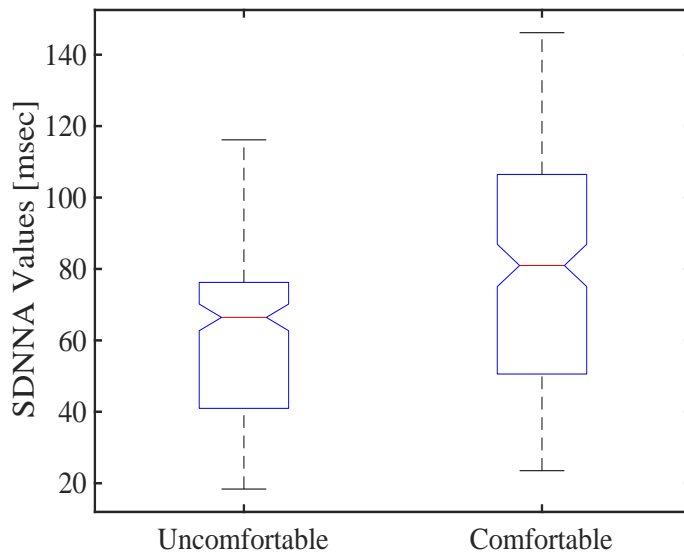
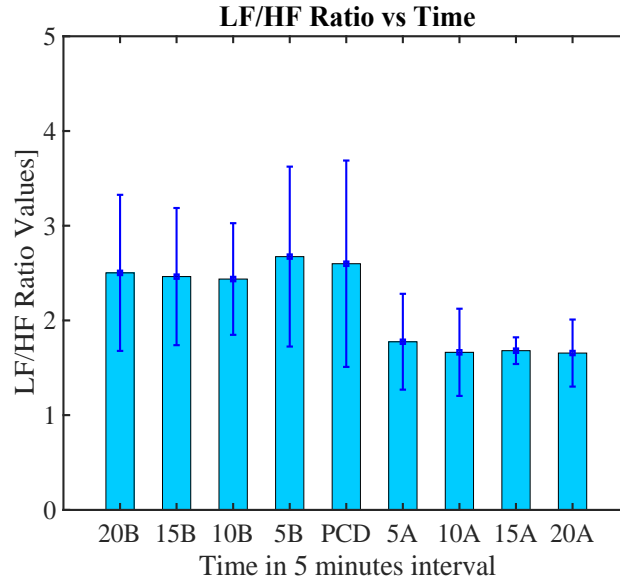


Figure 6- 11 Standard Deviation of NN Intervals Heart Beat Boxplot Uncomfortable vs Comfortable

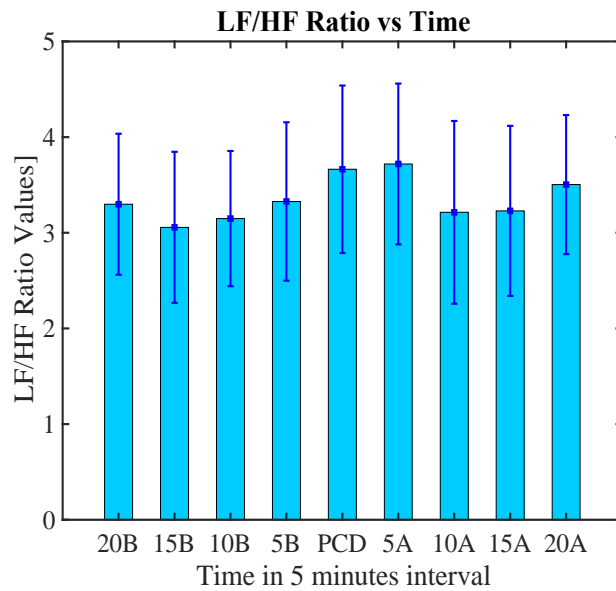
#### 6.6.4 Heart Rate Variability (Frequency Domain)

Figure 6-12 (a) and Figure 6-12 (b) show the time-dependent variation of LF/HF ratios for 20 minutes before and 20 minutes after requesting the PCD. The LF/HF ratios in this time frame were distinctively different among human subjects. Nevertheless, the majority of human subjects showed an increasing trend of LF/HF ratio as they reported being thermally uncomfortable in the environment. After the human subjects requested the PCD, the LF/HF ratios started decreasing as human subjects reported better thermal comfort levels. Similar to the analysis of SDNNA values, this study grouped human subjects according to the magnitude variation of in the LF/HF ratios. Human subjects with high magnitude variation and lower LF/HF ratio are shown in Figure 12 (a). This group of human subjects had higher tolerance to high temperatures since they requested the PCD during the second hour of the experiment. In contrast, human subjects with lower-magnitude of LF/HF ratios and higher LF/HF ratio requested the PCD during the first hour of the experiment. This group of human subjects are shown in Figure 6-12 (b). In general, the trend of LF/HF ratio

observed in this study suggests that high LF/HF ratios correspond to uncomfortable thermal levels for the human body and lower LF/HF ratio corresponds to comfortable levels for the human body. These results lead to the possibility of addressing individual thermal comfort based on the LF/HF ratios of human subjects. This analysis could also be an indicator of the performance of the PCD in providing thermally comfortable environments



(a)



(b)

Figure 6- 12 (a) LF/HF Ratio of High Variability Human Subjects (b) LF/HF Ratio of Low Variability Human Subjects over 20 minutes before and after Requesting PCD

The ANOVA analysis comparing the LF/HF ratios before and after requesting the PCD shows a statistically difference with ( $p\text{-value} < 0.001$ ). The comfort levels reported by the majority of human subjects before requesting the PCD varied from very uncomfortable to uncomfortable. Similarly, the comfort levels of human subjects after requesting PCD varied from neutral to comfortable. Therefore, the ANOVA analysis also indicates that there is a significant difference between LF/HF ratios at uncomfortable and comfortable thermal levels, as shown in Table 6-5. In these experiments, when the human subjects felt thermally uncomfortable, their LF/HF ratio had higher values compared to the LF/HF ratio when the human subjects felt thermally comfortable. The high LF/HF ratios in these experiments indicated the activation of the sympathetic nervous system, which activates and controls the thermoregulatory system for heat rejection. Furthermore, the decrease in LF/HF ratios indicated lower thermal stress on the human body due to the microclimate provided by the PCD. Human subjects had distinct LF/HF ratios between uncomfortable and comfortable levels during the experiments. Therefore, the box plot shown in Figure 6-13 shows an overlap between the boxes and the whiskers. This suggest that while some LF/HF ratios could be high for some human subjects, the same LF/HF ratio could be low for other human subjects.

Table 6- 5 ANOVA Results Uncomfortable vs Comfortable LF/HF Ratio ( $p\text{-value} < 0.001$ )

ANOVA Results Uncomfortable vs Comfortable LF/HF Ratio ( $p\text{-value} < 0.001$ )			
	N. of Human Subjects	Mean	STD
Uncomfortable	11	3.2	1.0
Comfortable	11	2.5	1.0



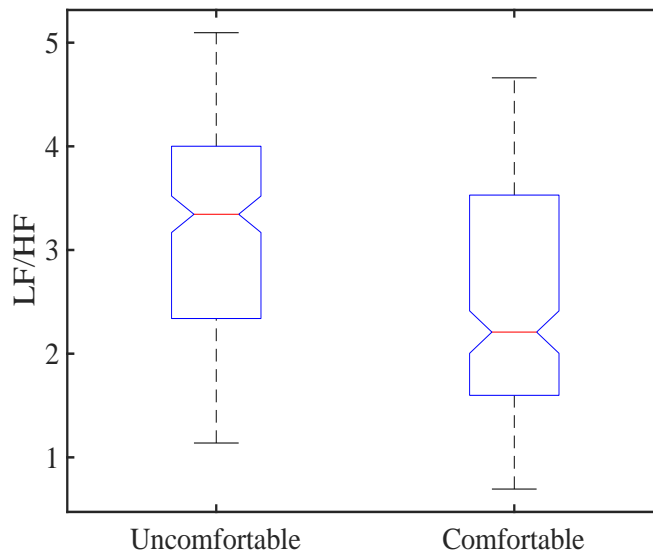


Figure 6- 13 LF/HF Ratio Boxplot Uncomfortable vs Comfortable

### 6.6.5 Relationship between Physiological Variables and Comfort Level

All human subjects were exposed to the same environmental temperatures for the same period of time. Each human subject was provided with a table to report their comfort level every 10 minutes for the duration of the experiments. However, the different reported comfort levels showed individual differences among human subjects, which are directly linked to the individual thermal preferences and their thermal adaptation capacity. These differences were also present in the physiological parameters that were monitored during the experiments. The analysis in the previous section demonstrated statistically significant responses of skin temperature, SDNNA values, and LF/HF ratios of the human subjects before and after requesting the PCD. These parameters are linked to the autonomic nervous system that controls the autonomous thermoregulation of the human body [136]. Understanding the relationship between each of these variables and the thermoregulatory system of the human body could automate the individual assessment of thermal comfort based on individual physiological parameters. Therefore, an individual analysis of the

relationship between each of these parameters and human subject comfort level responses is presented in this section.

Figure 6-14 (a-c) shows the relationship between skin temperature, SDNNA values, and LF/HF ratios with comfort level. This study proposes a linear relationship between each variable and thermal comfort. The results indicate an average  $R^2$  value of 0.75, 0.69, and 0.68 for skin temperature, SDNNA values, and LF/HF ratios, respectively, as shown in Figure 6-14 (d). Even though the linear trend is consistent among human subjects, there are significant differences in their magnitudes. The variability in physiological responses depends on the individual characteristics, such as genetics, lifestyle, age, and weight [137]. For example, the uncomfortable combination of parameters, including skin temperature, SDNNA values, and LF/HF ratios for ID3\_10 was a neutral set of parameters for human subject ID 3\_5. Therefore, this study highlights the importance of the individual assessment of thermal comfort to develop models considering individual physiological variables. In general, the results showed that high skin temperatures, low SDNNA, and high LF/HF ratio, relative to each human subject, are associated with thermally uncomfortable levels. In contrast, low skin temperature, high SDNNA, and low LF/HF ratio values are connected to the comfort levels. Therefore, the physiological responses for each human subject could be individualized, leading to personalized interpretation of thermal comfort in indoor spaces.

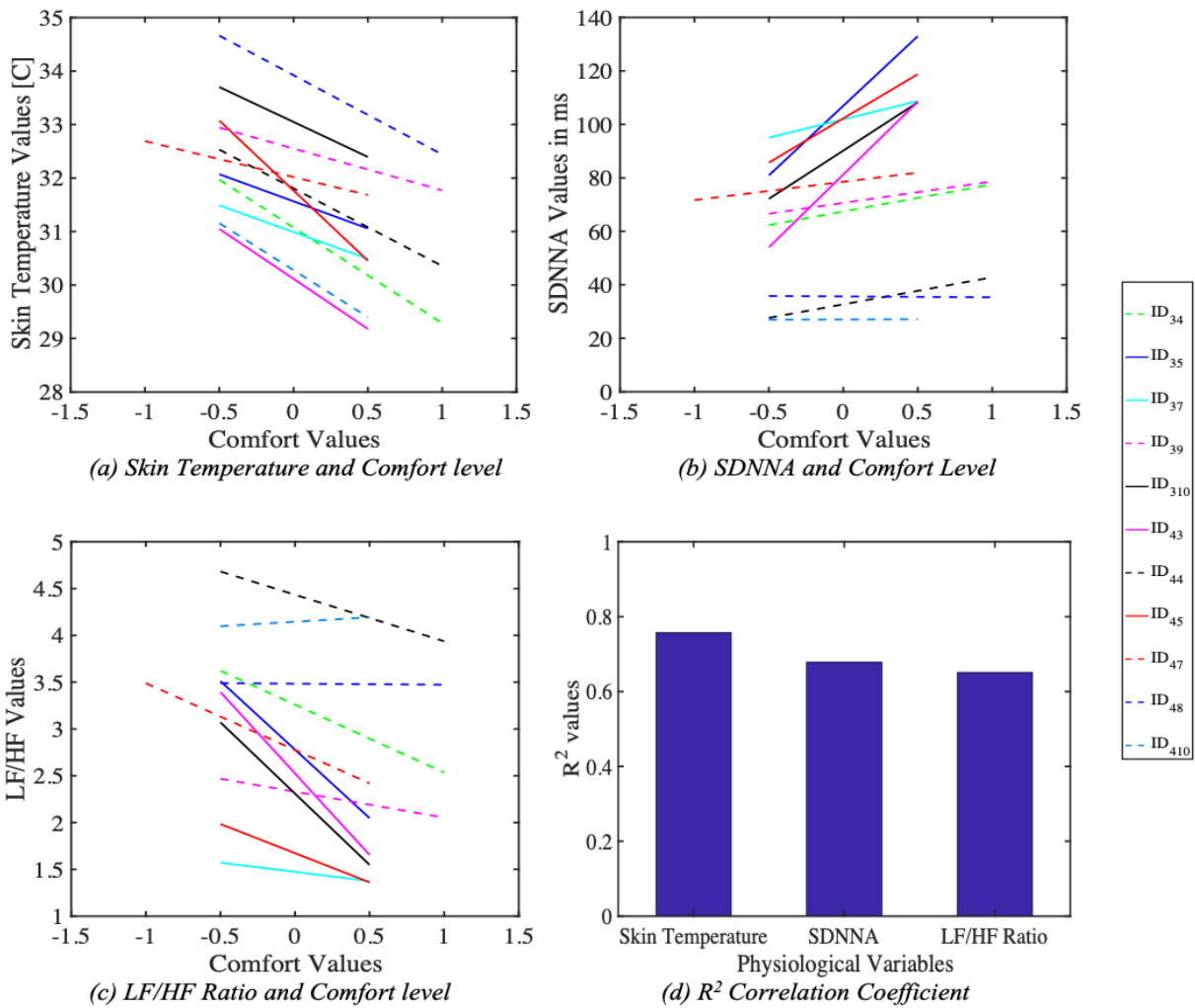


Figure 6- 14 Physiological Variables and Thermal Comfort Relationship

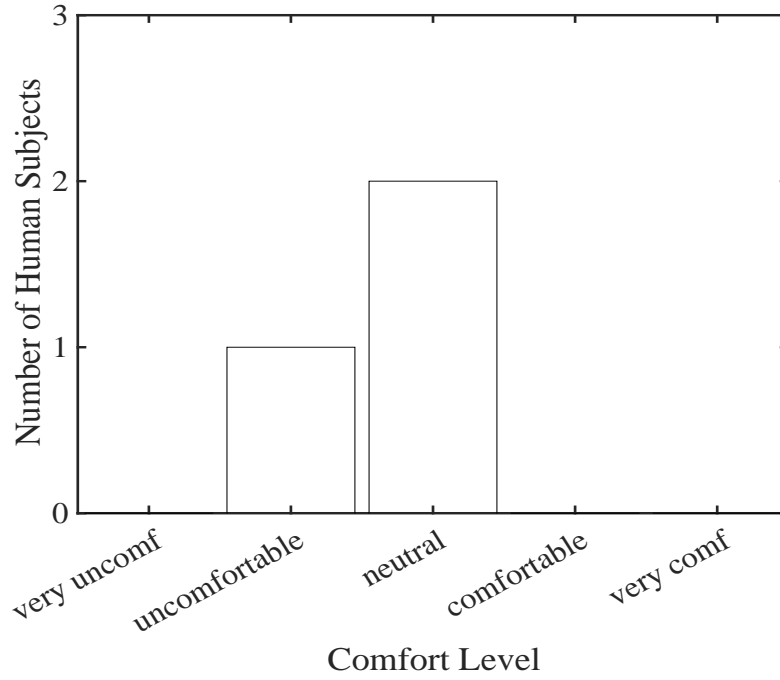
## 6.7 Discussion Section

The results provided quantitative responses in both the subjective and physiological data due to the effect of the PCD on the human body. The subjective responses showed a large variability in thermal preferences among human subjects. The physiological responses showed the individual capacity of human subjects to cope with the changes in the environmental temperatures. The trends in skin temperature, SDNNA values, and LF/HF ratio were the same for the majority of the human subjects when transitioning from thermally uncomfortable to comfortable levels. In

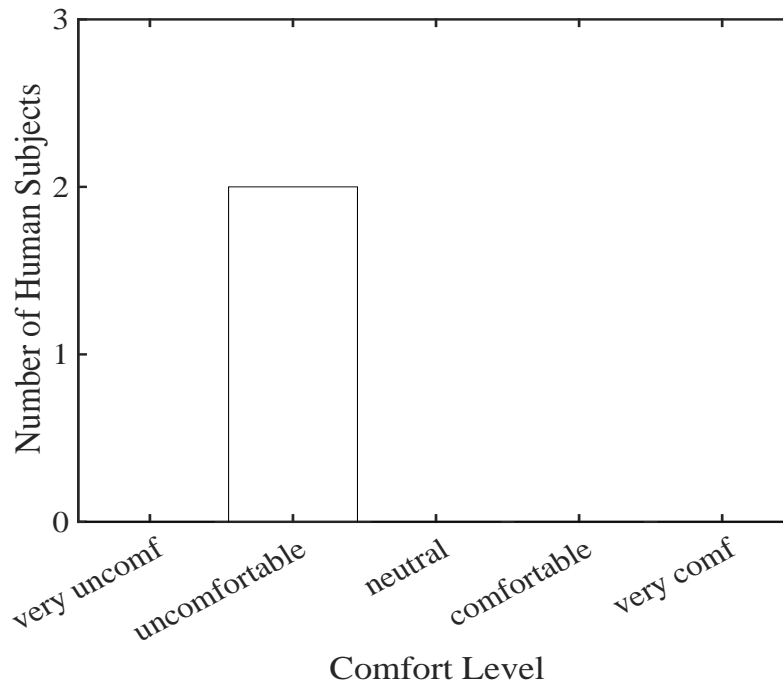
order to verify the observed results, this study conducted three control group experiments. These experiments consisted of providing human subjects with a PCD without its compressor-driven cooling capacity; in other words, a PCD that only operated its fan and moved warm room temperature air towards the human body. All the other factors of the experiment, such as the temperature change, the duration of the experiment, the physiological variables being monitored, and the amount of air supplied remained constant.

### **6.7.1 Subjective Response for the Control Group**

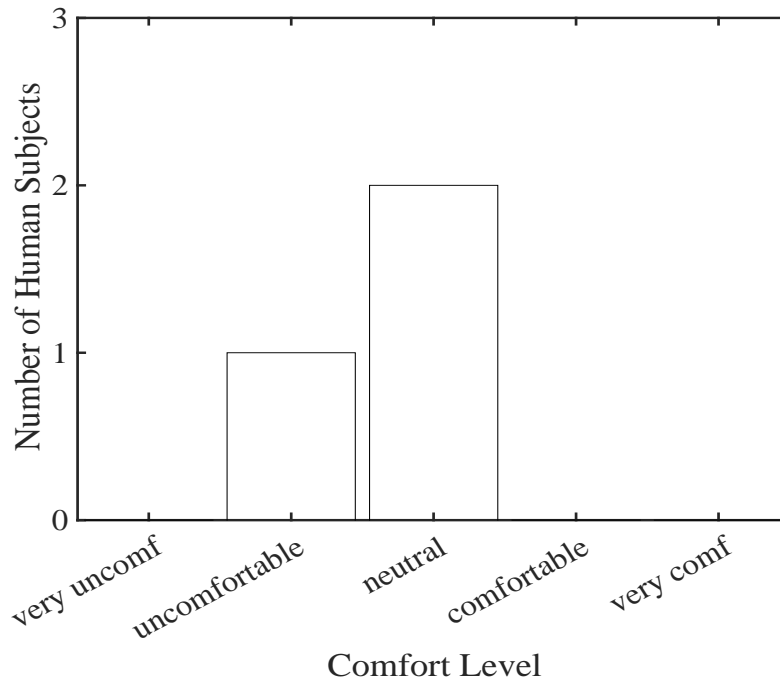
Similar to the regular experiments each human subject had variable comfort level and requested the PCD at different times. Figure 6-15 (a), (b), and (c) shows a histogram of the subjective responses at 10 minutes before requesting the PCD, at the moment of requesting the PCD, and 10 minutes after requesting the device. As shown on Figure 6-15 (b) when human subjects requested the three of them were uncomfortable, and 10 minutes after using the PCD they reported being neutral. On the contrary this same human subjects in the regular experiments reported comfortable and very comfortable thermal levels when using the PCD. The change in thermal comfort from uncomfortable to neutral is due to the convective effect of PCD and the physiological effect that PCD causes on human subjects.



(a) Subjective Responses 10 min before Requesting PCD



(b) Subjective Responses when Requesting PCD



(c) Subjective Responses 10 min After Requesting the PCD

Figure 6- 15 Distribution of Comfort Responses (a) 10 min before, (b) during, and (c)10 min After Requesting the PCD

### 6.7.2 Skin Temperature Response for the Control Group

In the control group experiments, the skin temperature of human subjects increased until the human body reached a thermally stable condition with the environment. Then, as soon as the human subjects requested the PCD, the air supplied towards the upper body (torso, arms, and face) decreased the skin temperature until finding a new thermal balance. Figure 6-16 shows the skin temperature response for the experiments in the control group. As shown in the figure, room temperature air supplied by the PCD’s fan was able, on average, to reduce the skin temperature approximately by 0.7°C that is a smaller temperature differential than 2°C obtained with full cooling capacity. This temperature reduction was a consequence of the convective effects of air movement around the human body. The statistical comparison between skin temperatures before and after the PC device showed no significant difference with a  $p\text{-value} > 0.05$ . These results,

including skin temperatures over time and their statistical analysis, suggested that the effect of the PCD's fan is insignificant in this scenario and had no potential to create a thermally comfortable microenvironment.

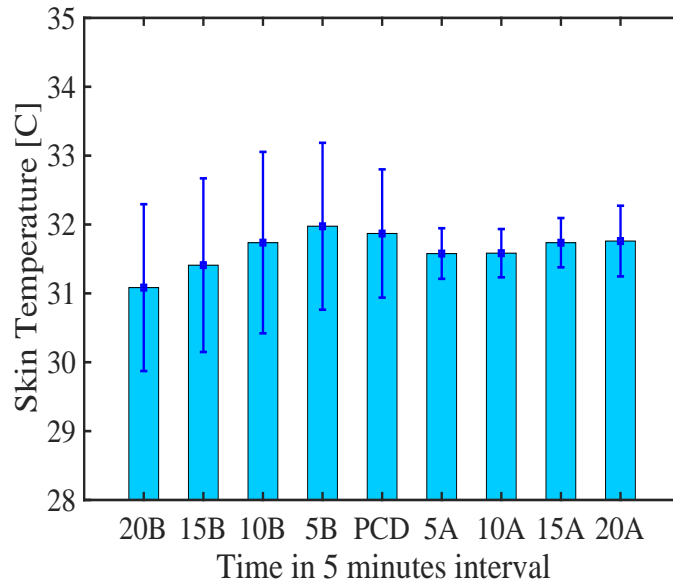


Figure 6- 16 Controlled-group Skin Temperature over 20 minutes before and after Requesting PCD

### 6.7.3 Heart Rate Variability (Time Domain) for the Control Group

The human subjects in the control group experiment were pooled from the high-individual variation of SDNNA group described in the result section. Human subjects in this group were selected due to their low tolerance to warm temperatures. Figure 6-17 shows the SDNNA values for the human subjects for control group experiments. The SDNNA values showed a decreasing trend as human subjects became thermally uncomfortable. After requesting the PCD, the SDNNA values slightly increased; however, these values did not increase as much as the values in the original experiment, specifically the values for the high-individual variation of SDNNA group. This slight increase could be attributed to the convective effect of room air movement around the

human body. An ANOVA test between the SDNNA values before and after requesting the PCD indicated no significant difference between these two cases. In addition, the human subjects reported being thermally neutral or uncomfortable after requesting the PCD.

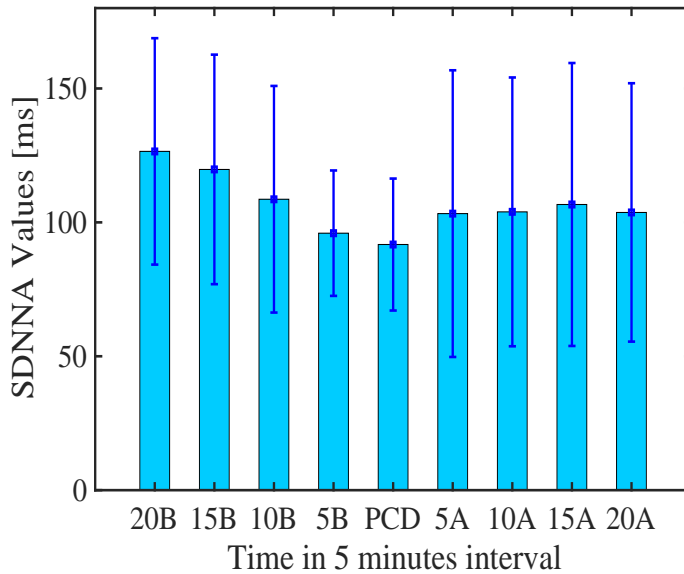


Figure 6- 17 Controlled-group SDNNA over 20 minutes before and after Requesting PCD

#### 6.7.4 Heart Rate Variability (Frequency Domain) for the Control Group

Similar to the original experiment results, the LF/HF ratio had an increasing trend as human subjects became thermally uncomfortable in the environment as shown in Figure 6-18. This increasing trend was directly associated with thermoregulatory system of each human body adapting to elevated environmental temperatures. After each human subject requested the PCD, the LF/HF ratio stabilized, but did not decrease as much as it did decrease in the original experiments. This response in HRV was consisted for the three human subjects in the controlled group experiments. In addition, the comparison of LF/HF ratio before and after the PCD showed no significance difference between the uncomfortable and comfortable thermal levels. This, again,



suggest that supplying room temperature air by the means of a fan is not sufficient to cause a change in the physiological parameters that are part of the human body thermoregulatory system. In addition, the different response in physiological variables between the original and control group experiments showed the potential to objectively evaluate individual thermal comfort using physiological variables.

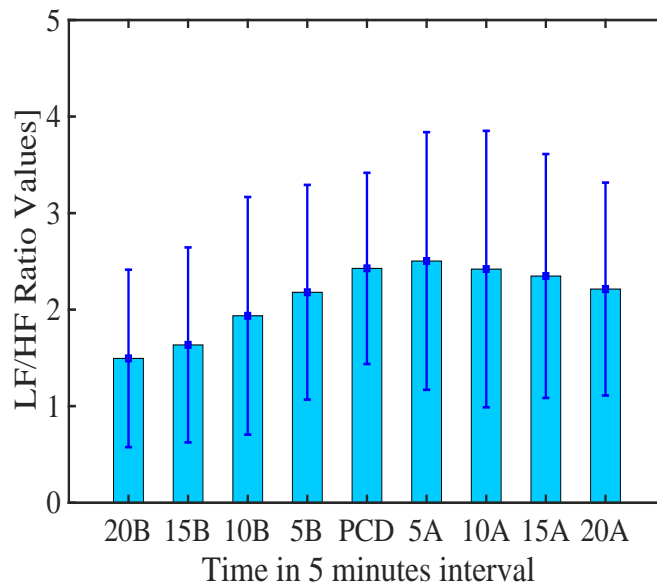


Figure 6- 18 Controlled-group LF/HF Ratio over 20 minutes before and after Requesting PCD

### 6.7.5 Physiological Changes at Different Thermal Comfort Levels

The human body is always adapting to changes in the environment. When environmental conditions change, the human body starts a physiological process, known as thermoregulation process, to maintain a stable internal condition [107]. The thermoregulation process is controlled by the autonomic nervous system [136]. Multiple studies have linked skin temperature and HRV, especially parameters such as SDNNA and LF/HF, to thermoregulation of the human body [138][136][131]. Due to the individual characteristics of the human body, the magnitude value of physiological responses varies among the human subjects; yet the trends in each variable are similar. According to a study, the trend of HRV, specifically LF/HF ratio, is an indicator of the

human thermoregulation under different environmental temperatures [107]. This is also true for subjective thermal preferences, where human subjects report different thermal comfort and thermal sensation levels for the same environmental condition [136].

The present results indicated that the magnitude and rate at which the skin temperature changes are different for each human subject. Consequently, the time to reach a stable temperature varies between 5 to 12 minutes and the air supplied by the PCD on average reduce the skin temperature by 2°C. The observed time and magnitude variation in this study is similar to the variations found in [107]. However, the aforementioned study used two full size and full equipped environmental chambers while our experiment achieved similar skin temperature response using a PCD, a significantly less intense technology that the one used to condition entire rooms. The results of this experiment indicated that high and low skin temperatures, relative to each human subject, are associated with individual thermal preferences. Consequently, the analysis on the correlation between skin temperature and thermal comfort level showed a correlation coefficient equal to 0.75. These findings suggested that skin temperature could be a potential indicator of thermal comfort as a function of environmental changes around the human body, and more importantly showed that PCDs have the potential to restore thermal comfort by creating a microenvironment that specifically targets the reduction in skin temperature.

The thermoreceptors in the skin act as temperature sensors and detect changes in the thermal environment around the human body. Further, these changes are delivered to the autonomic nervous system [138]. The autonomic system establishes the heat transfer between the human body and the environment. Due to the difference in autonomic systems and thermal preferences, the amount of heat removed from each human body, due to the PCD, varies. This study measured heat flux before and after each human subject requested the PCD. While the heat flux before using the

PCD averages 14 *Watts*, the heat flux after requesting the PCD averages 24 *Watts*, as shown in Figure 6-19. These results show the important role of the cooling capacity of the PCD device in creating a microenvironment that enhances the heat removal from the human body by a temperature differential and not only by the increase in convective heat transfer coefficient.

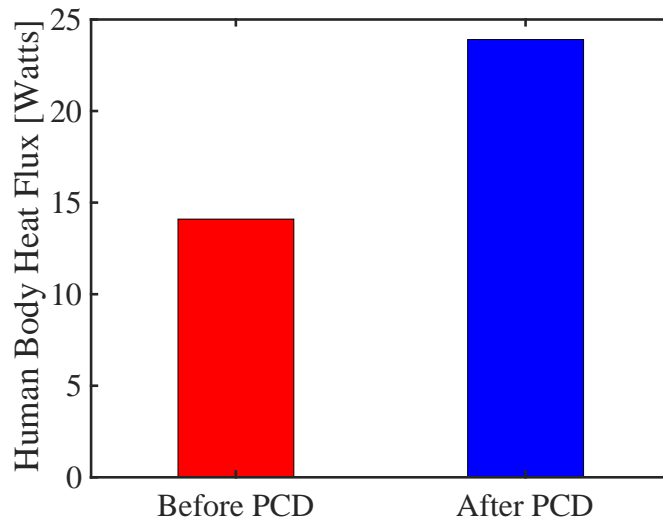


Figure 6- 19 Heat Flux Before and After PCD

The decrease of SDNNA values is due to a low ability of the human body to cope with emotional stressors. In contrast, the increase of SDNNA values is associated with relax/stress-free mode in the human body [134][139]. In our study, the SDNNA values consistently decreased until each human subject requested the PCD and increased as the PCD supplied cooled air. The magnitude and rate at which SDNNA values increased and decreased varied among human subject. Similarly, the time at which each human subject requested the PCD varied. These variations are due to the individual thermoregulation process of each human subject. According to SDNNA results, human subjects were grouped based on a high and low SDNNA values, as shown in Figure 11 (b). The low SDNNA group showed limited changes in the SDNNA values during the experiment and were able to delay requesting the PCD longer than the high SDNNA group. This could be associated

with individual thermal adaptation where the temperature range in the experiments was not sufficient to impact the SDNNA values. In contrast, the human subject group with high SDNNA values noticed the hot temperature and did not delay their request of the PCD, suggesting lower tolerance for warm/hot temperatures. Nevertheless, both groups showed a decreasing SDNNA trend during thermally uncomfortable levels and increasing SDNNA trend during comfortable levels. As a result, the individual analysis of the relationship between thermal comfort and SDNNA values showed correlation level, on average, of 0.68. This finding suggests that a constant monitoring of individual SDNNA values could provide useful information on individual thermal comfort. In addition, the microenvironment effect of the PCD in this experiment had positively impacted the subjective (surveys) and objective (SDNNA) values.

The frequency domain HRV analysis, specifically the LF/HF index, is associated with the balance between the parasympathetic nervous system (PNS) and the sympathetic nervous system (SNS). The parasympathetic nervous system (PNS) is related to the digest/rest activities that restore balance to the human body. In contrast, as the human body perceives changes or is exposed to stressful situation (physical or mental), it activates the SNS [138]. In our study results, the high LF/HF ratio indicates the activation of SNS in response of the heat stress perceived in the environment. The most common responses during the SNS in hot environments is the vasodilation to induced sweat to cool the skin and enhance heat losses. However, in our experiments, human subject did not show any signs of sweat since as soon as they reported uncomfortable conditions, they requested the PCD. As the PCD cools down the air around the human body, each human subject reported better thermal comfort values, and, consequently, the LF/HF ratio decreased, indicating that the PNS was engaged [107][136]. Based on the LF/HR results, two groups were identified by this research. The first group showed a low LF/HF ratio with very stable values over

the time frame of the experiments. In contrast, the second group had larger LF/HF, including a more dynamic response of LF/HF ratio values. The human subject in the first group tolerated longer the elevated temperatures before requesting the PCD. This suggest higher thermal tolerance to hot environments. Nonetheless, as human subjects in the first group requested the PCD, the decrease in LF/HF ratio was evident. The LF/HF ratio suggested that constant monitoring of LF/HF could provide useful insight towards the evaluation of individual thermal comfort. Our results showed a relationship between LF/HF and thermal comfort level with a correlation level, on average, equal to 0.67. These results indicate the potential implementation of LF/HF as an index for thermal comfort.

### **6.8 Summary**

This study investigated individual thermal comfort by simultaneously using survey, environmental, and physiological data instruments to understand impact of microenvironments created by Personalized Cooling Devices (PCDs) on human body. The experimental setup, in an environmental chamber, created an office-type space and controlled the air temperatures in a range between  $27 \pm 1^{\circ}\text{C}$  during the first hour and  $29 \pm 1^{\circ}\text{C}$  during the second hour of the experiment. The analysis demonstrates that PCD's microenvironments have an immediate physiological and subjective effect on the thermal comfort levels. The response time, on average, for both skin temperatures and heart rate variability is  $7 \pm 2$  minutes. Furthermore, the effect of the PCD's microenvironment conditions on the human body could be objectively quantify by monitoring physiological changes that drive the thermoregulation process in the human body. A significant relationship between measured skin temperatures and heart rate variability has been observed in the experiments. In contrast, the results showed no statistical relationship between heart rate and thermal comfort for studied human subjects. For these specific experimental conditions, the PCD

has the capability to reduce the skin temperature on average by 2°C and to decrease heart rate on average by 10 bpm. This reduction in thermal stress is due to the removal of  $24 \pm 6$  Watts from the human body via PCD cooling. The PCD enhances the human body heat dissipation which relaxes the autonomic nervous system; consequently, changing the LF/HF ratio, SDNNA values, and skin temperature. These physiological variables show significant differences when comparing their values before and after the PCD was introduced to the experiment. Since the PCD is the only external factor that was introduced into the experiment, the physiological changes were attributed to it. Therefore, the relationships established in this study between skin temperature and heart rate variability could be used to objectively evaluate the performance and interaction of different PCDs and human subjects.

## **Chapter 7**

### **Conclusions, and Recommendations for Future Studies**

Section 7.1 presents the key findings from this dissertation. Finally, the recommendation and future work are in section 7.2.

#### **7.1 Conclusions**

The analysis of the energy effect of PCD at the building level shows an increase in HVAC fan electrical energy consumption in the office building model. This increase in electrical energy is due to the extra load that the HVAC system experience when increasing the indoor setpoint during the peak hours of the day and decreasing the setpoint after the peak hour of the day. This HVAC fan effect is present in office buildings constructed pre-1980. On the other hand, in office buildings constructed post 2004 the HVAC fan electricity consumption show some savings. However, these savings are negligible at the building's overall energy balance since the HVAC fan energy load is only 4% of the total energy consumption of the building. Similarly, for midrise apartment building

pre-1980 and post-2004 the results show potential savings in HVAC fan electricity consumption, but they are negligible at the building overall energy balance due to the low contribution of the HVAC fan energy load. Therefore, in order to evaluate the total effect of introducing PCD to the building environment it is necessary to evaluate all the end-use energy available in the building.

The results of study show that increasing the temperature setpoint by 2.6°C during the peak hours of the day in the summer season could lead to energy savings between 10% to 70%, depending on the city. In addition, the results show costs savings associated with electricity. Midrise apartment buildings present the highest cost savings annually with \$130 per person for the city of Honolulu. These cost savings are the consequence of increasing the temperature setpoints during the electricity peak hours of the day when the electricity cost is highest while using PCDs to address thermal comfort of occupants. These cost savings are cities' dependent. This study proposes a method to identified potential cities that could benefit from adopting PCD technology based on cooling degree days and electricity rate. Cities with cooling degree days higher than 300 and the ratio of peak versus off-peak electricity price of 0.5 or higher, have the potential to show energy and cost savings. Overall the adoption of PCD has the potential decrease the cooling energy in the building while adding monetary savings due to electricity cost. The overall cost savings show a potential opportunity for the marketing of PCD technology in cities that have high cooling degree days and a significant difference between peak electricity price and off-peak electricity price.

The coupled simulations of CFD and Fanger's thermoregulation model is a useful tool to simulate the micro-environment of a human model using PCD. The results of the numerical simulations indicate that it is possible to remove approximately 23 Watts of sensible heat from the human body using an air nozzle of diameter equal to 8.0 cm, an airflow rate equal to 35 L/s (75 cfm), and 100

Watts cooling capacity. In addition, the results show a linear relationship between airflow rate and sensible heat removed from the human body. Airflow rates higher than 75 cfm more than 25 Watts of heat is removed from the human body. This indicates that the device is performing as intended and meets the required heat removal from the project specifications. In addition, the PPD calculations show a 26% dissatisfaction for seated model and a 5% dissatisfaction for standing model, which is under required PPD of 20% set by industry standards (ASHRAE) and the sponsoring agency Department of Energy (DOE). The results also indicate that PCD creates an uncomfortable environment for the seated model and a comfortable environment for the standing model. This discrepancy is associated with the amount of heat that the human body is set to generate under the two conditions, where the standing model generates more heat than the seated model. This specific result allows the study to propose higher operative room temperatures since the indoor temperature in this study is within the comfort zone defined by ASHRAE55. The results of this investigation show that it is possible to numerically evaluate thermal comfort as a function of airflow rate of PCD, amount of sensible heat removed from the human body, and cooling capacity of the PCD. However, numerical simulations cannot model physiological or psychological processes that are essential for individual thermal preferences. Therefore, experimental test that monitor human body key thermoregulation variables are necessary to evaluate the performance of the PCD.

This study assessed individual thermal comfort by simultaneously using survey, environmental, and physiological data instruments in microenvironments created by Personalized Cooling Device PCDs. The experimental setup, in an environmental chamber, created an office-type space and controlled the air temperature in a range between  $27 \pm 1^{\circ}\text{C}$  and  $29 \pm 1^{\circ}\text{C}$  for two hours. The analysis demonstrates that PCD's microenvironments have an immediate physiological and



subjective effect on the thermal comfort level. The response time, on average, of skin temperature and heart rate variability is  $7 \pm 2$  minutes. Furthermore, the effect of the PCD's micro-environment condition on the human body could be objectively quantify by monitoring physiological changes that drive the thermoregulation process in the human body. A significant relationship between skin temperature and heart rate variability has been established by this study and it is supported by other researchers. Based on these variables, this study reports that the PCD has the capability to reduce the skin temperature of human subjects approximately  $2^{\circ}\text{C}$  by helping the human body to remove  $24 \pm 6$  *Watts*. The PCD enhances the human body heat dissipation which relaxes the autonomic nervous system; consequently, changing the LF/HF ratio, SDNNA values, and skin temperature. These physiological variables show significant differences when comparing their values before and after the PCD was introduced to the experiment. Since the PCD is the only external factor that was introduced to the experiment, the physiological changes were attributed to it. This suggest that the relationships established in this study between skin temperature and heart rate variability to objectively evaluate the performance and interaction of different PCDs and human subjects.

This dissertation analysis the effect of PCD at the building and at the human level. The PCD technology shows potential for cooling energy savings and maintaining thermal comfort at warm indoor environmental conditions. In addition, this dissertation demonstrates that the PCD in this investigation has an effect on the physiological variables that control the human body thermoregulation systems. This suggest that PCD technology could be evaluated based on physiological variables. In addition, PCD technology could be adopted in indoor environments with limited access to HVAC systems or in places were thermal comfort is an important factor. Lastly, this dissertation demonstrates that occupants' thermal comfort could be assess by

monitoring physiological changes with the current sensor technology available in the market in a data-driven approach.

## **7.2 Recommendation and future work**

The data-driven approach for thermal comfort demonstrated in this study is the initial point to enable the evaluation of thermal comfort of human subjects when using PCDs. This dissertation was limited by the number of human subjects due to budget and time. Therefore, more human subject tests could potentially strengthen the relationship between thermal comfort and physiological variables.

Future studies should concentrate in human subject experiments and the deployment of the data-driven approach evaluation of thermal comfort. In these experiments, the researchers should consider evaluating the effect of PCD in a non-laboratory space to capture a more realistic interaction of human subjects and PCD. In addition, evaluating the interaction of PCD and human subject in a real scenario such as commercial or residential buildings will add uncertainty to the relationship found in this study, which could verify the strength of the relationship. Additionally, this dissertation recommends exploring the relationship between thermal comfort and productivity level when using PCD in warm environments. The complication and extra disturbances need to be considered and limited in the design of experiments stage to ensure a successful deployment and meaningful data collection.

Finally, a full deployment of PCD into commercial or residential buildings could lead to the validation of the overall energy analysis presented in this dissertation. However, this dissertation highly recommends using a market available PCD instead of a prototype version when conducting such a deployment. Using the actual device will enhance the user experience which is a key aspect of the potential benefits of PCD, more specifically RoCo.

## References

- [1] S. Vardoulakis *et al.*, “Impact of climate change on the domestic indoor environment and associated health risks in the UK,” *Environ. Int.*, vol. 85, pp. 299–313, 2015.
- [2] L. Pérez-Lombard, J. Ortiz, and C. Pout, “A review on buildings energy consumption information,” *Energy Build.*, vol. 40, no. 3, pp. 394–398, 2008.
- [3] M. Veselý and W. Zeiler, “Personalized conditioning and its impact on thermal comfort and energy performance - A review,” *Renew. Sustain. Energy Rev.*, vol. 34, pp. 401–408, 2014.
- [4] P. Höppe, “The physiological equivalent temperature - A universal index for the biometeorological assessment of the thermal environment,” *Int. J. Biometeorol.*, vol. 43, no. 2, pp. 71–75, 1999.
- [5] M. Heidarinejad, D. A. Dalgo, N. W. Mattise, and J. Srebric, “Personalized cooling as an energy efficiency technology for city energy footprint reduction,” *J. Clean. Prod.*, vol. 171, no. October, pp. 491–505, 2018.
- [6] American Physical Society, “Energy Future: Think Efficiency,” 2008.
- [7] M. C. Chang, “Room for improvement in low carbon economies of G7 and BRICS countries based on the analysis of energy efficiency and environmental Kuznets curves,”

- J. Clean. Prod.*, vol. 99, pp. 140–151, 2015.
- [8] A. K. Melikov, M. A. Skwarczynski, J. Kaczmarczyk, and J. Zabecky, “Use of personalized ventilation for improving health, comfort, and performance at high room temperature and humidity,” *Indoor Air*, vol. 23, no. 3, pp. 250–263, 2013.
- [9] S. Chen, W. Yang, H. Yoshino, M. D. Levine, K. Newhouse, and A. Hinge, “Definition of occupant behavior in residential buildings and its application to behavior analysis in case studies,” *Energy Build.*, vol. 104, pp. 1–13, 2015.
- [10] S. J.-L. Page J, Robinson D, “STOCHASTIC SIMULATION OF OCCUPANT PRESENCE AND BEHAVIOUR IN BUILDINGS Jessen Page , Darren Robinson and Jean-Louis Scartezini Solar Energy and Building Physics Laboratory ( LESO-PB ), Ecole Polytechnique Fédérale de Lausanne ( EPFL ), CH-1015 Lausanne ,” *Simulation*, pp. 757–764, 2007.
- [11] T. Maier, M. Krzaczek, and J. Tejchman, “Comparison of physical performances of the ventilation systems in low-energy residential houses,” *Energy Build.*, vol. 41, no. 3, pp. 337–353, 2009.
- [12] V. Martinaitis, E. K. Zavadskas, V. Motuziene, and T. Vilutiene, “Importance of occupancy information when simulating energy demand of energy efficient house: A case study,” *Energy Build.*, vol. 101, pp. 64–75, 2015.
- [13] K. Schakib-Ekbatan, F. Z. Çakici, M. Schweiker, and A. Wagner, “Does the occupant behavior match the energy concept of the building? - Analysis of a German naturally ventilated office building,” *Build. Environ.*, vol. 84, pp. 142–150, 2015.
- [14] D. Parker, E. Mills, and L. Rainer, “Accuracy of the Home Energy Saver Energy Calculation Methodology,” *ACEEE Summer Study Energy Effic. Build.*, pp. 206–222, 2012.
- [15] B. Jerry, *Desire for Control Personality, Social and Clinical Perspectives*. Elsevier Ltd, 1993.
- [16] T. Hong, S. C. Taylor-Lange, S. D’Oca, D. Yan, and S. P. Corgnati, “Advances in research and applications of energy-related occupant behavior in buildings,” *Energy Build.*, vol. 116, pp. 694–702, 2016.
- [17] E. Delzendeh, S. Wu, A. Lee, and Y. Zhou, “The impact of occupants ’ behaviours on building energy analysis : A research review,” *Renew. Sustain. Energy Rev.*, vol. 80, no. May, pp. 1061–1071, 2017.
- [18] P. Bluysen, *The Indoor Environemnt Handbook: how to make buildings healthy and comfortable*. London: Earthscan, 2009.
- [19] V. S. K. V Harish and A. Kumar, “A review on modeling and simulation of building energy systems,” *Renew. Sustain. Energy Rev.*, vol. 56, pp. 1272–1292, 2016.
- [20] M. Frontczak and P. Wargocki, “Literature survey on how different factors in fl uence human comfort in indoor environments,” *Build. Environ.*, vol. 46, no. 4, pp. 922–937, 2011.
- [21] H. B. Rijal, M. Honjo, R. Kobayashi, and T. Nakaya, “Investigation of comfort temperature , adaptive model and the window-opening behaviour in Japanese houses,” *Archit. Sci. Rev.*, vol. 8628, 2013.
- [22] P. O. Fanger, “Thermal Comfort,” *Robert E Krieger Publishing Company*, Florida, 1982.
- [23] X. . Ye, “Study on the mechanism and application of human thermal comfort,” Shanghai Jiao Tong University, 2005.
- [24] Y. . Liu, “Study on objective evaluation index of human body thermal comfort,” Shangai

- Jian Tong University, 2007.
- [25] T. B. B., “Urbanization: An Environmental Force to Be Reckoned With,” *Urbanization: An Environmental Force to Be Reckoned With*.
- [26] F. P. O. Bolashikov Z, Nikolev L, Melikov A.K., Kaczmarczyk J, “Personalized ventilation: air terminal devices with high efficiency,” *Proc. Heal. Build.*, pp. 850–855, 2003.
- [27] Y. Yang, J. Stapleton, B. T. Diagne, G. P. Kenny, and C. Q. Lan, “Man-portable personal cooling garment based on vacuum desiccant cooling,” *Appl. Therm. Eng.*, vol. 47, pp. 18–24, 2012.
- [28] K. M. Bendkowska W, Bogdan A, Kopias M, “Thermal manikin evaluation of microclimate cooling vests containing PCMs,” in *ITC and DC: Book of Proceedings of the 4th International Textile, Clothing and Design Conference e Magic World of Textiles*, 2008.
- [29] A. D. Flouris and S. S. Cheung, “Design and control optimization of microclimate liquid cooling systems underneath protective clothing,” *Ann. Biomed. Eng.*, vol. 34, no. 3, pp. 359–372, 2006.
- [30] T. A. C. Company, “How Evaporative Cooler Works.”
- [31] “The WARMING STORE.” [Online]. Available: [https://www.thewarmingstore.com/flexifreeze-ice-vest-zipper.html?productid=flexifreeze-ice-vest-zipper&channelid=FROOG&utm\\_source=CSE&utm\\_medium=GoogleShopping&utm\\_campaign=SolidCactus&gclid=EAIAIQobChMI8cTh3L6Q3gIVDIYNCh3xHAb1EAQYASABEgL5ofD\\_BwE](https://www.thewarmingstore.com/flexifreeze-ice-vest-zipper.html?productid=flexifreeze-ice-vest-zipper&channelid=FROOG&utm_source=CSE&utm_medium=GoogleShopping&utm_campaign=SolidCactus&gclid=EAIAIQobChMI8cTh3L6Q3gIVDIYNCh3xHAb1EAQYASABEgL5ofD_BwE).
- [32] “STACOOOL VEST.” [Online]. Available: [http://www.stacoolvest.com/stacool-premium-industrial-vest/?\\_vsrefdom=adwords&gclid=EAIAIQobChMI7eSissKQ3gIVrKGzCh2qWwarEAKYBCABEgLQ-PD\\_BwE](http://www.stacoolvest.com/stacool-premium-industrial-vest/?_vsrefdom=adwords&gclid=EAIAIQobChMI7eSissKQ3gIVrKGzCh2qWwarEAKYBCABEgLQ-PD_BwE).
- [33] “Home Esesentials Depot.” [Online]. Available: [https://www.google.com/search?rlz=1C5CHFA\\_enUS753US753&tbm=shop&q=phase+change+material+personalized+cooling+devices&tbs=vw:l,mr:1,price:1,ppr\\_min:600&sa=X&ved=0ahUKEwiU47rnw5DeAhWPMOAKHb1PBEGQvSsIoAIoAg&biw=1680&bih=922#spd=15895276980764205746](https://www.google.com/search?rlz=1C5CHFA_enUS753US753&tbm=shop&q=phase+change+material+personalized+cooling+devices&tbs=vw:l,mr:1,price:1,ppr_min:600&sa=X&ved=0ahUKEwiU47rnw5DeAhWPMOAKHb1PBEGQvSsIoAIoAg&biw=1680&bih=922#spd=15895276980764205746).
- [34] “ZoRo.” [Online]. Available: [https://www.zoro.com/coolshirt-systems-cooling-vest-1-28inl-bcw-1/i/G9411385/feature-product?gclid=EAIAIQobChMIxfiqlsyQ3gIVR1mGCh1pows\\_EAKYCiABEgJ6xfD\\_BwE](https://www.zoro.com/coolshirt-systems-cooling-vest-1-28inl-bcw-1/i/G9411385/feature-product?gclid=EAIAIQobChMIxfiqlsyQ3gIVR1mGCh1pows_EAKYCiABEgJ6xfD_BwE).
- [35] “Pegasus.” [Online]. Available: [https://www.pegasusautoracing.com/productselection.asp?Product=CS410&utm\\_source=google&utm\\_medium=cpc&utm\\_campaign=CS410&gclid=EAIAIQobChMIuMz7ic6Q3gIVyWSGCh22cgPcEAKYBSABEgIXRvD\\_BwE](https://www.pegasusautoracing.com/productselection.asp?Product=CS410&utm_source=google&utm_medium=cpc&utm_campaign=CS410&gclid=EAIAIQobChMIuMz7ic6Q3gIVyWSGCh22cgPcEAKYBSABEgIXRvD_BwE).
- [36] “Amazon.” [Online]. Available: [https://www.amazon.com/Compcooler-Backpack-Cooling-Performance-Underwear/dp/B07BTFLTGN/ref=asc\\_df\\_B07BTFLTGN/?tag=hyprod-20&linkCode=df0&hvadid=241944202239&hvpos=1o11&hvnetw=g&hvrand=7587653195756172035&hvppone=&hvptwo=&hvqmt=&hvdev=c&hvdcmdl=&hvlocint=&](https://www.amazon.com/Compcooler-Backpack-Cooling-Performance-Underwear/dp/B07BTFLTGN/ref=asc_df_B07BTFLTGN/?tag=hyprod-20&linkCode=df0&hvadid=241944202239&hvpos=1o11&hvnetw=g&hvrand=7587653195756172035&hvppone=&hvptwo=&hvqmt=&hvdev=c&hvdcmdl=&hvlocint=&)
- [37] “Sharper Image.” [Online]. Available: <https://www.sharperimage.com/si/view/product/Portable+Evaporative+Cooler/206051?p=>

- plist2470005&utm\_source=Google&utm\_medium=CPC&utm\_campaign=Shopping+Campaigns+High+Priority&Keyword=&device=c&creative=94259213663&cm\_mmc=CPC--Google--Shopping+Campaigns+High+Priority--94259213663&network=g&matchtype=&adpos=1o2&creative=94259213663&mkwid=hVr46QgQ%7Cpkw%7C%7Cpcrid%7C94259213663%7Cpmt%7C%7Cpdv%7Cc%7Cslid%7C%7C&gclid=EAIAIQobChMI8-\_gptOQ3gIVTVqGCh0zZAvOEAKYAiABEGJzy\_D\_BwE.
- [38] “Bed Bath & BEYOND.” [Online]. Available: [https://www.bedbathandbeyond.com/store/product/newair-af-1000b-portable-evaporative-cooler/1044548841?skuId=44548841&&mcid=PS\\_googlepla\\_nonbrand\\_outdoorutility\\_online&product\\_id=44548841&adtype=pla&product\\_channel=online&adpos=1o5&creative=223595886206&device=c&matchtype=&network=g&mrkgadid=558392987&mrkgclid=609&rkid=0&gclid=EAIAIQobChMI-e2K6dOQ3gIVgUCGCh0UAQvDEAKYBSABEGLXb\\_D\\_BwE&gclidsrc=aw.ds](https://www.bedbathandbeyond.com/store/product/newair-af-1000b-portable-evaporative-cooler/1044548841?skuId=44548841&&mcid=PS_googlepla_nonbrand_outdoorutility_online&product_id=44548841&adtype=pla&product_channel=online&adpos=1o5&creative=223595886206&device=c&matchtype=&network=g&mrkgadid=558392987&mrkgclid=609&rkid=0&gclid=EAIAIQobChMI-e2K6dOQ3gIVgUCGCh0UAQvDEAKYBSABEGLXb_D_BwE&gclidsrc=aw.ds).
- [39] A. Makhoul, K. Ghali, and N. Ghaddar, “Thermal comfort and energy performance of a low-mixing ceiling-mounted personalized ventilator system,” *Build. Environ.*, vol. 60, pp. 126–136, 2013.
- [40] S. Schiavon and A. K. Melikov, “Energy-saving strategies with personalized ventilation in cold climates,” *Energy Build.*, vol. 41, no. 5, pp. 543–550, 2009.
- [41] A. Makhoul, K. Ghali, and N. Ghaddar, “Desk fans for the control of the convection flow around occupants using ceiling mounted personalized ventilation,” *Build. Environ.*, vol. 59, pp. 336–348, 2013.
- [42] E. Foda and K. Sirén, “Design strategy for maximizing the energy-efficiency of a localized floor-heating system using a thermal manikin with human thermoregulatory control,” *Energy Build.*, vol. 51, pp. 111–121, 2012.
- [43] W. Chakroun, N. Ghaddar, and K. Ghali, “Chilled ceiling and displacement ventilation aided with personalized evaporative cooler,” *Energy Build.*, vol. 43, no. 11, pp. 3250–3257, 2011.
- [44] S. Schiavon and C. Sekhar, “Energy analysis of the personalized ventilation system in hot and humid climates,” *Energy Build.*, no. May, 2010.
- [45] P. O. Fanger *et al.*, “Findings of Personalized Ventilation Studies in a Hot and Humid Climate Findings of Personalized Ventilation Studies in a,” vol. 9669, 2011.
- [46] U. C. Berkeley, “Localized comfort control with a desktop task conditioning system : Laboratory and field measurements Center for the Built Environment,” no. October 2016, 1993.
- [47] H. Amai, S. Tanabe, T. Akimoto, and T. Genma, “Thermal sensation and comfort with different task conditioning systems,” vol. 42, pp. 3955–3964, 2007.
- [48] A. Melikov, T. Ivanova, and G. Stefanova, “Seat headrest-incorporated personalized ventilation : Thermal comfort and inhaled air quality,” *Build. Environ.*, vol. 47, pp. 100–108, 2012.
- [49] M. A. Sekhar S, Gon N, Maheswaran C, Cheong K, Tham K and Fanger P.O., “Energy efficiency potential of a personalized ventilation system in tropics,” in *Healthy Buildings*, 2003, vol. 2, pp. 668–689.
- [50] N. Ghaddar, K. Ghali, and W. Chakroun, “Evaporative cooler improves transient thermal comfort in chilled ceiling displacement ventilation conditioned space,” *Energy Build.*, vol. 61, pp. 51–60, 2013.

- [51] H. Zhang, E. Arens, D. Kim, E. Buchberger, F. Bauman, and C. Huizenga, "Comfort, perceived air quality, and work performance in a low-power task-ambient conditioning system," *Build. Environ.*, vol. 45, no. 1, pp. 29–39, 2010.
- [52] ASHRAE, "Thermal environmental conditions for human occupancy," *ASHRAE Inc.*, vol. 2010, p. 42, 2010.
- [53] Z. L. Huizenga, Charlie, Abbaszadeh S, "Indoor Environmental Quality ( IEQ ) Air Quality and Thermal Comfort in Office Buildings : Results of a Large Indoor Environmental Quality Survey," 2006.
- [54] D. Li, C. C. Menassa, and V. R. Kamat, "Personalized human comfort in indoor building environments under diverse conditioning modes," vol. 126, no. September, pp. 304–317, 2017.
- [55] F. P. Melikov A, Arakelian R, Halkjaer L, "Spot cooling – part 2: Recommendations for design of spot cooling systems," *ASHRAE Trans.*, vol. 100, pp. 500–510, 1994.
- [56] N. Gong *et al.*, "The Acceptable Air Velocity Range for Local Air Movement in The Tropics The Acceptable Air Velocity Range for Local Air Movement in The Tropics," vol. 9669, 2011.
- [57] C. V Grivel F, "Ambient temperatures preferred by young European males and females at rest," *Ergonomics*, vol. 34, no. 3, pp. 365–378, 1991.
- [58] I. Holmør, "Personal cooling with phase change materials to improve thermal comfort from a heat wave perspective," pp. 523–530, 2012.
- [59] A. K. Melikov, G. L. Knudsen, and A. K. Melikov, "Human Response to an Individually Controlled Microenvironment Human Response to an," vol. 9669, 2011.
- [60] S. Watanabe, A. K. Melikov, and G. L. Knudsen, "Design of an individually controlled system for an optimal thermal microenvironment," *Build. Environ.*, vol. 45, no. 3, pp. 549–558, 2010.
- [61] Y. Zhai, H. Zhang, Y. Zhang, W. Pasut, E. Arens, and Q. Meng, "Comfort under personally controlled air movement in warm and humid environments," *Build. Environ.*, vol. 65, pp. 109–117, 2013.
- [62] A. Makhoul, K. Ghali, and N. Ghaddar, "The Energy Saving Potential and the Associated Thermal Comfort of Displacement Ventilation Systems Assisted by Personalised Ventilation," *Indoor Built Environ.*, no. January 2015, 2013.
- [63] N. S. Dan and L. K. Voigt, "Modelling ow and heat transfer around a seated human body by computational uid dynamics," vol. 38, pp. 753–762, 2003.
- [64] Z. J. Murakami S, Kato S, "Development of a computational thermal manikin—CFD analysis of thermal environment around human body," in *Tsinghua-HVAC-95*, 1995, pp. 349–354.
- [65] M. Beaton *et al.*, "Ventilation for Acceptable," 2004.
- [66] J. S. Russo, T. Q. Dang, and H. E. Khalifa, "Computational analysis of reduced-mixing personal ventilation jets," *Build. Environ.*, vol. 44, no. 8, pp. 1559–1567, 2009.
- [67] J. Srebric, V. Vukovic, G. He, and X. Yang, "CFD boundary conditions for contaminant dispersion , heat transfer and airflow simulations around human occupants in indoor environments," *Build. Environ.*, vol. 43, pp. 294–303, 2008.
- [68] N. Gao, J. Niu, and H. Zhang, "Coupling CFD and Human Body Thermoregulation Model for the Assessment of Personalized Ventilation Coupling CFD and Human Body Thermoregulation Model for the Assessment of Personalized Ventilation," *HVAC R Res.*, vol. 9669, no. April, 2017.

- [69] S. Murakami, S. Kato, and J. Zeng, “Combined simulation of air flow, radiation and moisture transport for heat release from a human body,” vol. 35, 2000.
- [70] S. Zhu, D. Dalgo, J. Srebric, and S. Kato, “Cooling efficiency of a spot-type personalized air-conditioner,” *Build. Environ.*, vol. 121, pp. 35–48, 2017.
- [71] Z. E. Conceiça, P. Rosa, A. L. V. Custo, R. L. Andrade, and M. J. P. A. Meira, “Evaluation of comfort level in desks equipped with two personalized ventilation systems in slightly warm environments,” *Build. Environ.*, vol. 45, pp. 601–609, 2010.
- [72] Zhang H, “Human thermal sensation and comfort in transient and non-uniform thermal environments,” 2003.
- [73] J. Niu, N. G. Å, M. Phoebe, and Z. Huigang, “Experimental study on a chair-based personalized ventilation system,” vol. 42, pp. 913–925, 2007.
- [74] J. Kaczmarczyk, A. K. Melikov, and P. O. Fanger, “Human response to personalized ventilation and mixing ventilation,” *Indoor Air*, vol. 14, no. Suppl 8, pp. 17–29, 2004.
- [75] D. Faulkner, W. J. Fisk, D. P. Sullivan, and S. M. Lee, “Ventilation efficiencies and thermal comfort results of a desk-edge-mounted task ventilation system,” *Indoor Air*, vol. 14 Suppl 8, no. Suppl 8, pp. 92–97, 2004.
- [76] R. Li, S. C. Sekhar, and A. K. Melikov, “Thermal comfort and IAQ assessment of under-floor air distribution system integrated with personalized ventilation in hot and humid climate,” *Build. Environ.*, vol. 45, no. 9, pp. 1906–1913, 2010.
- [77] W. Pasut, E. Arens, H. Zhang, and Y. Zhai, “Enabling energy-efficient approaches to thermal comfort using room air motion,” *Build. Environ.*, vol. 79, pp. 13–19, 2014.
- [78] H. Zhang *et al.*, “Air movement preferences observed in office buildings,” pp. 349–360, 2007.
- [79] C. Pan, H. Chiang, M. Yen, and C. Wang, “Thermal comfort and energy saving of a personalized PFCU air-conditioning system,” *Energy Build.*, vol. 37, pp. 443–449, 2005.
- [80] S. C. Sekhar *et al.*, “Findings of personalized ventilation studies in a hot and humid climate,” *HVAC R Res.*, vol. 11, no. 4, pp. 603–620, 2005.
- [81] J. Kaczmarczyk, A. Melikov, Z. Bolashikov, L. Nikolaev, and P. O. Fanger, “Human response to five designs of personalized ventilation,” *HVAC R Res.*, vol. 12, no. 2, pp. 367–384, 2006.
- [82] J. Kaczmarczyk, A. Melikov, and D. Sliva, “Effect of warm air supplied facially on occupants’ comfort,” *Build. Environ.*, vol. 45, no. 4, pp. 848–855, 2010.
- [83] G. A. F. A. and B. L., “A standard predictive index of human response to the thermal environment,” *ASHRAE Trans.*, vol. 92, pp. 709–731, 1986.
- [84] Y. Yao, Z. Lian, W. Liu, and C. Jiang, “Heart rate variation and electroencephalograph – the potential physiological factors for thermal comfort study,” pp. 93–101, 2009.
- [85] P. The, “Temperature and comfort monitoring systems for humans.”
- [86] Y. Yang, R. Yao, B. Li, H. Liu, and L. Jiang, “A method of evaluating the accuracy of human body thermoregulation models,” *Build. Environ.*, vol. 87, pp. 1–9, 2015.
- [87] H. Zhu, H. Wang, Z. Liu, G. Kou, C. Li, and D. Li, “Experimental study on the variations in human skin temperature under simulated weightlessness,” *Build. Environ.*, vol. 117, pp. 135–145, 2017.
- [88] D. W. Å, H. Zhang, E. Arens, and C. Huizenga, “Observations of upper-extremity skin temperature and corresponding overall-body thermal sensations and comfort,” vol. 42, pp. 3933–3943, 2007.
- [89] Y. Yao, Z. Lian, W. Liu, and Q. Shen, “Experimental study on skin temperature and



- thermal comfort of the human body in a recumbent posture under uniform thermal environments,” *Indoor Built Environ.*, vol. 16, no. 6, pp. 505–518, 2007.
- [90] W. X. and P. F, “Estimating thermal transient comfort,” *ASHRAE Trans.*, vol. 98, pp. 182–188, 1992.
- [91] “Dynamic Simulation of Human Heat Transfer and Thermal Comfort,” 1998.
- [92] de D. R, R. J, and P. O. Fanger, “Thermal Sensations Resulting From Sudden Ambient Temperature Changes,” *Indoor Air*, vol. 3, no. 3, pp. 181–192, 1993.
- [93] J. H. Choi, V. Loftness, and D. W. Lee, “Investigation of the possibility of the use of heart rate as a human factor for thermal sensation models,” *Build. Environ.*, vol. 50, pp. 165–175, 2012.
- [94] D. Fiala, K. J. Lomas, and M. Stohrer, “modeling in physiology,” 2018.
- [95] M. Humphreys, M. McCartney, J. Nicol, and I. Raja, “AN ANALYSIS OF SOME OBSERVATIONS OF THERMAL COMFORT IN AN EQUATORIAL CLIMATE BY,” *Indoor Air*, pp. 602–607, 1959.
- [96] S. Y. Sim *et al.*, “Skin Temperatures,” *Sensors*, vol. 16, pp. 1–11, 2016.
- [97] P. O. Fanger, “Thermal Comfort: Analysis and Applications in Environmental Engineering,” *Danish Tech. Press*, 1970.
- [98] J. Xiong, Z. Lian, X. Zhou, J. You, and Y. Lin, “Potential indicators for the effect of temperature steps on human health and thermal comfort,” *Energy Build.*, vol. 113, pp. 87–98, 2016.
- [99] MedicineNet, “Medical Definition of Parasympathetic nervous system.” [Online]. Available: <http://www.medicinenet.com/script/main/art.asp?articlekey=4770>. [Accessed: 19-Apr-2017].
- [100] ScienceDaily, “ScienceDaily.” [Online]. Available: [https://www.sciencedaily.com/terms/sympathetic\\_nervous\\_system.htm](https://www.sciencedaily.com/terms/sympathetic_nervous_system.htm). [Accessed: 19-Apr-2017].
- [101] L. Lan, P. Wargocki, D. P. Wyon, and Z. Lian, “Effects of thermal discomfort in an office on perceived air quality, SBS symptoms, physiological responses, and human performance,” *Indoor Air*, vol. 21, no. 5, pp. 376–390, 2011.
- [102] T. Akimoto, S. ichi Tanabe, T. Yanai, and M. Sasaki, “Thermal comfort and productivity - Evaluation of workplace environment in a task conditioned office,” *Build. Environ.*, vol. 45, no. 1, pp. 45–50, 2010.
- [103] J. Verhaart, “Climate Chamber Tests for Measuring Performance Characteristics of a Personal Cooling System,” pp. 1–9, 2015.
- [104] X. Zhou, Z. Lian, and L. Lan, “Experimental study on a bedside personalized ventilation system for improving sleep comfort and quality,” *Indoor Built Environ.*, vol. 23, no. 2, pp. 313–323, 2014.
- [105] X. Jin, D. Zhou, and D. Li, “Physiology,” *Mil. Med. Sci.*, 1999.
- [106] C. P. Chen, R. L. Hwang, S. Y. Chang, and Y. T. Lu, “Effects of temperature steps on human skin physiology and thermal sensation response,” *Build. Environ.*, vol. 46, no. 11, pp. 2387–2397, 2011.
- [107] W. Liu, Z. Lian, and Y. Liu, “Heart rate variability at different thermal comfort levels,” *Eur. J. Appl. Physiol.*, vol. 103, no. 3, pp. 361–366, 2008.
- [108] L. Berglund and D. Cunningham, “Parameters of human discomfort in warm environments,” in *ASHRAE Transactions*, 1986.
- [109] G. Havenith and I. Holme, “Personal factors in thermal comfort assessment : clothing

- properties and metabolic heat production,” *Energy Build.*, vol. 34, pp. 581–591, 2002.
- [110] R. Edelberg, *Electrical Activity of the Skin: Its Measurements and Uses in Psychophysiology*. New York: Holt, Rinehart & Winston, 1972.
- [111] D. Filingeri, D. Fournet, S. Hodder, and G. Havenith, “Neurophysiology of Tactile Perception : A Tribute to Steven Tactile cues significantly modulate the perception of sweat-induced skin wetness independently of the level of physical skin wetness,” *J. Neurophysiol.*, no. Montell 2008, pp. 3462–3473, 2018.
- [112] J. H. Choi and D. Yeom, “Study of data-driven thermal sensation prediction model as a function of local body skin temperatures in a built environment,” *Build. Environ.*, vol. 121, pp. 130–147, 2017.
- [113] IMotions, “GSR Pocket Guide The pocket guide,” pp. 1–36, 2016.
- [114] S. Anand, N. Selvaraj, A. Jaryal, J. Santhosh, and K. Deepak, “Assessment of heart rate variability derived from finger-tip photoplethysmography as compared to electrocardiography,” *J. Med. Eng. Technol. details, Incl. Instr. authors subsc*, vol. 32, no. May 2014, pp. 479–484, 2008.
- [115] IMotions, “Measuring the Heart – How do ECG and PPG Work?,” 2017. .
- [116] R. C. Peng, X. L. Zhou, W. H. Lin, and Y. T. Zhang, “Extraction of heart rate variability from smartphone photoplethysmograms,” *Comput. Math. Methods Med.*, vol. 2015, no. January, 2015.
- [117] M. N. K. Boulos, S. Wheeler, C. Tavares, and R. Jones, “How smartphones are changing the face of mobile and participatory healthcare : an overview , with example from eCAALYX,” *Biomed. Eng. Online*, vol. 10, no. 1, p. 24, 2011.
- [118] M. J. Gregoski *et al.*, “Development and Validation of a Smartphone Heart Rate Acquisition Application for Health Promotion and Wellness Telehealth Applications,” *Int. J. Telemed. Appl.*, vol. 2012, p. 7 pages, 2012.
- [119] X. F. Teng and Y. T. Zhang, “STUDY ON THE PEAK INTERVAL VAFUABLITY OF,” *Jt. Res. Cent. Biomed. Eng.*, pp. 140–141.
- [120] W. Johnston and Y. Mendelson, “EXTRACTING HEART RATE VARIABILITY FROM A WEARABLE REFLECTANCE PULSE OXIMETER,” in *IEEE 31st Annual Northeast Bioengineering Conference*, pp. 157–158.
- [121] M. Bolanos, H. Nazeran, and Haltiwanger, “Comparison of heart rate variability signal features derived from electrocardiography and photoplethysmography in healthy individuals,” in *Proceedings of the 28th IEEE EMBS Annual International Conference*, 2006, pp. 4289–4294.
- [122] N. Selvaraj, J. Santhosh, and S. Anand, “Feasibility of photoplethysmographic signal for assessment of autonomic response using heart rate variability analysis,” in *IFMBE Proceedings*, 2007, pp. 391–395.
- [123] M. Heidarinejad, “RELATIVE SIGNIFICANCE OF HEAT TRANSFER PROCESSES TO QUANTIFY TRADEOFFS BETWEEN COMPLEXITY AND ACCURACY OF ENERGY SIMULATIONS WITH A BUILDING,” Pennsylvania State, 2016.
- [124] D. Betzer, “A Comprehensive System of Energy Intensity Indicators for the U.S.”
- [125] D. Deru M, Field K, Studer D, Benne K, Griffith B, Torcellini P, Liu B, Halverson M, Winiarski D, Yazdanian M, Huang J, Crawley, “U.S. Department of Energy Commercial Reference Building Models of the National Building Stock,” 2011.
- [126] Y. Du, “Battery Powered Portable Vapor Compression Cycle System With Pcm Condenser,” p. 84, 2016.

- [127] PRICE, “Engineering Guide Air Distribution.”
- [128] H. Shin, “Ambient temperature effect on pulse rate variability as an alternative to heart rate variability in young adult,” *J. Clin. Monit. Comput.*, vol. 30, no. 6, pp. 939–948, 2016.
- [129] T. Chaudhuri, D. Zhai, Y. C. Soh, H. Li, and L. Xie, “Random forest based thermal comfort prediction from gender-specific physiological parameters using wearable sensing technology,” *Energy Build.*, vol. 166, pp. 391–406, 2018.
- [130] T. Chaudhuri, D. Zhai, Y. C. Soh, H. Li, and L. Xie, “Thermal comfort prediction using normalized skin temperature in a uniform built environment,” *Energy Build.*, vol. 159, pp. 426–440, 2018.
- [131] L. a Fleisher, S. M. Frank, D. I. Sessler, C. Cheng, T. Matsukawa, and C. a Vannier, “Thermoregulation and heart rate variability.,” *Clin. Sci. (Lond).*, vol. 90, no. 2, pp. 97–103, 1996.
- [132] R. Dhumane, Y. Du, J. Ling, V. Aute, R. Radermacher, and M. H. Bldg, “Transient Modeling of a Thermosiphon based Air Conditioner with Compact Thermal Storage : Modeling and Validation,” *Int. Compress. Eng. Refrig. Air Cond. High Perform. Build. Conf.*, no. Vcc, pp. 1–10, 2016.
- [133] S. . D. F. . F. N. et al. Assad, “Correlating Heart Rate Variability with Mental Fatigue,” *Qualifying, A Major Report, Proj.*, 2012.
- [134] D. Kim, Y. Seo, J. Cho, and C.-H. Cho, “Detection of subjects with higher self-reporting stress scores using heart rate variability patterns during the day.,” *Conf. Proc. IEEE Eng. Med. Biol. Soc.*, vol. 2008, no. July 2016, pp. 682–685, 2008.
- [135] E. Olsson, “Heart Rate Variability in Stress-related Fatigue, Adolescent Anxiety and Depression and its Connection to Lifestyle,” *Vasa*, 2010.
- [136] H. Zhu, H. Wang, Z. Liu, D. Li, G. Kou, and C. Li, “Experimental study on the human thermal comfort based on the heart rate variability (HRV) analysis under different environments,” *Sci. Total Environ.*, vol. 616–617, pp. 1124–1133, 2018.
- [137] S. Sammito and I. Böckelmann, “Factors influencing heart rate variability,” *Int. Cardiovasc. Forum J.*, vol. 6, pp. 18–22, 2016.
- [138] K. N. Nkurikiyeyezu, Y. Suzuki, and G. F. Lopez, “Heart rate variability as a predictive biomarker of thermal comfort,” *J. Ambient Intell. Humaniz. Comput.*, vol. 0, no. 0, pp. 1–13, 2017.
- [139] Medicore, “Heart Rate Variability Analysis System,” 2010.